



Durham E-Theses

Wavefunctions and wavefunctionals in complex configuration space

Leonard, David

How to cite:

Leonard, David (2007) *Wavefunctions and wavefunctionals in complex configuration space*, Durham theses, Durham University. Available at Durham E-Theses Online: <http://etheses.dur.ac.uk/3930/>

Use policy

The full-text may be used and/or reproduced, and given to third parties in any format or medium, without prior permission or charge, for personal research or study, educational, or not-for-profit purposes provided that:

- a full bibliographic reference is made to the original source
- a [link](#) is made to the metadata record in Durham E-Theses
- the full-text is not changed in any way

The full-text must not be sold in any format or medium without the formal permission of the copyright holders.

Please consult the [full Durham E-Theses policy](#) for further details.

Wavefunctions & Wavefunctionals in Complex Configuration Space

David Leonard

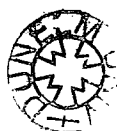
The copyright of this thesis rests with the author or the university to which it was submitted. No quotation from it, or information derived from it may be published without the prior written consent of the author or university, and any information derived from it should be acknowledged.

A Thesis presented for the degree of
Doctor of Philosophy



Centre for Particle Theory
Department of Mathematical Sciences
Durham University
England

August 2007



13 FEB 2008

Wavefunctions & Wavefunctionals in Complex Configuration Space

David Leonard

Submitted for the degree of Doctor of Philosophy

August 2007

Abstract

We show how to evaluate divergent asymptotic series using a modified Borel resummation method. We develop and test this technique using three different perturbative expansions of the anharmonic oscillator. In the first two expansions this provides the energy eigenvalues directly; however, in the third method we tune the wavefunctions to achieve the correct large x behaviour, as first illustrated in [1]. This tuning technique allows us to determine the energy eigenvalues up to an arbitrary level of accuracy with remarkable efficiency. We give numerical evidence to explain this behaviour. We also refine the modified Borel summation technique to improve its accuracy. The main sources of error are investigated with reasonable error corrections calculated. Having developed a suitable resummation technique we show how to generate a type of local expansion for vacuum, one- and two-particle states in the Schrödinger representation of quantum field theory. We also develop a large distance expansion of the S matrix in terms of a momentum cut-off. Computer programs capable of producing the local expansions of the wavefunctionals and S matrix to an arbitrary order are generated.

Declaration

The work in this thesis is based on research carried out at the Centre for Particle Theory, Department of Mathematical Sciences, Durham University, England. No part of this thesis has been submitted elsewhere for any other degree or qualification.

Chapters 2 and 5 contain relevant background material for which no claim of originality is made. The remainder of this thesis is based on my own work in collaboration with Paul Mansfield unless referenced to the contrary in the text. Chapter 3 follows [2], whilst chapter 4 is based on [1] and [2]. The material in chapter 6 contains unpublished research.

Copyright © 2007 by David Leonard.

“The copyright of this thesis rests with the author. No quotations from it should be published without the author’s prior written consent and information derived from it should be acknowledged”.

Acknowledgements

It is a pleasure to thank Professor Paul Mansfield for his patience and advice during the course of my studies in Durham. He was my supervisor during the fourth year of study in my Masters Degree and yet remarkably took on the challenge of helping me through my PhD.

It is also a pleasure to thank friends and family who have shown support throughout the course of my studies in Durham. Anna Lishman, Gina Titchener, Mark Goodsell, Lisa Müller, Gavin Hardman and Jenny Richardson have kindly tolerated my presence as office cohabitants. Their support has been invaluable and far outweighs any damage caused by the ‘vortex’¹ as it quickened pace. In particular it is a pleasure to thank those at Peterlee Parachute Centre. Although sometimes too diverting this community has been an important part of my life in Durham.

I would also like to acknowledge the Particle Physics and Astronomy Research Council (PPARC). Undoubtedly this work would not have been produced without the financial support they have awarded me.

¹See <http://www.phdcomics.com>

Contents

Abstract	ii
Declaration	iii
Acknowledgements	iv
1 Introduction	1
2 Harmonic Oscillators and Resummation	4
2.1 Asymptotic and Divergent Series	5
2.2 Padé Approximants	6
2.3 Borel Transformation	7
2.4 Symanzik Scaling	8
3 Direct Resummation of the Anharmonic Oscillator	9
3.1 Bender-Wu Expansion	12
3.2 Semi-Classical Expansion	16
3.3 A Shifted Expansion	22
3.4 Error Estimates	25
3.5 Summary	28
4 Tuning the Boundary Condition	29
4.1 Tuning for Large x	30
4.2 Excited States	36
4.3 Other Potentials	39
4.4 Numerical Investigation and Explanation	39

4.4.1	The Ground State - Zeros, Poles and Cuts	40
4.4.2	Excited States - Large x behaviour	43
4.5	Summary	47
4.6	Appendix	47
5	Schrödinger Representation of Quantum Field Theory	49
5.1	Functional Calculus	51
5.1.1	Functional Differential Equations	52
5.1.2	Functional Integration	54
5.2	Scalar Field Theory	56
5.2.1	Massive Free Scalar Field Theory	59
5.3	Renormalisability of the Schrödinger Equation	61
5.4	Locality of the Wavefunctional	65
5.4.1	Massive Free Scalar Field Theory	66
5.5	Reconstructing the Full Vacuum Functional	69
5.6	A Schrödinger Equation for the Local Expansion	71
5.7	Summary	75
6	A Large Distance Expansion of the S Matrix	76
6.1	Finding a Semi-Classical Wavefunctional	77
6.1.1	Ground State	77
6.1.2	One-Particle State	79
6.1.3	Two-Particle State	81
6.2	Generating the S Matrix	83
6.2.1	A Tree-Level Example	86
6.3	The Local Field Expansion	90
6.3.1	Ground State	90
6.3.2	One-Particle State	94
6.3.3	Two-Particle State	97
6.4	Computing the S Matrix: Functional Integration	99
6.5	The Computer Program	101
6.6	Summary	102

7	Conclusions and Further Research	104
	Appendix	107
A	Computer Programs: Large Distance Expansions	107
A.1	Generating the Basis Elements	107
A.2	Setting up the Problem	112
A.3	Solving the Schrödinger Equation	130
A.3.1	Ground State	130
A.3.2	One-Particle State	132
A.3.3	Z and b_2	134
A.3.4	Two-Particle State	136
A.4	Findind the S Matrix	137
A.4.1	Functional Integration	138
A.4.2	The S Matrix	147
	Bibliography	154

List of Figures

3.1	Plot of $L_{30}(\lambda)$ and $L_{29}(\lambda)$ with $\alpha = \alpha_M$	15
3.2	Ratio of coefficients of \hbar^n in b_2	18
3.3	Plot of $L_{30}(\lambda)$ and $L_{29}(\lambda)$ with $\hbar = 0.05$	20
4.1	$L_N(\lambda)$ with $N = 19, 20$ for $a_2 = -3/16$	32
4.2	ρ , E and a_3 as functions of a_2	34
4.3	E as a function of ρ	35
4.4	$T(\lambda)$ with an odd prefactor	38
4.5	Location of zeros of $\Psi(s)$	42
4.6	Prefactors corresponding to the first three excitations	45
4.7	P for values of c_1 either side of $e_1 = -0.1458432840772$	46
4.8	Q for values of c_1 either side of $\tau_1 \approx -0.1458432840772$	46
5.1	Key-hole shaped contour of integration	68

List of Tables

3.1	Results for resummation of E in the coupling.	14
3.2	Results of resummation in the semi-classical expansion	18
3.3	Infinite coupling values of b_3	22
3.4	Results of resummation in the shifted semi-classical expansion	24
3.5	Corrected couplings due to dominant singularity contributions	27
4.1	Quartic excited energy eigenvalues with $\rho = 0$	48

Chapter 1

Introduction

Quantum field theory (QFT) is undoubtedly the most successful mathematical theory we have in particle physics to date. It arose from efforts to unify quantum mechanics and special relativity particularly in many particle systems where particles can be created and annihilated. QFT describes phenomena on scales ranging from the sub atomic to the cosmological. It is the mathematical framework for describing the standard model of particle physics within which three of the four fundamental forces of nature are unified. QFT also has applications in nuclear, atomic, condensed matter physics and cosmology. The standard model of particle physics exhibits many symmetries such as $U(1) \otimes SU(2) \otimes SU(3)$ gauge invariance and Lorentz covariance.

Despite this, QFT has been troubled with difficulties since its inception. The biggest problem in physics today is perhaps how to unify the fourth fundamental force in nature, gravity. A QFT of gravity is currently viewed as an effective field theory valid below some cut-off scale. A quantum theory of gravity valid on scales of 10^{-33} cm and below therefore has to be described by a more fundamental theory. Present candidates include the use of extended objects such as strings and membranes or additional symmetries. This does not mean that QFT has been exhausted as a source of information about physical phenomena. In the development of a theory beyond the standard model the tools and lessons of QFT will undoubtedly still be of great importance. In a similar manner quantum mechanics is a useful testing ground for quantum field theory, as we show in this thesis.



QFT theory is also fraught with technical difficulties. Perturbative techniques to extract physical observables from a theory often fail, particularly in strongly coupled theories. For example the renormalisation group implies that the energy eigenvalues in Yang-Mills theory cannot be solved for perturbatively. Our repository of mathematical techniques to deal with non-perturbative solutions is extremely limited. Lattice field theory is probably the most important numerical technique for extracting these physical observables.

Unlike relativity, which is based on fundamental physical concepts, QFT is difficult to motivate at a physical level. The Schrödinger representation of QFT however is perhaps the best approach from the point of view of maintaining as much connection to fundamental physical concepts as possible. In particular it is more closely related to the original concept of quantum mechanics. This representation of QFT has largely gone undeveloped since its conception. This is due to technical difficulties in the definition and ability to work in this representation. Some of these problems, however, have been overcome by, for example, the work of Symanzik [3] [4]. We give a more detailed discussion of the Schrödinger representation, its difficulties and how some of these have been overcome in chapter 5.

Quantum mechanics is conceptually and technically more simple than QFT; however, many of the problems regarding divergence of perturbative solutions and the existence of non-perturbative effects are still found. The Bender-Wu asymptotic expansion of the quartic anharmonic oscillator energy eigenvalue for example is known to be divergent for all non-zero values of the coupling. In quantum mechanics a variety of techniques have been used and developed to produce accurate and in some cases exact energy eigenvalues. These quantum mechanical systems will therefore be of importance in developing techniques that we later intend to use in quantum field theory.

In chapter 2 we present some basic concepts of asymptotic series and resummation techniques. Chapter 3 presents and develops one of the key concepts of this thesis by introducing a modified Borel resummation technique. We develop this technique by producing energy eigenvalues using the quartic anharmonic oscillator as a toy theory. We improve the technique in a number of ways including the

introduction of some basic error bounds.

In chapter 4 we outline a remarkably efficient method for generating solutions to quantum anharmonic oscillators with an x^{2M} potential. We solve the Schrödinger equation in terms of a free parameter which is then tuned to give the correct boundary condition by generating a power series expansion of the wavefunction in x and applying a modified Borel resummation technique to obtain the large x behaviour. The process allows us to calculate energy eigenvalues to an arbitrary level of accuracy. High degrees of precision are achieved even with modest computing power. This technique extends to all levels of excitation and produces the correct solution to the double-well oscillators even though they are dominated by non-perturbative effects.

In chapter 5 we introduce the Schrödinger representation of QFT, specifically focussing on scalar field theory. We discuss a type of local expansion for the ϕ^4 field theory vacuum wavefunctional and show how a modified Borel resummation technique can be used to extract the full wavefunctional. In chapter 6 we further develop the idea of expanding the wavefunctionals of ϕ^4 field theory. We show how to produce a semi-classical expansion of the vacuum, one-particle and two-particle states. We then develop a method of extracting the S-matrix from the wavefunctionals. We explicitly demonstrate this using the semi-classical expansion. The concept of a local expansion of the wavefunctionals is extended to one and two-particle states. These local expansions are then used to generate a large-distance expansion of the S-matrix. We write computer programs to achieve this and discuss these in more detail in appendix A.

Chapter 2

Harmonic Oscillators and Resummation

Harmonic oscillators are a corner-stone of many branches of physics. Consequently a large variety of methods have been used to study the eigenvalue properties of anharmonic oscillators (see [5] [6] and references therein for a general review). High levels of accuracy have always been difficult to achieve due to slow convergence or often non-convergence of asymptotic perturbative expansions. For example the Bender-Wu [7] expansion of the quartic anharmonic oscillator ground state energy eigenvalue in positive powers of the coupling is known to be divergent for all non-zero values of the coupling. Methods of resumming asymptotic series [8] have been applied to generate approximate eigenvalues [9] [10]. In addition some types of anharmonic oscillators are dominated by non-perturbative effects such as instantons [11]. More innovative approaches have been required to produce a greater level of accuracy and account for these non-perturbative effects [12] [13] [14] [15]. In addition to the numerical approaches some progress has been made in determining the analytic structure of certain anharmonic oscillators [16] [17]. In particular [17] outlines a type of anharmonic oscillator which is quasi exactly solvable with certain parts of the spectrum known exactly.

These problems extend into quantum field theory. For example, the renormalisation group implies that the energy eigenvalues in Yang-Mills theory cannot be solved for perturbatively. Strongly coupled theories in particular are hard to deal

with using traditional techniques. Anharmonic oscillators are therefore of great interest because of their applicability in many branches of physics and because their mathematical properties often mirror those of other physical systems.

In this chapter we define the concept of an asymptotic series. In particular we define the Gervy asymptotic expansion since the perturbative solutions of the quartic anharmonic oscillator in the coupling and Planck's constant are both of this type. Since these types of expansion are known to be divergent we discuss the use of Padé approximants and Borel transforms as methods of resumming these series. Suitable reference material includes [8] and [18].

2.1 Asymptotic and Divergent Series

Suppose a function f is analytic in some sector S and a formal power series is given by $\hat{f} = \sum_{n=0}^{\infty} a_n z^n$. We say that $f(z)$ asymptotically equals $\hat{f}(z)$ as $z \rightarrow 0$ in S if there exists $C > 0$ such that $|r_f(z, N)| \leq C$ for every non negative N with $z \in S$ where

$$r_f(z, N) \equiv z^{-N} \left(f(z) - \sum_{n=0}^{N-1} a_n z^n \right). \quad (2.1.1)$$

Note that $r_f(z, N+1) = z^{-1} (r_f(z, N) - a_N)$. So if $r_f(z, N+1)$ is bounded at the origin then

$$\lim_{z \rightarrow 0} r_f(z, N) = a_N. \quad (2.1.2)$$

This shows that an analytic $f(z)$ has a unique asymptotic expansion.

An asymptotic expansion, however, does not necessarily correspond to a unique analytic function. Therefore a perturbative series does not necessarily specify a physical system uniquely. For example the function $\Re(cz^{-k}) > 0$ with $c > 0$ when $|\arg(z)| < \pi/2/k$. Therefore $\exp(-cz^{-k}) \rightarrow 0$ when $z \rightarrow 0$ within this sector. This implies that $f(z)$ would have the same asymptotic expansion as $f(z) + \exp(-cz^{-k})$, hence our claim that an asymptotic expansion does not necessarily correspond to a unique analytic function.

Equivalently we may also say that $\hat{f}(z)$ is the asymptotic expansion of $f(z)$. Given $k > 0$ we may say that \hat{f} is the asymptotic expansion of f of (Gervy) order

k^{-1} if there exist $C, K > 0$ such that for every non-negative integer N

$$|r_f(z, N)| \leq CK^N \Gamma(1 + N/k). \quad (2.1.3)$$

Gervy asymptotic expansions occur in many physical systems, including the Bender-Wu [19] perturbative expansion of the quartic anharmonic oscillator in the coupling. We will also encounter a Gervy asymptotic expansion in the semi-classical solution of this oscillator in section 3.2. One technique that has been applied to these types of expansion is a Borel-resummed Padé approximants technique.

2.2 Padé Approximants

With $M + N = K$, the $[M, N]$ Padé approximant of a function $f(z)$ with a truncated series expansion of order K ,

$$\hat{f}(z) = \sum_{n=0}^K f_n z^n \quad (2.2.1)$$

is given by

$$f^{[M,N]} = \frac{a_0 + a_1 z + \cdots + a_M z^M}{1 + b_1 z + \cdots + b_N z^N} \quad (2.2.2)$$

where the a_n and b_n are chosen in such a way that the truncated series expansion up to order K of $f^{[M,N]}$ is given by $\hat{f}(z)$. That is

$$f^{[M,N]} - \hat{f}(z) = O(z^{K+1}) = 0. \quad (2.2.3)$$

The coefficients a_n and b_n in principle can be chosen uniquely as follows. Multiplying (2.2.3) by the denominator of $f^{[M,N]}$ gives us

$$\sum_{n=0}^K \sum_{m=0}^n f_{n-m} b_m z^n = \sum_{n=0}^M a_n z^n + O(z^{K+1}) \quad (2.2.4)$$

with $b_0 = 1$. Comparing coefficients of z^n for $0 \leq n \leq K$ gives us $K + 1$ equations which in principle uniquely determine the $K + 1$ a_n and b_n . Firstly, consider the z^n coefficients of (2.2.4) with $M < n < K + 1$,

$$\sum_{m=0}^n f_{n-m} b_m. \quad (2.2.5)$$

These allow us to determine the b_n uniquely in terms of the given f_n using the usual algorithms and techniques for solving the simultaneous equations.

The a_n are then determined by looking at the z^n coefficients of (2.2.4) with $0 \leq n \leq M$. The linear equations are solved for the a_n , for each n , substituting the a_m with $m < n$ and all of the b_m, f_n in at each stage.

Whilst the series (2.2.1) may only converge within some circle $|z| < R$ it is possible that the Padé approximant may converge outside this region. Padé approximants can therefore be used to define an analytic continuation of $\hat{f}(z)$ outside of this region.

One advantage of the Padé method is that even at low orders of approximation the Padé approximation is able to describe functions with poles. This is in contrast to the standard power series expansions.

We note that the Bender-Wu asymptotic expansion of the quartic anharmonic oscillator is one such asymptotic expansion for which Padé approximants have been used [9]. In this paper it was proved that the diagonal Padé approximants of the perturbative energy eigenvalue series converge towards the correct eigenvalue.

2.3 Borel Transformation

The Borel sum, $B(z)$ of an asymptotic series such as (2.2.1) is defined by dividing the z^n coefficients, f_n by $n!$. That is

$$B(z) \equiv \sum_{n=0}^{\infty} \frac{f_n}{n!} z^n. \quad (2.3.1)$$

Using the integral representation of the gamma function

$$n! = \Gamma(n+1) = \int_0^{\infty} dt e^{-t} t^n \quad (2.3.2)$$

we can reinsert the factorials at each stage:

$$f(z) = \sum \frac{f_n}{n!} z^n n! \quad (2.3.3)$$

$$= \sum \frac{f_n}{n!} \int_0^{\infty} dt e^{-t} (zt)^n \quad (2.3.4)$$

$$= \int_0^{\infty} dt e^{-t} B(zt). \quad (2.3.5)$$

This (2.3.5) is the Borel transformation of the Borel sum (2.3.1).

It is pointless to directly apply the Borel transform to a truncated Borel sum since this simply reproduces the original divergent series. In general a form of analytic continuation of the Borel sum must be found and then inversion applied. The Padé approximant technique is one method of performing this continuation. In [10] a type of Borel sum was applied to the Padé approximants of the quartic anharmonic oscillator and proved that this does produce the correct energy eigenvalues. These numerical approximations appeared to be better than those obtained with the direct use of the Padé approximants.

We note that the Borel sum of a Gervy asymptotic expansion will be convergent within a non-zero radius. This is due to the dampening of the gamma function in the expansion's coefficients.

2.4 Symanzik Scaling

In a semi-classical solution of a quantum mechanical model, Symanzik noted that the energy eigenvalues are often related via a type of scaling transformation [20]. For example, a Hamiltonian

$$H(\rho, g) = p^2 + \rho x^2 + gx^4 \quad (2.4.1)$$

may undergo a scaling $x \rightarrow cx$. This scales the Hamiltonian

$$H(\rho, g) \rightarrow \frac{p^2}{c^2} + \rho c^2 x^2 + gcx^4 = \frac{1}{c^2} H(\rho c^4, gc^6). \quad (2.4.2)$$

In this example there is actually only one free parameter that we should consider. The remaining degree of freedom can be eliminated without loss of generality by a Symanzik scaling type argument. In particular, the energy eigenvalues are related by choosing $c = g^{-1/6}$

$$E_n(1, g) = g^{1/3} E_n(g^{-2/3}, 1). \quad (2.4.3)$$

Chapter 3

Direct Resummation of the Anharmonic Oscillator

One technique that has been of interest in the Schrödinger representation of both quantum field theory and quantum mechanics is a modified type of Borel resummation [21] [22] [23] [24]. The aim of this chapter is to explore this particular method of resummation. It is important to test and develop the accuracy of our technique in a theory with known results so that we can confidently apply it to problems in which other techniques fail. Since energy eigenvalues are already known for the quantum mechanical anharmonic oscillator to a high degree of accuracy, we shall apply the resummation technique to this problem. That is, we look for solutions to

$$-\frac{d^2\Psi}{dx^2} + \rho x^2\Psi + gx^4\Psi = E\Psi \quad (3.0.1)$$

$$\lim_{|x|\rightarrow\infty} \Psi = 0 \quad (3.0.2)$$

where x is defined along the real axis and we choose units in which $\hbar = 2m = 1$. We will generate three different perturbative expansions of the quartic anharmonic oscillator wavefunction as follows:

- An expansion in the coupling, g (Bender-Wu expansion)
- An expansion in Planck's constant, \hbar (the semi-classical expansion)
- An expansion in powers of x

In the first two approaches we take a perturbative expansion of the energy eigenvalue and directly resum to find an approximate result. In the third method we resum the large x behaviour of the wavefunction. This provides a variational technique in which the energy is tuned to ensure the correct boundary condition (3.0.2) is observed. This technique is remarkably efficient and provides energy eigenvalues up to an arbitrary level of accuracy. In this chapter we focus on the first two expansions. The third expansion is considered separately in chapter 4 due to its special interest and efficiency. First we must develop a method of resummation.

The method of resummation we shall employ allows us to extract the small s properties from an asymptotic expansion which is only valid for large s . Therefore consider an asymptotic expansion of a function $f(s)$ in inverse powers of s :

$$f(s) \approx a_0 + \frac{c_1}{s} + \frac{c_2}{s^2} + \frac{c_3}{s^3} + \frac{c_4}{s^4} + \frac{c_5}{s^5} + \dots \quad (3.0.3)$$

We analytically continue $f(s)$ into the complex s plane, then Cauchy's theorem relates the large s to small $s = s_0$ behaviour of $f(s)$ via the integral

$$L(\lambda) = \int_C ds \frac{e^{\lambda(s-s_0)}}{s-s_0} f(s) \quad (3.0.4)$$

where C is a large circular contour centred on the origin. We only assume $f(s)$ to be analytic in the half plane $\Re(s - s_0) \geq 0$. Any singularity contributions to (3.0.4) in the half plane $\Re(s - s_0) < 0$ are exponentially damped by λ so that $\lim_{\lambda \rightarrow \infty} L(\lambda) = f(s_0)$.

We approximate $L(\lambda)$ using a truncated version of the asymptotic expansion (3.0.3) and expanding the $s - s_0$ denominator in powers of s_0/s truncated to some order P . Thus we define

$$\begin{aligned} L_N(\lambda) &= \int_C ds e^{\lambda(s-s_0)} \sum_{p=0}^P \frac{s_0^p}{s^{p+1}} \sum_{n=0}^N \frac{c_n}{s^n} \\ &= \sum_{n=0}^N \sum_{p=0}^P c_n \frac{e^{-\lambda s_0} s_0^p \lambda^{n+p}}{\Gamma(n+p+1)} \approx L(\lambda) \end{aligned} \quad (3.0.5)$$

where in completing the integral we used the identity [25]

$$\int_C ds s^{-n} \exp(\lambda s) = 2\pi i \lambda^{n-1} / \Gamma(n) \quad (3.0.6)$$

for $n < 0$. The introduction of the gamma functions in this series improves the convergence of the original asymptotic expansion. We note, however, that $L_N(\lambda)$ is only a good approximation to $L(\lambda)$ within a limited range of λ . For sufficiently large λ the series will be dominated by the highest powers of λ and exhibits a rapidly increasing or decreasing behaviour depending on the sign of the coefficient. We also note the similarity of this method to that of Borel summation. The Borel transform of an asymptotic series results in the introduction of an additional $1/n!$ factor in each c_n . The Borel procedure, however, requires us to analytically continue the Borel transformed series before inversion. This is accomplished via techniques such as Padé approximants or conformal mapping. The advantage of our technique is that this analytic continuation is encoded in the contour integral.

We take λ as large as practicably possible with the constraint that $L_N(\lambda)$ be a good approximation to $L(\lambda)$. This is best achieved by requiring maximal $\lambda = \lambda_M$ such that $L_N(\lambda)$ differs from $L_{N-1}(\lambda)$ by no more than a set amount. In this chapter we will choose λ_M so that they differ by no more than 10^{-3} percent. More terms (greater N) allows for a larger λ and therefore better dampening of any singularity contributions.

One method for increasing the singularity dampening for a given N is to introduce a new parameter, α by replacing $f(s)$ with $f(s^\alpha)$ and s_0 with $s_0^{1/\alpha}$ in $L(\lambda)$. For $\alpha > 1$ the size of the last term in L_N relative to its penultimate term L_{N-1} is reduced due to the gamma function in (3.0.5). This allows us to take a larger value of λ whilst $L_N(\lambda)$ remains a good approximation to $L(\lambda)$. Increasing α , however, causes singularities of f to be rotated about the origin. For α too large the singularities enter the half plane $\Re(s - s_0) \geq 0$, at which point they are no longer exponentially suppressed. $L(\lambda)$ will then exhibit oscillations resulting from these singularity contributions. We therefore take $\alpha = \alpha_M$ to be as large as possible but still ensuring $L_N(\lambda)$ is monotonic as a function of λ for $\lambda < \lambda_M$. The technique originally (i.e. without the introduction of α) only worked for functions which are analytic in the half plane $\Re(s - s_0) \geq 0$. With the introduction of α we could also consider functions in which $f(s)$ has singularities with $\Re(s - s_0) \geq 0$. By reducing $\alpha < 1$ we can rotate these singularities back into the half plane $\Re(s - s_0) < 0$, where

they become exponentially dampened.

In all three approaches we will solve the anharmonic oscillator ground state by writing $\Psi = e^W$ since the ground state of any quantum mechanical system has no nodes. In the case of the quartic anharmonic oscillator (3.0.1), the potential and boundary condition are even in x . We therefore expand W in the form $W = \sum_{n=1}^{\infty} a_n x^{2n}$. Substituting this expansion into the differential equation (3.0.1) and comparing coefficients of the x^{2n} we get relations between the a_n as follows

$$-2a_1 = E, \quad -12a_2 - 4a_1^2 + \rho = 0, \quad -30a_3 - 16a_1a_2 + g = 0 \quad (3.0.7)$$

and for $n \geq 3$

$$a_{n+1} = - \left(\sum_{m=1}^n 4m(n-m+1)a_m a_{n-m+1} \right) / (2(n+1)(2n+1)). \quad (3.0.8)$$

The equation (3.0.8) allows us to find a_{n+1} in terms of the a_m with $m \leq n$. We can therefore solve all of the a_n in terms of a_1 , a_2 and a_3 . In turn these first three coefficients are determined by the physical parameters E , ρ and g via (3.0.7). However, for a given ρ and g only specific values of E allow the solution to satisfy the boundary condition (3.0.2). In sections 3.1, 3.2 and chapter 4 we propose different methods for eliminating this final degree of freedom.

3.1 Bender-Wu Expansion

Bender and Wu [19] showed how to construct the ground state energy by summing all connected Feynman diagrams with no external legs. In general a Feynman diagram with $2n$ external legs has at least $n - 1$ vertices. So we ensure that an x^{2n} term is at least order $n - 1$ in the coupling by making the expansion $a_n = \sum_{m=n-1}^{\infty} a_{n,m} g^m$. This is a similar approach to another method outlined by Bender and Wu in the same paper. We substitute this coupling expansion into the above relations between the a_n and compare coefficients of g^n . The first coefficient is given by $a_{1,0}^2 = 1/4$ which requires a choice of sign for $a_{1,0}$. In keeping with the Bender-Wu methods [19] we choose a negative sign. In chapter 4 we show that this sign choice is required to ensure the correct boundary condition (3.0.2).

Having made the choice for $a_{1,0}$, the remaining coefficients are uniquely determined. We first find each $a_{n,n-1}$ by looking at the g^{n-1} coefficient in (3.0.7) and (3.0.8). The g^n coefficients give $a_{n,n}$ then the g^{n+1} coefficients give the $a_{n,n+1}$ etc. At each stage we are substituting in the previous solutions. Eventually we can find each a_n up to any order in g . Of course the coefficients will also depend on ρ however for the purpose of this section we set $\rho = 1$ without loss of generality since the eigenvalues for arbitrary ρ may be reproduced via a form of Symanzik scaling.

We now have a solution for the ground state wavefunction of (3.0.1) as the exponential of a power series in x and g . The energy eigenvalue is computed from a_1 using (3.0.7) as a power series in g . This gives the well known [19] [26] [27] Rayleigh-Schrödinger perturbation expansion for $E(g)$,

$$E = 1 + \frac{3}{4}g - \frac{21}{16}g^2 + \frac{333}{64}g^3 - \frac{30885}{1024}g^4 + \frac{916731}{4096}g^5 - \frac{65518401}{32768}g^6 + \dots \quad (3.1.1)$$

This expansion has a zero radius of convergence, as can be seen from the asymptotic form of the $a_{1,n}$ coefficients at large n as given by Bender and Wu [19]. It has been used to generate some energy eigenvalues via a Borel-resummed Padé approximants technique [9] [10] although many other techniques have been used to find the energy eigenvalues more accurately and efficiently, e.g. [1] [12] [13] [14] [15] [28] [29].

We will apply our resummation method to $E(g)$ in an attempt to get meaningful results for non zero values of g . To do this we analytically continue g in the complex $s = 1/g$ plane. We write $s_0 = 1/g$ and $c_n = -2a_{1,n}$ then apply the contour integral technique so that $L_N(\lambda)$ in (3.0.5) approximates the energy.

The results generated via our resummation method are listed in Table 3.1 (recall α_M and λ_M represent the optimal values of α and λ) and compared to the results as generated by the method [1]. We label the eigenvalues generated by [1] E_{best} since they are accurate to within the number of significant figures expressed. The seemingly strange choices for g that we use become more natural in the semi-classical expansion as outlined in the next section. We use the same values of g in both sections to allow comparison.

The results for small g are quite impressive, with errors in the region of 10^{-3} to 10^{-4} percent. However, for larger g the results are less impressive, with the error approximately 23.8% for the largest value of g .

g	α_M	λ_M	L_{30}	E_{best}	Error (%)
0.05783	1.6398	2.9266	1.0397406	1.0397505	0.00095
0.13458	2.4250	7.6353	1.0846489	1.0846523	0.00031
0.23702	2.8159	10.4624	1.1359213	1.1359237	0.00021
0.37556	2.8160	9.9602	1.1952265	1.1952286	0.00017
0.56672	2.8160	9.6275	1.2649090	1.2649111	0.00017
0.83794	2.8159	9.3800	1.3483970	1.3483997	0.00020
1.23759	2.8160	9.1841	1.4509422	1.4509525	0.00071
1.85793	2.8160	9.0197	1.5810649	1.5811388	0.00467
2.89469	2.8160	8.8769	1.7536476	1.7541160	0.02671
4.83194	2.8160	8.7472	1.9974138	2.0000000	0.12948
9.19266	2.8160	8.6252	2.3766424	2.3904572	0.58127
23.50256	2.8160	8.5039	3.0767794	3.1622777	2.77882
206.09853	2.8160	8.3641	5.1098167	6.3245553	23.77265

Table 3.1: Results for resummation of E in the coupling.

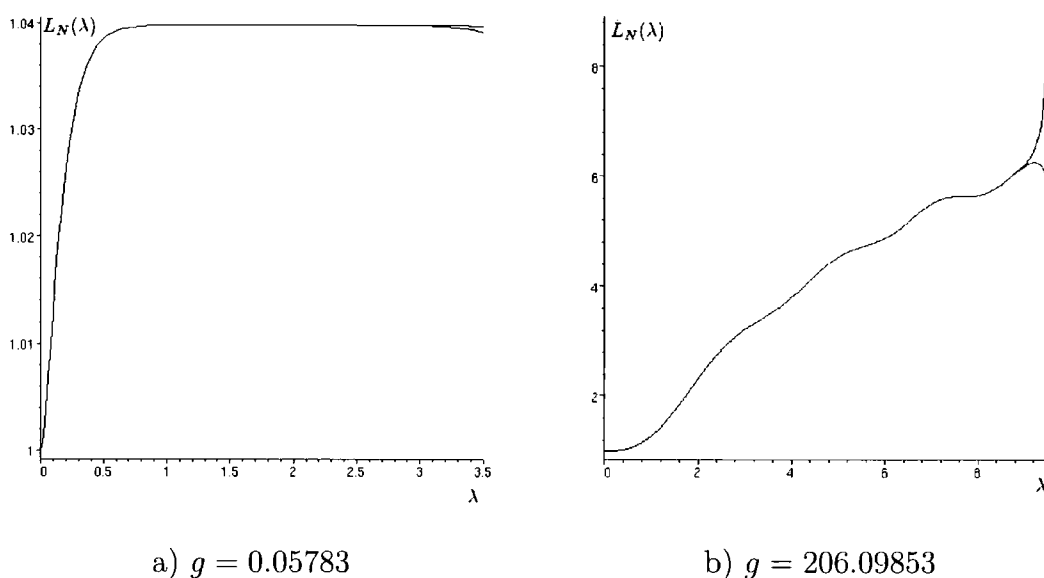
Figure 3.1: Plot of $L_{30}(\lambda)$ and $L_{29}(\lambda)$ with $\alpha = \alpha_M$

Figure 3.1a (a small g example) shows the expected behaviour of $L_{29}(\lambda)$ and $L_{30}(\lambda)$ with $P = 50$. For sufficiently large λ the two curves become a good approximation to $L(\lambda)$ and we see a flattening of the curve. For λ sufficiently large we notice an appreciable divergence of the two curves. Figure 3.1b, where g is relatively large has somewhat different behaviour. Here we notice that the curves have not started to flatten before they appreciably diverge. For these larger g we need more terms (greater N) in the expansion so that we may consider larger λ where the curve starts to flatten. Additionally we note that this curve exhibits oscillatory behaviour although it remains monotonic. When we introduced the requirement for the curve to be monotonic we assumed that a singularity contribution would consist of an exponentially weighted sinusoidal correction to a flat curve. In this case we do not have sufficient terms to consider λ in the region where it becomes flat but instead are considering a region of the curve where it is still appreciably increasing. If we considered more terms with this value of α we might well find our monotonic condition is violated. Given the behaviour observed in Figure 3.1b it is not surprising that we have such a large error.

In the next subsection we show that¹ $E \sim g^{1/3}$. Therefore as $g \rightarrow \infty$ or equiva-

¹This can be seen by Symanzik scaling of the Hamiltonian [20].

lently $s_0 \rightarrow 0$ we notice that E has a singularity. It is this singularity that is causing difficulty in the resummation process since we need larger λ for large g to ensure it is damped sufficiently. This in turn requires a larger N . The problems no doubt could be solved if we took a sufficient number of terms in the expansion of E however this would be at the expense of greater computing resources. In the next subsection we outline a more efficient method in which the singularity contribution is absent. We will therefore be able to calculate the infinite coupling limit. This is something that cannot be done via resummation of the Bender-Wu expansion.

3.2 Semi-Classical Expansion

In this section we resum a semi-classical expansion in \hbar for the a_n coefficients in W . We write $\Psi = e^{W/\hbar}$ and consider the modified differential equation

$$-\hbar^2 \frac{d^2 \Psi}{dx^2} + (b_0 + b_1 x^2 + b_2 x^4) \Psi = 0. \quad (3.2.1)$$

The original problem (3.0.1) in which $\hbar = 2m = 1$ is then recovered via a rescaling $x \rightarrow cx$ provided

$$E = -b_0 \frac{c^2}{\hbar^2}, \quad 1 = b_1 \frac{c^4}{\hbar^2}, \quad g = b_2 \frac{c^6}{\hbar^2}. \quad (3.2.2)$$

We substitute Ψ into the \hbar -dependent differential equation to generate relations between the a_n . The equivalent expressions to (3.0.7) are

$$b_0 = 2a_1 \hbar, \quad b_1 = 4a_1^2 + 12a_2 \hbar, \quad b_2 = 16a_1 a_2 + 30a_3 \hbar \quad (3.2.3)$$

and the new version of (3.0.8) is

$$2\hbar(n+1)(2n+1)a_{n+1} + \sum_{m=1}^n 4m(n-m+1)a_m a_{n-m+1} = 0. \quad (3.2.4)$$

The advantage of performing this rescaling is that we now have some freedom to choose a_1 and a_2 . We will restrict the choice, however, by requiring $\hbar \geq 0$, with both c and \hbar real. This will allow us to choose a_1 and a_2 up to a sign. We will choose $a_1 = -1/2$ and $a_2 = -1/8$. We show in chapter 4 that this is the appropriate sign

choice to ensure that the boundary condition (3.0.2) is satisfied. With these choices (3.2.3) simplifies to

$$b_0 = -\hbar, \quad b_1 = 1 - \frac{3}{2}\hbar, \quad b_2 = 1 + 30a_3\hbar. \quad (3.2.5)$$

Some particularly useful relations can be derived by eliminating c from (3.2.2)

$$E = -\frac{b_0}{\hbar\sqrt{b_1}}, \quad g = -\frac{E^3}{b_0^3}\hbar^4 b_2, \quad (3.2.6)$$

and then substituting in (3.2.5),

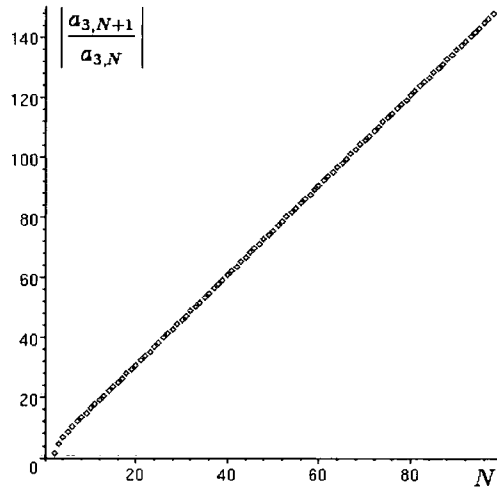
$$E = \frac{1}{\sqrt{1 - \frac{3}{2}\hbar}}, \quad g = \hbar(1 + 30a_3\hbar)E^3. \quad (3.2.7)$$

We now assume an expansion $a_n = \sum_{m=0}^{\infty} a_{n,m}\hbar^m$ for each $n \geq 3$. This is substituted into (3.2.4) and coefficients of \hbar^m compared for each n . We first compare coefficients of \hbar^0 to get the $a_{n,0}$, then the coefficients of \hbar^1 give the $a_{n,1}$ etc. At each stage previous results are substituted into the new equation. By continuing this process sufficiently many times we can find each a_n to any order required. A simple program can therefore be created to calculate b_2 (by using the \hbar expansion of a_3) as an expansion in \hbar . The first few orders are

$$b_2 = 1 + \frac{5}{8}\hbar - \frac{35}{32}\hbar^2 + \frac{2555}{512}\hbar^3 - \frac{69545}{2048}\hbar^4 + \frac{4849705}{16384}\hbar^5 - \frac{202337485}{65536}\hbar^6 + \dots \quad (3.2.8)$$

The expansion of b_2 in \hbar is an alternating sign series, so we plot the ratio of successive coefficients of \hbar^n in b_2 in such a way that we are dividing by the preceding term and removing the minus sign. We illustrate this in Figure 3.2 for the first 100 coefficients and note the approximate linear behaviour for large orders. This suggests that the asymptotic behaviour of the coefficients in b_2 has the form $(-1)^{n+1}k_1^n\Gamma(n+k_2)$ where k_1 and k_2 are real constants. Such asymptotic expansions have a zero radius of convergence as demonstrated via the alternating sign series test.

We shall therefore resum (3.2.5) for a particular $s_0 \equiv 1/\hbar$, from which E and g can be calculated. The c_n in $L_N(\lambda)$ now correspond to the coefficients of \hbar^n in the b_2 expansion. We note that $\hbar = 0$ corresponds to $g = 0$ and $E = 1$ whilst $\hbar \rightarrow 2/3$ corresponds to $g \rightarrow \infty$. We actually find that $\hbar \in [0, 2/3)$ corresponds to $g \in [0, \infty)$, which can be confirmed by the results of [1]. We therefore calculate some couplings

Figure 3.2: Ratio of coefficients of h^n in b_2

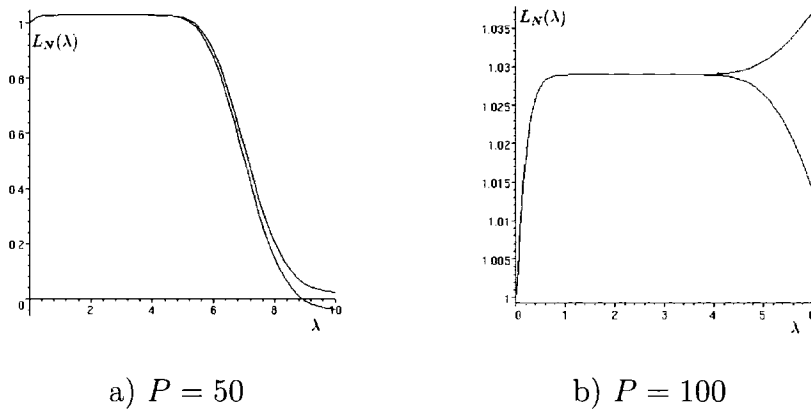
\hbar	α_M	λ_M	\mathbf{b}_2	\mathbf{g}_{est}	\mathbf{g}_{best}	Err ($10^{-4}\%$)
0.05	1.5190	3.5078	1.0289799	0.0578315	0.0578320	8.85
0.10	2.2473	8.4878	1.0546589	0.1345810	0.1345815	3.68
0.15	2.5696	11.0496	1.0780575	0.2370176	0.2370183	2.69
0.20	2.7754	12.7628	1.0997450	0.3755562	0.3755570	2.20
0.25	2.8514	13.2331	1.1200769	0.5667191	0.5667201	1.83
0.30	2.8555	13.0189	1.1392958	0.8379415	0.8379430	1.71
0.35	2.8557	12.8266	1.1575774	1.2375925	1.2375945	1.66
0.40	2.8557	12.6736	1.1750540	1.8579236	1.8579267	1.65
0.45	2.8557	12.5499	1.1918288	2.8946853	2.8946902	1.70
0.50	2.8557	12.4457	1.2079838	4.8319353	4.8319442	1.83
0.55	2.8557	12.3584	1.2235859	9.1926365	9.1926555	2.07
0.60	2.8557	12.2820	1.2386905	23.5024991	23.5025564	2.44
0.65	2.8557	12.2158	1.2533439	206.0979166	206.0985278	2.97

Table 3.2: Results of resummation in the semi-classical expansion

and energy eigenvalues within this range. The results, g_{est} , are given in Table 3.2 again compared to results, g_{best} (accurate to the stated number of significant Figures) generated from [1]. The energy eigenvalues produced are exact; however, it is the coupling that we are trying to approximate via the resummation process. We note that errors in the coupling are in the order of $10^{-4}\%$. Most importantly however, the error remains within this order of magnitude for the full spectrum of \hbar , in contrast to resummation in the coupling. We can attribute this success to the fact that $\hbar \in [0, 2/3)$ as opposed to $g \in [0, \infty)$ and that the resummation process is most effective for small \hbar or g . Also we encountered difficulties in resumming the coupling expansion for large g due to the singularity at the origin in the s plane. This problem has been removed in the semi-classical expansion.

For higher \hbar we expect the error to be greater since the contribution from singularities increases. It is interesting to note, however, that whilst this is true for the larger values of \hbar , the highest error is when $\hbar = 0.05$. We attribute this to an insufficiently large value of P . We plot $L_{30}(\lambda)$ and $L_{29}(\lambda)$ in Figure 3.3a with $P = 50$ and note the decaying behaviour of the curves. With $P = 100$, say, we recover the expected behaviour of a flattening curve followed by the divergence of the two curves. One curve increases whilst one decreases from the point of divergence, as illustrated in Figure 3.3b. This is because the expansion of $(s - s_0^{1/\alpha})^{-1}$ in powers of $s_0^{1/\alpha}/s$ is only valid for large s . Whilst this is a valid assumption given the contour of integration, the series does require more terms to achieve a suitable level of approximation when s_0 becomes larger, or equivalently \hbar becomes smaller. The error as a result of truncation in this expansion is systematic, hence the decaying nature of the curve for larger values of λ . This effect becomes more pronounced for larger α . It is possible that α becomes sufficiently large to cause this decaying behaviour before singularity contributions becomes significant. However, in this case the curve will still fail the monotonic condition. We resultingly take both a smaller α and a smaller λ and therefore get greater singularity contributions than if we had taken a larger P . Despite the improvement expected with larger P we are still able to extract good approximations with $P = 50$.

The case $\hbar \rightarrow 2/3$ is particularly interesting because this corresponds to the

Figure 3.3: Plot of $L_{30}(\lambda)$ and $L_{29}(\lambda)$ with $\hbar = 0.05$

infinite coupling limit. With $E_\infty = (3/b_2(2/3)/2)^{1/3}$ this limit corresponds to $E \rightarrow E_\infty g^{1/3}$. Using our resummation method we find $E_\infty = 1.0603632150$, compared to the value $E_\infty = 1.06036209$ which is exact to the stated number of significant figures. That is an error of $1.06 \times 10^{-4}\%$. Parisi [30] was also able to calculate this limit as $E_\infty = 1.06038$.

The method outlined so far for the ground state can be generalised to find the energy and wavefunctions of the excited states. We write the q th excited state $\Psi = P_q \Psi_0$ with energy $E = E_q + E_0$. Now consider

$$-\hbar^2 \frac{d^2 \Psi}{dx^2} + (b_0 + b_3 + b_1 x^2 + b_2 x^4) \Psi = 0 \quad (3.2.9)$$

which using (3.2.1) reduces to

$$-\hbar^2 \frac{d^2 P_q}{dx^2} - 2W' \hbar \frac{dP_q}{dx} + b_3 P_q = 0. \quad (3.2.10)$$

We scale $x \rightarrow cx$ to recover the AHO oscillator (3.0.1) provided that in addition to (3.2.7) we also have

$$E_q = -\frac{b_3 c^2}{\hbar^2} = -\frac{b_3}{\hbar} E_0 = -\frac{b_3}{\hbar \sqrt{1 - \frac{3}{2}\hbar}}. \quad (3.2.11)$$

We now need to find b_3 and U_q using (3.2.10), which is easily done using a similar approach to that described for the ground state. That is, expand

$$U = \sum_{n=0}^{\infty} \sum_{m=0}^{\infty} c_{n,m} \hbar^m x^n, \quad (3.2.12)$$

$$b_3 = \sum_{m=0}^{\infty} b_{3,m} \hbar^m, \quad (3.2.13)$$

and substitute into (3.2.10). By comparing coefficients of \hbar^k and x^n we get

$$-\sum_{i=0}^k b_{3,i} c_{n,k-i} + (n+2)(n+1)c_{n+2,k-2} + 4 \sum_{m=1}^{(n+1)/2} \sum_{i=0}^{k-1} m(n+2-2m)a_{m,i} c_{n+2-2m,k-i-1} = 0. \quad (3.2.14)$$

for $k > 1$. The $k = 0$ case reveals $b_{3,0} = 0$ or $c_{0,n} = 0$ for all n . Clearly the former is required. The $k = 1$ case is given by

$$-b_{3,1}c_{n,0} + 4\hbar \sum_{m=1}^{(n+1)/2} m(n+2-2m)a_{m,0}c_{n+2-2m,0} = 0. \quad (3.2.15)$$

We consider this equation for each n starting with $n = 0$ and find at each stage that $c_{n,0} = 0$ until we reach a point where

$$b_{3,1} = 4na_{1,0} = -2n. \quad (3.2.16)$$

Clearly $b_{3,1} = 0$ is required for the ground state, $q = 0$. Note also that a Taylor expansion of (3.2.11) would reveal $b_{3,1} = E_{q,0}$. This corresponds to the q th harmonic oscillator with energy eigenvalues $E = 2q + 1$ or $E_{q,0} = 2q$. So we have $c_{n,0} = 0$ for $n < q$ and $b_{3,1} = 2q$.

We can fix one of the x^n coefficients in U_q by a choice of normalisation and therefore set $c_{q,0} = 1$ with the remaining $c_{q,n} = 0$. Now consider the $k = 2$ case for each n then $k = 3$ etc. We see that at each stage (3.2.14) can be solved for $c_{n,k-1}$ provided $n \neq q$ or if $n = q$ we get $b_{3,k}$.

By solving a series of linear equations we have managed to determine b_3 and U_q and hence found the excited wavefunctions and energies up to any order required. We can then apply our resummation method to evaluate the series expansion.

One advantage of this method is that we can calculate the energy eigenvalues for an infinite coupling. We have already seen that this is given when $\hbar = 2/3$. By using (3.2.11) and (3.2.7) we can write

$$E_q = -\frac{b_3}{\hbar} \left(\frac{g}{\hbar b_2} \right)^{\frac{1}{3}}. \quad (3.2.17)$$

So in the infinite coupling limit, $\hbar \rightarrow 2/3$ we have $E_q = E_{q,\infty} g^{1/3}$ where

$$E_{q,\infty} = -\frac{3}{2} b_3 (2/3) E_{0,\infty}. \quad (3.2.18)$$

q	α_M	λ_M	b_3^{est}	b_3^{best}	Error (%)
1	3.3554	17.9902	-1.722251	-1.722249	0.0001
2	3.2057	15.4576	-4.020691	-4.020850	0.0040
3	3.1254	13.8688	-6.654020	-6.654572	0.0083
4	3.0734	12.7075	-9.555955	-9.557404	0.0152
5	3.0341	11.7759	-12.681877	-12.686239	0.0344
6	3.0046	11.0209	-16.000874	-16.012209	0.0708
7	2.9831	10.4064	-19.489826	-19.514237	0.1251
8	2.9675	9.8993	-23.130233	-23.176133	0.1980
9	2.9560	9.4721	-26.906049	-26.984993	0.2926
10	2.9473	9.1068	-30.803510	-30.930247	0.4098

Table 3.3: Infinite coupling values of b_3

Applying our resummation method we can calculate b_3 and hence $E_{q,\infty}$. A table listing the first ten approximations of b_3 , labeled b_3^{est} , is given in Table 3.3.

3.3 A Shifted Expansion

Let us momentarily remove α from $L(\lambda)$ by setting $\alpha = 1$. We were unable to directly evaluate $L(\lambda)$ even having replaced $f(s)$ with the truncated asymptotic expansion. This was due to the $s - s_0$ denominator in the integrand, which we expanded to give a sum of integrals of the form

$$\int_C ds \frac{e^{\lambda s}}{s^n} = \frac{\lambda^n}{\Gamma(n)} \quad (3.3.1)$$

which are more easily evaluated. Unfortunately the expansion of this denominator required summing over two variables in $L_N(\lambda)$. We truncated the expansion of the $(s - s_0)^{-1}$ term to a relatively high order to avoid complications arising from a truncated form of this expansion. This effectively meant we had to compute a series involving a sum of NP terms. With our chosen N and P this amounted to 1500 terms.

Instead we shall briefly investigate the possibility of shifting $s \rightarrow s + s_0$ in $L(\lambda)$

and then using the truncated expansion of $f(s)$ to approximate $L(\lambda)$. That is, we write

$$f(s + s_0) = \sum_{n=0}^{\infty} \frac{c_n}{(s + s_0)^n} = \sum_{n=0}^{\infty} \frac{\tilde{c}_n}{s^n} \quad (3.3.2)$$

by expanding the $(s + s_0)^{-n}$ terms in powers of s_0/s . Our new coefficients \tilde{c}_n would then be dependent on s_0 , so a separate expansion would be required for each s_0 we try to evaluate.

We then truncate the new expansion and substitute into $L(\lambda)$. Having done this we reinsert the parameter α with the substitution $s \rightarrow s^\alpha$.

$$L_N(\lambda) = \sum_{n=0}^N \tilde{c}_n \frac{\lambda^{\alpha n}}{\Gamma(\alpha n)}. \quad (3.3.3)$$

The advantage of this type of expansion is that we no longer need to worry about a double summation truncated to order N and P . This reduces the computational time to evaluate the series but also prevents the problems encountered in 3.2 as a result of truncation in P .

We should note, however, that the α parameter in the original L_N (3.0.5) is different to the α in (3.3.3). In the original formulation α caused singularities to be rotated about the origin. This is still the case in the new formulation; however, we now have a different origin since s has been shifted. It will depend on the location of singularities as to which method will allow a larger α and therefore better dampening of pole contributions.

We complete our resummation process by using the shifted \hbar expansion and present the results, g_{est} , in Table 3.4. We note that the errors are considerably larger than in the previous method. So whilst this method does have some advantages it is clearly less efficient for the semi-classical expansion. We attribute this to the different geometry involved when rotating poles by varying α . It is clear that in the shifted method we have smaller values of α_M and therefore λ_M , which results in less dampening of any pole contributions. Although this method is inferior for the expansion of b_2 we should note that, depending on the location of singularities it may prove to be better in other expansions and therefore should not be ignored.

We could question, however, whether it is fair to compare this method with $N = 30$ to the previous method, which effectively had $NP = 1500$ terms. In the shifted

\hbar	α_M	λ_M	\mathbf{b}_2	\mathbf{g}_{est}	\mathbf{g}_{best}	Err (%)
0.05	1.0000	0.5166	1.0289943	0.0578329	0.0578320	0.002
0.10	1.0040	0.5631	1.0545995	0.1345734	0.1345815	0.006
0.15	1.0627	0.7669	1.0791362	0.2372547	0.2370183	0.100
0.20	1.0971	0.9049	1.1021792	0.3763874	0.3755570	0.221
0.25	1.1303	1.0487	1.1244110	0.5689119	0.5667201	0.387
0.30	1.1569	1.1569	1.1457268	0.8426714	0.8379430	0.564
0.35	1.1832	1.3033	1.1665395	1.2471800	1.2375945	0.775
0.40	1.2060	1.4223	1.1866922	1.8763800	1.8579267	0.993
0.45	1.2264	1.5340	1.2062905	2.9298231	2.8946902	1.214
0.50	1.2435	1.6317	1.2252384	4.9010160	4.8319442	1.429
0.55	1.2625	1.7442	1.2441147	9.3469363	9.1926555	1.678
0.60	1.2777	1.8371	1.2622842	23.9503681	23.5025564	1.905
0.65	1.2941	1.9401	1.2803813	210.5377762	206.0985278	2.154

Table 3.4: Results of resummation in the shifted semi-classical expansion

example we could afford to take more terms given the reduced computational power required to perform the resummation. We note, however, that in some perturbative expansions calculating an expansion to higher orders can often be the limiting factor.

3.4 Error Estimates

There are two main sources of error in our prescription for evaluating $f(s_0)$. The first is due to $L_N(\lambda)$ only being an approximation to $L(\lambda)$. We require $L_N(\lambda)$ to differ from $L_{N-1}(\lambda)$ by no more than, say, σ percent. Therefore we can think of σ as being an error. Smaller σ requires evaluating $L(\lambda)$ for a smaller λ , which has the unwanted side effect of reducing the exponential dampening of any singularities of $f(s)$ in the left half plane. This is the second source of error. We shall outline a method for estimating the error in $L(\lambda)$ as a result of singularity contributions.

Consider a pole of $f(s)$ located at s_p . We will only be working with asymptotic expansions for which all coefficients, a_n are real. This implies that for a pole to exist at s_p we must necessarily have a pole at the conjugate location s_p^* . We shall for now assume that $f(s)$ has just one pair of poles in the left half s plane but is analytic on the remainder of the complex plane. The pair of conjugate poles gives a contribution to (3.0.4) of the form

$$c \cos(\lambda y_p + \nu) e^{\lambda(x_p - s_0^{1/\alpha})} \quad (3.4.1)$$

where $s_p^{1/\alpha}$ is split into real and imaginary parts $s_p^{1/\alpha} = x_p + iy_p$ and c, ν are real numbers. In the large λ limit this contribution approaches zero provided α is not taken so large as to rotate the poles into the right half plane. For a general α the correction (3.4.1) looks like an oscillating curve either growing or decreasing in amplitude. For $x_p > s_0^{1/\alpha}$ the oscillations are growing and for $x_p < s_0^{1/\alpha}$ the oscillations are being damped. We will use this to tune α until the oscillations are fixed in amplitude, say $\alpha = \alpha_T$, at which point $x_p = s_0^{1/\alpha}$. Having determined x_p we determine y_p by calculating the period of oscillations. This is best achieved by considering the λ derivative of $L_N(\lambda)$ and looking for zeros with $\alpha = \alpha_T$. The phase ν and amplitude c are then easily calculated by fixing the location of zeros in the

derivative of $L_N(\lambda)$ and also ensuring the correct amplitude of the sinusoidal curve.

Now with $\alpha = \alpha_T$ the pole contribution is

$$\frac{e^{\lambda y_p i}}{i y_p} \rho_T + cc = c \cos(\lambda y_p + \nu) \quad (3.4.2)$$

where ρ_T is the residue of $f(s^{\alpha_T})$ at s_p^{1/α_T} and cc denotes the complex conjugate. So we have determined ρ_T numerically in terms of the parameters c , y_p and ν .

We want to evaluate $L(\lambda)$ (or $L_N(\lambda)$) when $\alpha = \alpha_M$, the maximal value of α for which the curve is still monotonic. With this value of α the pole contribution is

$$\rho_M \frac{e^{\lambda(s_c - s_0^{1/\alpha_M})}}{s_c - s_0^{1/\alpha_M}} + cc \quad (3.4.3)$$

where

$$s_c \equiv \left(s_0^{1/\alpha_T} + i y_p \right)^{\alpha_T/\alpha_M} \quad (3.4.4)$$

and ρ_M is the residue of $f(s^{\alpha_M})$ at s_c . We can relate ρ_T and ρ_M via

$$\rho_T = \rho_M \frac{\alpha_M}{\alpha_T} \frac{s_c}{s_p^{1/\alpha_T}} \quad (3.4.5)$$

and therefore can calculate the pole contribution from (3.4.3). We think of σ as being the error in approximating $L(\lambda)$ with $L_N(\lambda)$ which in this case was chosen to be $\sigma = 10^{-3}\%$, and (3.4.3) as being the correction to $L(\lambda)$ as an approximation to $f(s_0)$ as a result of a pole pair contribution.

In general $f(s)$ will not have just one pair of poles but a number of poles and cuts. The contributions from these singularities will be exponentially weighted with singularities lying furthest to the right being most dominant. Due to this exponential weighting a cut contribution will look like a pole dominated by the right most end of the cut. We can therefore apply our procedure assuming the existence of just one pole pair and then interpret the correction (3.4.3) as being the dominant or leading order correction. We note, however, that the right-most end of a cut can actually change as it is rotated by increasing α . The left and right ends of a cut may actually switch if α becomes too large. In this case the error estimate may not be the most dominant but will be a more minor correction.

In order to apply our technique we will require sufficient terms to ensure at least two peaks or troughs for $\alpha = \alpha_T$. These must exist within a region where $L_N(\lambda)$

g_{best}	α_T	g_{corr}	Resum Err	Corrected Err	Relative Err
0.057832	1.0000	0.057833	0.00165	0.00002	90
0.134581	1.0040	0.134613	0.00600	0.00023	26
0.237018	1.0627	0.237378	0.09976	0.00152	66
0.375557	1.0971	0.376543	0.22112	0.00263	84
0.566720	1.1303	0.568924	0.38674	0.00389	99
0.837943	1.1569	0.842246	0.56430	0.00514	110
1.237595	1.1832	1.243168	0.77452	0.00450	172
1.857927	1.2060	1.866679	0.99322	0.00471	211
2.894690	1.2264	2.908286	1.21370	0.00470	258
4.831944	1.2435	4.864863	1.42948	0.00681	210
9.192656	1.2625	9.237419	1.67830	0.00487	345
23.502556	1.2777	23.666373	1.90537	0.00697	273
206.098528	1.2941	207.519940	2.15394	0.00690	312

Table 3.5: Corrected couplings due to dominant singularity contributions

is a good approximation to $L(\lambda)$. Clearly $N = 30$ in the Bender-Wu expansion is insufficient for large couplings, as $L_N(\lambda)$ did not approximate $L(\lambda)$ sufficiently well. We also note that with the semi-classical expansion, the errors are of the order $10^{-4}\%$. So in this case the dominant error is provided by σ . In fact the exact values lie between L_{30} and L_{29} in this expansion, so σ is actually an error bound. It would, however, be pointless to calculate the error correction due to singularities without first reducing σ (or N). We will instead apply this technique to the shifted semi-classical expansion (section 3.3). In this technique we found the actual error to be much greater than σ .

We subtract the dominant singularity correction and list the results (g_{corr}) in Table 3.5. The percentage errors after resummation, and percentage errors having subtracted the dominant singularity contribution, are listed. The relative error is the ratio of these two errors and indicates that the percentage error has improved by a factor of between 90 and 312. We expect the error as a result of singularities is greater for larger \hbar , and this is reflected in these increasing corrections for higher \hbar .

3.5 Summary

The concept of direct resummation to approximate a divergent asymptotic expansion is important despite the existence of more accurate techniques for calculating anharmonic oscillator energy eigenvalues. We produce a particularly efficient method for finding such energy eigenvalues in the next chapter. It will not always be possible to apply this technique to other physical problems such as calculating the S matrix in later chapters. Hence the need for this resummation method.

We have shown that the modified Borel summation technique can produce reasonably accurate results from perturbative expansions that are divergent. This is achieved with a relatively modest number of terms. We have improved the accuracy of the procedure and investigated some of the major sources of error. Subtracting these leading order corrections also resulted in better approximations.

Chapter 4

Tuning the Boundary Condition

In this chapter we will outline a method of constructing solutions to the Schrödinger equation for an anharmonic oscillator of the form

$$-\frac{d^2\Psi}{dx^2} + \rho x^2\Psi + gx^{2M}\Psi = E\Psi \quad (4.0.1)$$

$$\lim_{|x|\rightarrow\infty} \Psi = 0 \quad (4.0.2)$$

where x is real and units are defined such that Planck's constant and the mass are set to unity, $\hbar = 2m = 1$. We do this initially by constructing a solution to the differential equation (4.0.1) in terms of one free parameter for a given ρ and g . We then vary this parameter until we observe the correct large x behaviour determined by the boundary condition (4.0.2) using a contour integral method of resummation. We find the energy eigenvalues with an arbitrary level of accuracy. The process is easily automated to produce very high levels of precision even with modest computing power.

In section 4.1 we will outline the basic method for the ground state of the quartic oscillator, $M = 2$. In section 4.2 we will extend the method to produce excited wavefunctions and energy eigenvalues. Finally in section 4.3 we will show how this method can be extended to general anharmonic oscillators with an x^{2M} potential as in (4.0.1). Having set up the basic method we offer a more detailed investigation in section 4.4 as to why this technique works so well.

4.1 Tuning for Large x

In this section we will find the ground-state wavefunction and energy eigenvalues corresponding to the quartic anharmonic oscillator obtained from (4.0.1) by setting $M = 2$. Since the ground state has no nodes we will construct the wavefunction in the form $\Psi = \exp(W)$. We will make an even-powered x expansion $W = \sum_{n=1}^{\infty} a_n x^{2n}$ since both the potential term and boundary condition are even. The coefficients a_n are then determined in terms of the parameters ρ , g and E via (4.0.1). Having chosen two of these parameters, the third must be determined by ensuring the correct boundary condition (4.0.2), which implies that $W \sim -\sqrt{g}x^3/3$ for large positive real x . Since our expansion for W in positive powers of x is only valid for small x we shall resum by analytically continuing x into the complex $s \equiv 1/x$ plane and using Cauchy's theorem to examine the large x behaviour. We define

$$L(\lambda) = \frac{1}{2\pi i} \frac{1}{\lambda^3} \int_C ds \frac{e^{\lambda s}}{s} W(s). \quad (4.1.1)$$

where C is a large circular contour about the origin in the complex s plane. The large x asymptotic behaviour implied by the differential equation requires $W(s)$ to have a third order pole at the origin. This contributes a term $-\sqrt{g}/18$ to $L(\lambda)$ by Cauchy's theorem. When the boundary condition is satisfied we find that any remaining singularities of $W(s)$ lie to the left of the imaginary axis. The contribution from these is exponentially suppressed in $L(\lambda)$ so that in the large λ limit only the singular contribution at the origin remains, $\lim_{\lambda \rightarrow \infty} L(\lambda) = -\sqrt{g}/18$. In reality (4.1.1) is not calculated exactly but by truncating W at some order x^{2N} . Thus

$$L_N(\lambda) \equiv \frac{1}{2\pi i} \frac{1}{\lambda^3} \int_C ds \frac{e^{\lambda s}}{s} \sum_{n=1}^N \frac{a_n}{s^{2n}} = \sum_{n=1}^N a_n \frac{\lambda^{2n-3}}{\Gamma(2n+1)} \approx L(\lambda) \quad (4.1.2)$$

where in the evaluation of the contour integral we used the identity

$$\int_C ds s^{-n} \exp(\lambda s) = 2\pi i \lambda^n / \Gamma(n) \quad (4.1.3)$$

for $n < 0$ [25].

We proceed by finding our x expansion in W and looking for the correct behaviour in $L_N(\lambda)$. We will consider solutions with a fixed coupling $g = 1$, without

loss of generality, and look at the relationship between E and ρ . We do this without loss of generality since our parameters are related by scaling properties of the Hamiltonian, as first noted by Symanzik and discussed in [20]. To help us we will scale $x \rightarrow cx$ ($c \in \mathbb{R}$) in the differential equation (4.0.1) in such a way that we are free to place a restriction on our expansion for W . We can choose $k \equiv a_1/a_2$ at least up to a sign, say $k = \pm 4$. Now substituting W into our scaled differential equation and comparing coefficients of x^{2n}

$$Ec^2 = -2a_1 \quad (4.1.4)$$

$$\rho c^4 = 4a_1^2 + 12a_2 \quad (4.1.5)$$

$$c^6 = 16a_1a_2 + 30a_3. \quad (4.1.6)$$

We eliminate c to find expressions for E and ρ in terms of a_2 and a_3

$$E = \frac{-2ka_2}{(16ka_2^2 + 30a_3)^{\frac{1}{3}}} \quad (4.1.7)$$

$$\rho = \frac{4k^2a_2^2 + 12a_2}{(16ka_2^2 + 30a_3)^{\frac{2}{3}}}, \quad (4.1.8)$$

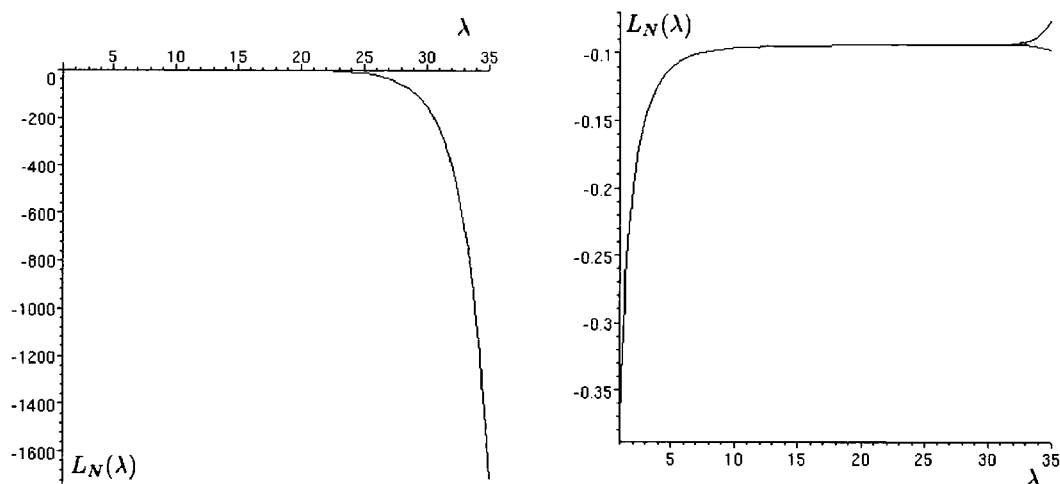
whilst for $n \geq 3$ we have

$$a_{n+1} = - \left(\sum_{m=1}^n 4m(n-m+1)a_m a_{n-m+1} \right) / (2(n+1)(2n+1)), \quad (4.1.9)$$

giving a_{n+1} in terms of a_2 and a_3 .

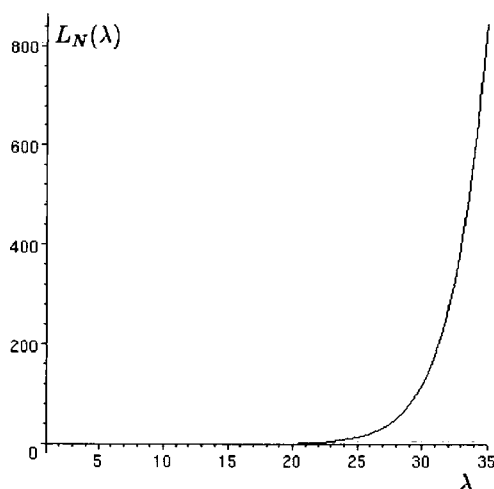
Our goal is now to determine a_3 for a given a_2 in such a way that the boundary condition is satisfied. We do this by tuning a_3 until the correct large λ behaviour is observed in $L_N(\lambda)$. To illustrate the process we shall choose positive k , $k = 4$ and $a_2 = -3/16$. With this sign choice and a_2 we get a zero ρ term. This is a useful case to consider because it is easily compared with existing literature, but is also interesting because it corresponds to the strong coupling problem via Symanzik scaling of the Hamiltonian. We choose a fairly modest N initially, guess a value of a_3 then plot $L_N(\lambda)$ and $L_{N-1}(\lambda)$. L_N and L_{N-1} only provide a good approximation to $L(\lambda)$ for values of λ up to the point where they appreciably diverge from each other. Therefore we restrict our consideration of λ to within this range.

With a_3 too small we encounter a curve rapidly decreasing such as in figure 4.1a. With a_3 too large we encounter a curve rapidly increasing as in figure 4.1c. An



a) $a_3 = 0.015$ - too small

b) $a_3 = 0.0193604$ - optimal



c) $a_3 = 0.025$ - too big

Figure 4.1: $L_N(\lambda)$ with $N = 19, 20$ for $a_2 = -3/16$

optimal value of a_3 will give a curve flattening as we increase λ as in 4.1b. We tune a_3 until we achieve this. As a_3 gets closer to its correct value the exponential behaviour in figures 4.1a and 4.1c becomes less pronounced within our range of acceptable λ and flatness becomes a less well defined concept. This determines our level of accuracy for determining a_3 . To improve our accuracy we must increase N in order to consider larger λ . As we consider these larger λ we again encounter the exponentially increasing / decreasing behaviour, which enables us to further tune a_3 to a greater accuracy.

We completed this procedure in this zero- ρ case and determined a_3 to 6 significant figures with $N = 20$. With $N = 100$ we tune a_3 to 30 significant figures and with $N = 300$ we get

$$a_3 = 0.01936043720245950419201997531721233596425589581549397570027615152, \quad (4.1.10)$$

to 65 significant figures and we find $L(\lambda) \approx -0.0934774$, which is remarkably close to the predicted value of -0.0934723 . This calculated figure of a_3 is accurate to the stated number of digits, i.e. 65 significant figures and in agreement with existing literature [12] [13] [14] [15] at least up to the 10-16 significant figures they quote. With a_3 determined we calculate the ground state energy via (4.1.7)

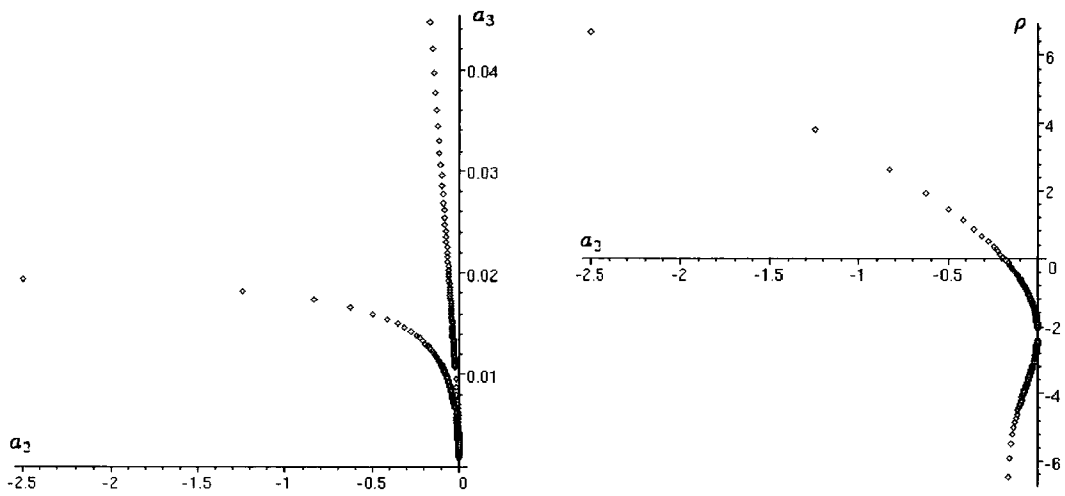
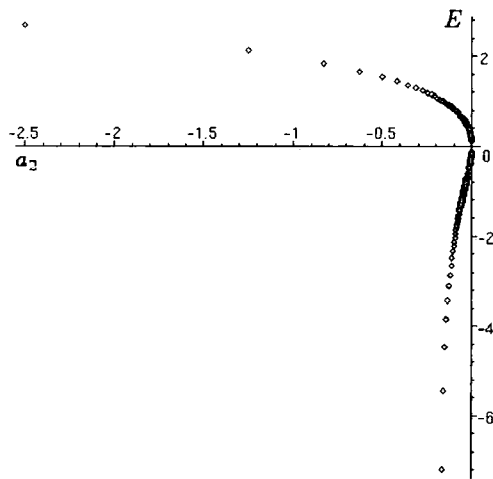
$$E_0 = 1.0603620904841828996470460166926635455152087285289779332162452417 \quad (4.1.11)$$

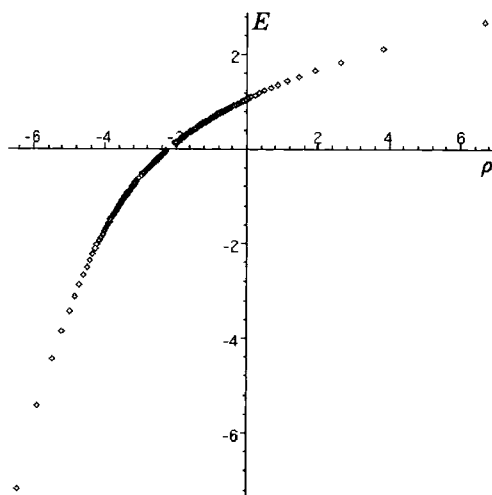
again quoted accurately up to 65 significant figures.

Calculating large numbers of terms is easy, even with modest computing power, given the linear nature of the calculations. The tuning process is easily automated.

We repeat this for various a_2 and plot the results in figures 4.1 and 4.3. The two branches correspond to differing sign choices of k . With $k = +4$ we found solutions corresponding to positive energy. The solutions have a positive ρ term for $a_2 < -3/16$ and a negative term for $-3/16 < a_2 \leq 0$. With $k = -4$ and $0 > a_2 > -3/16$ we found negative energy eigenvalues corresponding to $\rho < 0$.

We also verify that non-zero ρ terms correspond to the literature by for example calculating the $\rho = -1$, $g = 1$ energy eigenvalue. In doing so we must tune a_2 with $k = +4$ to obtain the correct ρ term. We found that $a_2 = 0.004048768355681543705$ approximated $\rho = -1$ with an error in the order of 10^{-16} . This value of a_2 is within $\pm 5^{-21}$ of the correct a_2 required to evaluate ρ exactly. The energy eigenvalue produced from this approximate value of a_2 gave us the same eigenvalue as stated in previous literature to within the 16 significant figures available for comparison. This is an example of an eigenvalue where instanton effects would normally dominate and perturbative techniques in \hbar or g would fail.

a) a_3 as a function of a_2 b) ρ as a function of a_2 c) E as a function of a_2 Figure 4.2: ρ , E and a_3 as functions of a_2 .

Figure 4.3: E as a function of ρ

We now explain why this method of tuning is so sensitive. With $M = 2$ the differential equation (4.0.1) without the boundary condition (4.0.2) in general has an asymptotic large positive x solution of the form

$$\Psi_l = \exp\left(-\frac{\sqrt{g}}{3}x^3\right) + A \exp\left(\frac{\sqrt{g}}{3}x^3\right). \quad (4.1.12)$$

For $A < 0$, Ψ_l has zeros along the real x axis; however, for $A > 0$, Ψ_l has zeros in the complex x plane off the real axis. Our boundary condition (4.0.2) requires us to take $A = 0$, in which case Ψ_l has no zeros. We note that for $A \neq 0$, $\log \Psi_l$ will have a pole (possibly part of a cut). Such a pole contribution in the right-half x plane would spoil our resummation of the large x behaviour. In section 4.4 we numerically determine the location of zeros in our wavefunctions for varying a_3 and show that they numerically approximate the location of the zeros in our asymptotic large x solution for varying A . Thus varying a_3 corresponds to varying A in (4.1.12). The presence of these poles is responsible for the rapidly increasing/decreasing behaviour for values of a_3 on either side of the correct one due to the exponential factor in (4.1.1). It is this behaviour that allows us to select the correct value of a_3 to any specified level of accuracy.

4.2 Excited States

We now construct the excited states and energy eigenvalues of the quartic anharmonic oscillator. Firstly we write the q th excited state as $\Psi_q = P_q \Psi_0$, where the energy is $E = E_q + E_0$, and Ψ_0 is the ground state obtained in the previous section. For q odd P_q is odd and for q even P_q is even. We therefore expand $P = \sum_{n=0}^{\infty} c_n x^n$ and sum only over even or odd values of n as appropriate. We set either c_0 or c_1 to unity as a choice of normalisation. The remaining c_n and E_q are then solved for using a recurrence relation in terms of either c_2 or c_3 . This is easily obtained from our new differential equation, which comes from substituting Ψ_q into (4.0.1) to obtain

$$\frac{d^2 P}{dx^2} + 2 \frac{dW}{dx} \frac{dP_q}{dx} + E_q P_q = 0. \quad (4.2.1)$$

This differential equation has two types of large x solution. Either

$$P \sim \exp\left(-\frac{E_q}{2\sqrt{g}x}\right) \quad \text{or} \quad P \sim \exp(2\sqrt{g}x^3). \quad (4.2.2)$$

For the correct boundary condition (4.0.2) we must choose the first type of solution.

We therefore construct

$$T_N(\lambda) \equiv \frac{1}{2\pi i} \int_C ds \frac{e^{\lambda s}}{s} \sum_{n=0}^N \frac{c_n}{s^{2n\alpha}} = \sum_{n=0}^N c_n \frac{\lambda^{2n\alpha}}{\Gamma(2n\alpha + 1)} \quad (4.2.3)$$

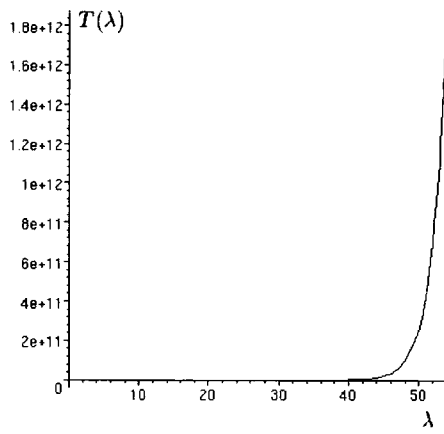
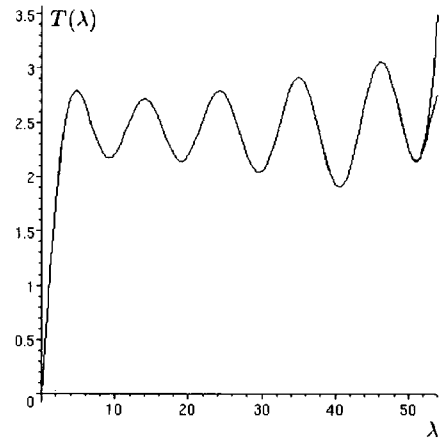
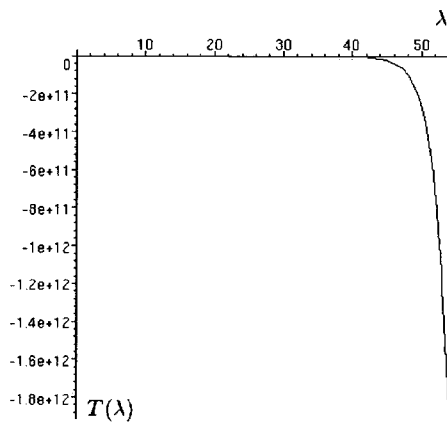
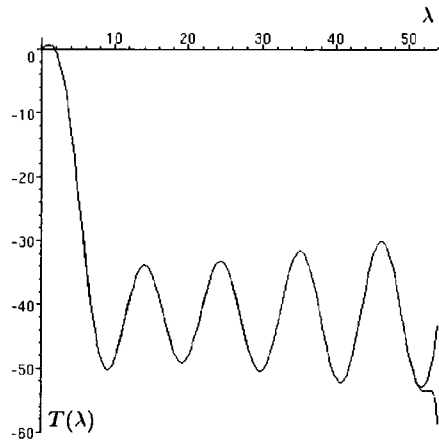
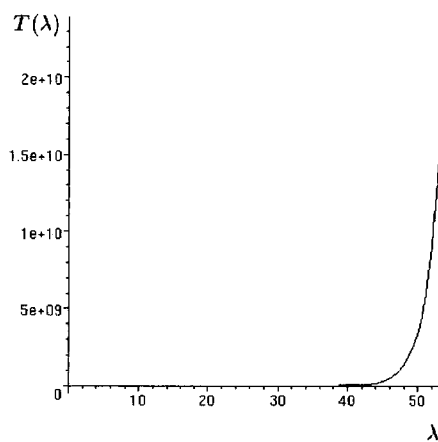
and look for a flat curve as we tune c_2 or c_3 . We have introduced an additional parameter α by substituting $s \rightarrow s^\alpha$ in $P(s)$ since we find that $P(s)$ has a more limited region of analyticity than $W(s)$ when the boundary condition is satisfied. Here we only assume that $P(s)$ is analytic in some wedge shaped region radiating from the origin and containing the real axis. Singularities outside of this region of analyticity are observed in $T_N(\lambda)$ in the form of oscillations. They can, however, be rotated in the complex s plane so that they lie to the left of the imaginary axis by reducing the parameter $\alpha < 1$. Having done this the singularities become exponentially suppressed.

We illustrate the process in the zero ρ case for the odd eigenfunctions. There will be multiple values of $\tau \equiv -c_3$ that correspond to different levels of odd excitation. Let us label these τ_n in such a way that $\tau_{n+1} > \tau_n$. With $\tau < \tau_1$ we obtain a rapidly increasing curve; however, with $\tau_1 < \tau < \tau_2$ we get a rapidly decreasing curve (figure

4.4). We follow our tuning procedure in the same manner as for the ground state; however, this time we do not encounter a flat curve but oscillations. These result from a pole or cut outside of our region of analyticity. We could, however, take a smaller α to recover a flat curve and proceed with our tuning procedure. For $\tau = \tau_1$ we found $\alpha = 0.6$ sufficient to achieve this.

We can produce the full spectrum of eigenvalues by continuing to vary τ . We find that as τ passes through a value τ_n we switch from the rapidly growing to rapidly decreasing behaviour. With $\tau_3 > \tau > \tau_2$ for example we switch back to the rapidly increasing curve. This alternating behaviour continues with higher excitations, as illustrated in figure 4.4. Exactly the same procedure works for even excitations but we vary c_2 instead of c_3 . Having found an eigenstate through this method we cannot immediately tell which energy level it corresponds to. To do this we could plot the prefactor using a similar contour integral method of resummation. We then count the number of nodes. We did this for some of the lower excitations. We calculated excited states up to $q = 39$ with $g = 1$ and again found exact agreement to the quoted level of accuracy in previous literature [12] [13] [14] [15]. We give some of these eigenvalues in the appendix.

Whilst we cannot attribute the rapidly increasing / decreasing behaviour of $T_N(\lambda)$ to zeros in P_q we believe that a similar effect is encountered this time due to the large x behaviour. There were two types of large x behaviour (4.2.2) that we were able to derive from the differential equation (4.2.1). We chose the first in order to satisfy our boundary condition (4.0.2). When c_2 or c_3 do not correspond to an energy eigenstate we believe that we are obtaining the second type of solution. We note that such large x behaviour would give an additional pole contribution to $T(\lambda)$. Again our resummation is conveniently spoiled. In section 4.4 we numerically verify this result by plotting P for large real values of x for a range of c_3 by exploiting Cauchy's theorem.

a) $\tau = 0.1$ b) $\tau \approx \tau_1 \approx 0.14584$ c) $\tau = 0.2$ d) $\tau \approx \tau_2 \approx 1.99546$  $\tau = 2$ Figure 4.4: $T(\lambda)$ with an odd prefactor

4.3 Other Potentials

In this section we consider other values of M in 4.0.1. The large positive x behaviour is now $W \sim -\sqrt{g}x^{M+1}/(M+1)$. We should therefore redefine our $L_N(\lambda)$ for a general x^{2M} potential

$$L_N^M(\lambda) \equiv \frac{1}{2\pi i} \frac{1}{\lambda^{(M+1)\alpha}} \int_C ds \frac{e^{\lambda s}}{s} \sum_{n=1}^N \frac{a_n}{s^{2n\alpha}} = \sum_{n=1}^N a_n \frac{\lambda^{(2n-M-1)\alpha}}{\Gamma(2n\alpha+1)}. \quad (4.3.1)$$

where again we introduce the parameter α , since for $M > 2$ we find that $W(s)$ is analytic within a more limited region. Our prescription of reducing $\alpha < 1$ will therefore be required to rotate these singularities to the left of the imaginary axis where they become exponentially suppressed.

Our a_n are again determined via the differential equation in the same manner as before. We apply the rescaling $x \rightarrow cx$ so that we can fix $a_1/a_2 = \pm 4$ as before. We pick a value of a_2 and use (4.1.9) to solve for all of the coefficients in terms of a_{n+1} . This relation now holds for $n \geq 2$ but not $n = M$. In its place we have

$$c^6 g = 2(M+1)(2M+1)a_{M+1} + \sum_{n=1}^M 4n(M-n+1)a_M a_{n-M+1} \quad (4.3.2)$$

which is then substituted into (4.1.4) and (4.1.5) to give E and ρ .

Our procedure is now the same as for the $M = 2$ case. We do find, however, that for increasing M the region of analyticity becomes smaller and therefore an increasingly small α is required. We performed this procedure with M ranging from 2 to 50 for $g = 1$ and found results matching those in [13] for $M = 2, 3, 4$. Having determined the ground state we have applied the technique outlined in section 4.2 to obtain some excited energy eigenvalues. Again these are in complete agreement with [13].

4.4 Numerical Investigation and Explanation

In this section we numerically investigate the behaviour of solutions to the quartic anharmonic oscillator differential equation. We show how the location of zeros in Ψ vary depending on the choice of a_3 and how the large- x behaviour of U in the

excited states is dependent on c_2 or c_3 . Whilst our evidence is numerical and by no means rigorous this does offer a good explanation as to why this tuning technique works so well.

4.4.1 The Ground State - Zeros, Poles and Cuts

If we solve the differential equation (3.0.1) for its large positive x behaviour without the boundary condition (3.0.2) we find two asymptotic solutions, $W = \pm\sqrt{g}x^3/3$. The general large- x solution to (3.0.1) is therefore of the form

$$\Psi_l = \exp\left(-\frac{\sqrt{g}}{3}x^3\right) + A \exp\left(\frac{\sqrt{g}}{3}x^3\right). \quad (4.4.1)$$

The boundary condition (3.0.2), however, requires us to take $A = 0$. Ψ_l in general has zeros at specific points in the complex x plane depending on A . The only exception to this is when $A = 0$, at which point we only asymptotically approach zero as $x \rightarrow \infty$. For $A < 0$ these zeros lie along the real axis whereas for $A > 0$ they lie off the real axis, somewhere in the complex x plane. There will also be contours in the complex x plane along which Ψ_l is purely real and negative. The zeros and negative regions in Ψ_l will be manifested as cuts and poles in $\log \Psi_l$.

It is clear that any pole or cut in the right half complex x plane would result in an exponentially increasing or decreasing $L_N(\lambda)$. Oscillations will occur due to a pole lying off the real axis; however, we took modest N to ensure we only see the beginning of the oscillation and hence the appearance of a rapidly increasing or decreasing curve. We hypothesised in [1] that it is the pole contributions that are being observed in $L_N(\lambda)$. In this section we present numerical evidence to support the hypothesis. We are essentially tuning the solution until $A = 0$. For $A \neq 0$ the resummation is conveniently spoiled in such a way that we are able to refine the solution. In this section we will employ Cauchy's theorem to determine the location of zeros in the solutions to the differential equation as constructed in the previous section. We will then be able to observe the dependence of these zeros on a_3 . Whilst we have so far only presented an argument based on the large- x behaviour of Ψ we will find that the location of zeros in Ψ_l do indeed correspond approximately to the location of zeros in the full solution.

We note that since the coefficients a_n in W (and a Taylor-expanded W_l) are all real, any cut or pole in the upper half s plane should necessarily be mirrored in the lower s plane. Let us momentarily assume that in the right-half s plane $W(s)$ only contains poles located at s_p and s_p^* . We then construct

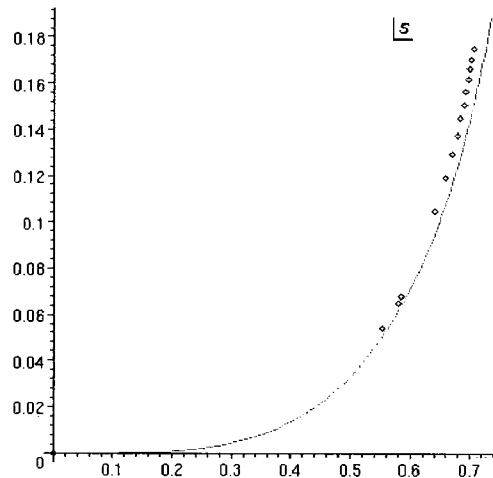
$$S(\lambda) = \frac{1}{2\pi i} \int_C ds \frac{e^{\lambda(s-s_0)}}{s-s_0} W(s) \quad (4.4.2)$$

$$\sim W(s_0) + c \cos(\lambda s_p^{\Im} + \nu) e^{\lambda(s_p^{\Re} - s_0)} \quad (4.4.3)$$

where c, ν are real numbers and s_p is split into real and imaginary parts, $s_p^{\Re} + i s_p^{\Im}$. If we had included a cut contribution instead of a pole then we would expect contributions from the whole cut with each portion of the cut weighted by the exponential factor. In Ψ_l the zero lies on the right end of a region of negativity corresponding to a potential cut in W_l and therefore is the dominant singularity contribution in our contour integral if $W = W_l$. So whilst $W(s)$ does not necessarily have just one pole in the positive right quadrant we will model the cuts by a pole representing a weighted average. Since the zero is the dominant contributor we will find that $S(\lambda)$ at least in the case of W_l allows us to reasonably approximate the location of our zero. We will apply this model to our original Ψ and predict zeros close to the zeros of Ψ_l . As usual we use the truncated expansion of W to approximate $S(\lambda)$ by $S_N(\lambda)$.

With the above construction we are in a position to numerically determine the location of the conjugate poles. Initially we will assume that $s_p^{\Im} \neq 0$ and plot $S_N(\lambda)$ for a given s_0 . We expect to see oscillations in the curve either growing ($s_p^{\Re} > s_0$), decaying ($s_p^{\Re} < s_0$) or fixed in amplitude. We tune s_0 until we achieve the latter, at which point we have $s_p^{\Re} = s_0$. With this s_0 we can determine the frequency of the oscillations in $S_N(\lambda)$, this gives us s_p^{\Im} .

If we do not observe the oscillatory behaviour in $S_N(\lambda)$ even with N, P sufficiently large then it may be that $s_p^{\Im} = 0$. If this is the case then we use $S_N(\lambda)$ to approximate $W(s_0)$ for $s_0 > s_p$. As s_0 becomes closer to s_p , however, the effect of our pole becomes more significant since the exponential dampening factor becomes reduced. We must therefore take larger λ , which in return requires larger N . Alternatively we can try increasing $\alpha > 1$. This causes the final term in S_N to be reduced

Figure 4.5: Location of zeros of $\Psi(s)$

in comparison to the penultimate term due to the Γ function. This again allows a larger λ and hence greater exponential dampening. Ultimately, though, we are unable to extract $W(s_0)$ from $S_N(\lambda)$ for $s_0 \leq s_p$, and indeed the process becomes more difficult as s_0 approaches s_p . We can, however, determine s_p by approximating Ψ to a linear behaviour in this region. We justify this by solving the differential equation in a region where W' and W'' are more dominant than any potential term. Numerically this linear behaviour appears to work well, at least within the region that we were realistically able to plot.

For a_3 too small we find that the zeros lie along the real s axis with zeros approaching $s = 0$ (i.e. $x = \infty$) and indeed attaining this value as a_3 becomes appropriate for the correct boundary condition to be satisfied. For a_3 too large we find that the location of zeros lie off the real axis and into the complex plane. They appear to lie on some contour which approaches $s = 0$ as a_3 approaches its correct value. We plot the location of some of these complex zeros of Ψ in figure 4.5¹. We have restricted this plot to one quadrant only; however, the plot would necessarily be mirrored into all four quadrants. The solid line represents the location of zeros of Ψ_l , (4.4.1), as constructed at the beginning of this section with A considered a

¹We have actually scaled the complex plane so that $s^3 \rightarrow \sqrt{16a_1a_2 + 30a_3}s^3/3$ for simplicity of calculation in figure 4.5

variable parameter.

We note that the two sets of zeros are not in exact agreement, although there does appear to be a correlation. We attribute the differences largely due to Ψ_t being a small- s approximation and we therefore expect the approximation to improve as $|s| \rightarrow 0$ which appears to be happening in the plot. Unfortunately it becomes increasingly difficult to numerically calculate zeros of Ψ as we get closer to the origin since the period of oscillation becomes very large. In order to measure this period we need to be able to plot at least the first few oscillations. This requires an increasingly large λ , which in turn increasingly requires a large number of terms.

We also question how accurately our numerical technique can accurately determine the location of zeros. As an example we calculate analytically the location of the zeros in $\Psi_t = \exp(x^3) + \exp(-x^3)$. Applying the resummation process to $\log(\Psi_t)$ expanded in positive powers of x we are able to numerically calculate the location of the zero. We find analytically that a zero exists at $s = 0.745 + 0.43i$, whereas numerically we find it exists at $s = 0.738 + 0.429i$. Given the scale of the plot this error is relatively insignificant.

4.4.2 Excited States - Large x behaviour

We substitute $\Psi_q = P_q \Psi_0$ into the differential equation (3.0.1) to produce a new differential equation satisfied by P_q ,

$$\frac{d^2 P}{dx^2} + 2 \frac{dW}{dx} \frac{dP_q}{dx} + E_q P_q = 0. \quad (4.4.4)$$

Taking $W \sim -\sqrt{g}x^3/3$, this differential equation exhibits two types of large x asymptotic solution

$$P \sim \exp\left(-\frac{E_q}{2\sqrt{g}x}\right) \quad \text{or} \quad P \sim \exp\left(\frac{2\sqrt{g}x^3}{3}\right). \quad (4.4.5)$$

We necessarily choose the first of these to ensure the boundary condition (3.0.2) is satisfied. When the boundary condition is satisfied $U_N(\lambda)$ produces a flat curve (having adjusted α appropriately), which would be expected if we have correctly chosen the large asymptotic behaviour. If the second type of asymptotic behaviour is chosen then we would expect to observe a correction to $T_N(\lambda)$ due to a singularity

at $s = 0$. We hypothesised in [1] that when c_2 or c_3 does not correspond to an energy eigenstate then we are observing the second type of asymptotic large x behaviour.

Using the resummation technique already outlined, the prefactors corresponding to different levels of excitation may be plotted. The prefactors corresponding to the 1st, 2nd and 3rd excited states are shown in figure 4.6 both on a large and small x scale. Since these functions are either odd or even we restrict the domain to $x \geq 0$. As would be expected, the prefactor corresponding to the first excited state has one zero located at the origin. The 2nd excited state has two zeros and the 3rd excited state has 3 zeros when considered along the whole of the real axis. The tuning procedure did not provide a method for determining which level of excitation we have, just that we had determined an energy eigenstate. Using our resummation method to plot the prefactor we are able to confirm which energy eigenstate has been found by counting the number of nodes. The technique in section 3.2 provides an alternative method. We could use resummation in a \hbar expansion to approximate c_2 or c_3 and then use the tuning method to determine the value more accurately.

We note that for large x these prefactors asymptotically approach some constant value, as predicted. For example the prefactor corresponding to some energies either side of the first excited state energy level are shown in figure 4.7. For $\tau_1 < \tau < \tau_2$ we see that P quickly becomes very large. This is similarly true for $\tau < \tau_1$; however, this time P becomes large in the negative direction. This appears not to be the result of a pole or cut, otherwise for large x the resummation technique would exhibit singularity contributions. Instead we find that the prefactor is simply resumming to large values and these values are increasing in size rapidly. We test the hypothesis that we are observing prefactors with large- x behaviour determined by the second type of asymptotic behaviour in (4.4.5) by plotting

$$Q \equiv \log |P| - \frac{2}{3}\sqrt{g}x^3. \quad (4.4.6)$$

If the hypothesis is correct then we expect Q to approach a constant for large x . We plot these graphs for those same values of c_1 as before and display them in figure 4.8. As predicted, these plots do flatten out for large x , at least on the scale of $\exp(x^3)$. This numerically supports our hypothesis.

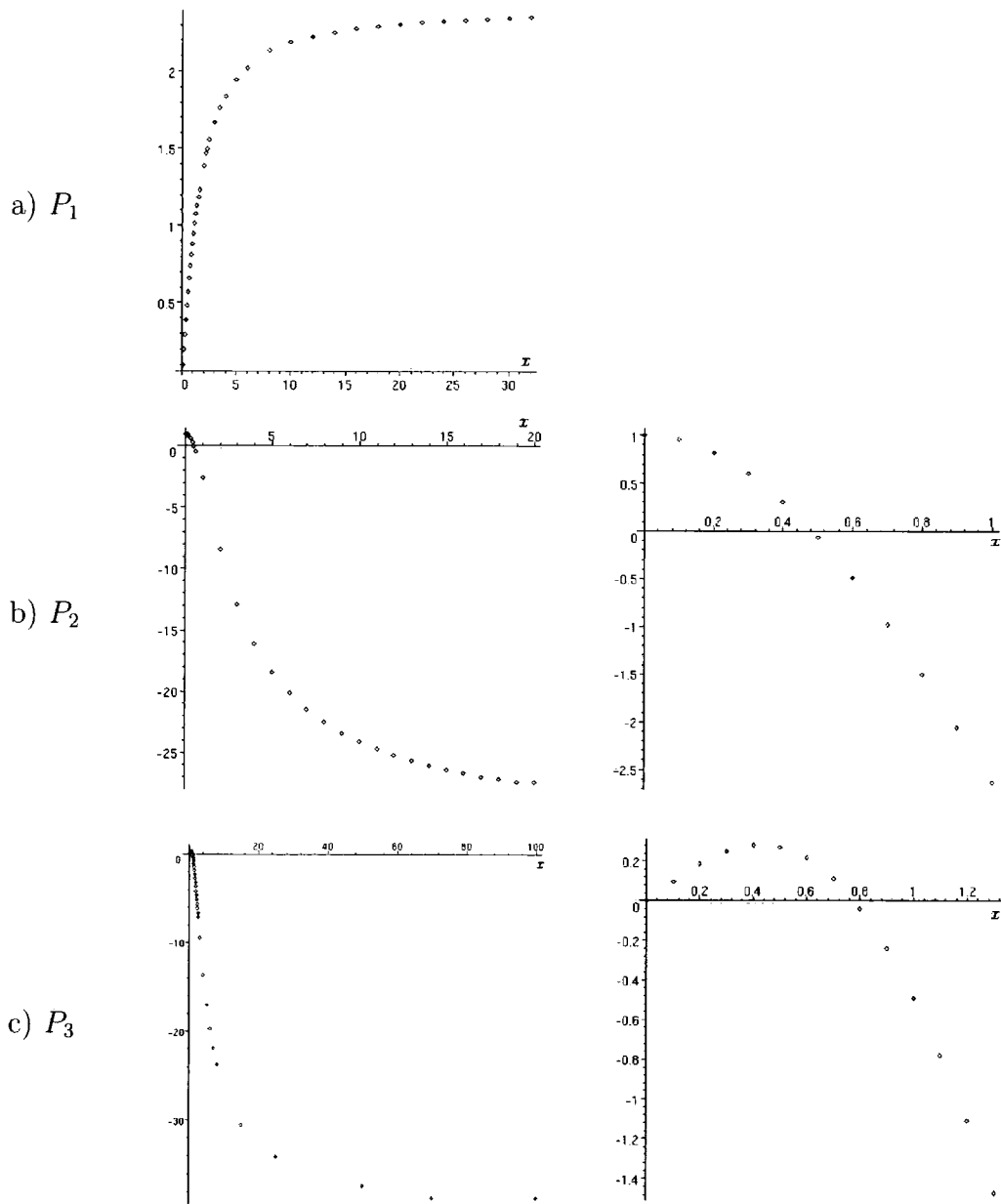
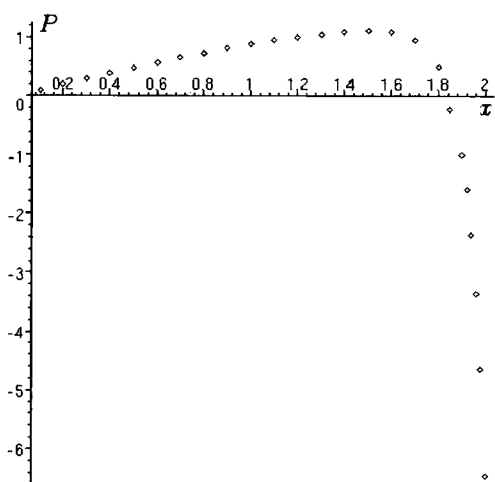
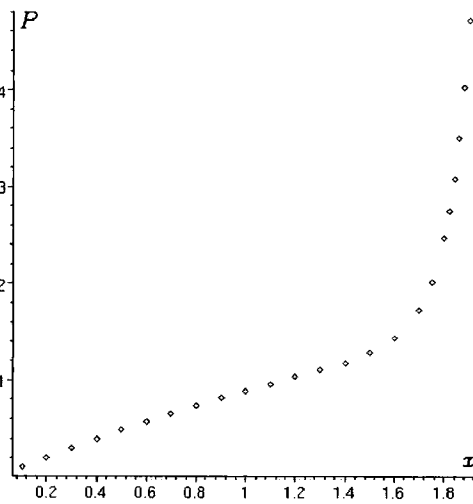


Figure 4.6: Prefactors corresponding to the first three excitations

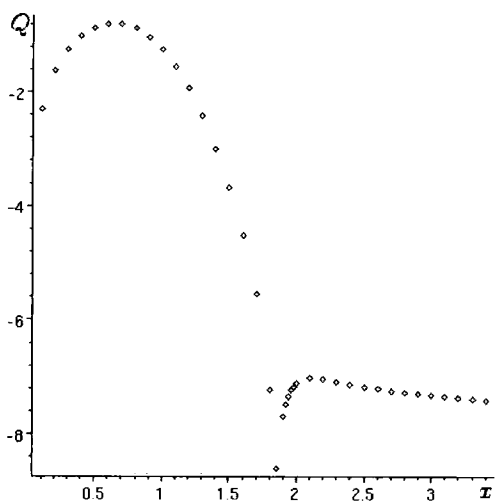


a) $c_1 = -0.15$

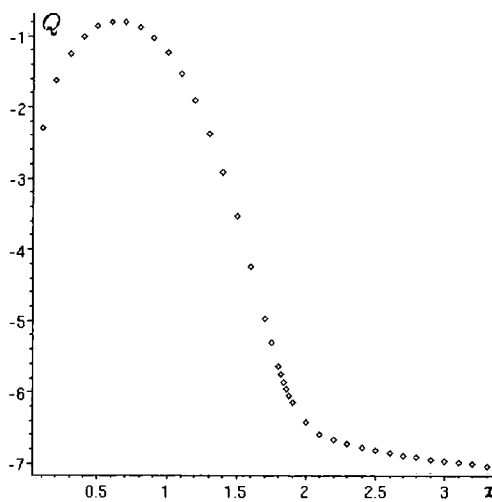


b) $c_1 = -0.14$

Figure 4.7: P for values of c_1 either side of $e_1 = -0.1458432840772$



a) $c_1 = -0.15$



b) $c_1 = -0.14$

Figure 4.8: Q for values of c_1 either side of $\tau_1 \approx -0.1458432840772$

4.5 Summary

We have developed a method for calculating the relationship between the physical parameters of a general x^{2M} anharmonic oscillator. The equations we solve are linear and the process of refining our estimate is easily automated. We can calculate the physical quantities and wavefunctions for all levels of excitation to an arbitrary level of accuracy, with an error that can be reduced by increasing the number of terms in our expansion. Using modest computing power we have demonstrated that high degrees of accuracy can be obtained very quickly. Our technique overcomes some of the deficiencies of traditional perturbative techniques which rely on coupling-constant expansions and so do not immediately reveal the effects of instantons, for example. We note that the analytic continuation of quantum mechanical systems into complex configuration space has recently been studied in \mathcal{PT} symmetric quantum mechanics (see [31] and references therein). We believe that understanding the properties of Hermitian theories in the complex plane is still of great interest.

Finally we note that in the case of the quasi-exactly-solvable solutions studied in [17], the expansion of both W and P in powers of x becomes truncated. In this type of solution it is more obvious that the correct boundary condition is satisfied by the large- x behaviour. This is trivially reflected in our resummation technique. We have numerically verified that the results of [17] are correctly reproduced for some specific choices of an x^6 polynomial potential.

4.6 Appendix

In table 4.1 we give some of the excited energy eigenvalues for the $\rho = 0$ quartic ($M = 2$) anharmonic oscillator. The results represent accurate eigenvalues rounded to 48 significant figures.

q	$E_0 + E_q$
1	3.79967302980139416878309418851256895776606546733
2	7.455697937986738392156591347185767488137819536750
3	11.6447455113781620208503732813709364365508721620
4	16.2618260188502259378949544303846135342445865045
5	21.2383729182359400241497111135886363767048320597
20	122.604639000999455020762971417615181874976633223
38	284.068590581400743150496281208125064777084713267
39	293.948458266006085433669997483521626303445899275

Table 4.1: Quartic excited energy eigenvalues with $\rho = 0$

Chapter 5

Schrödinger Representation of Quantum Field Theory

The Schrödinger representation of quantum field theory (SRQFT) is a natural extension of ordinary quantum mechanics. In quantum mechanics we start with a Hamiltonian which is quantised by imposing canonical commutation relations between the coordinate operators and the conjugate momenta. In the coordinate representation we work with a basis in which the position operator is diagonal, $\hat{x}|x\rangle = x|x\rangle$. We assume that such a basis satisfies orthonormality and completeness conditions. A general state $|\Psi\rangle$ may then be represented by a function $\Psi(x) \equiv \langle x|\Psi\rangle$ so that

$$|\Psi\rangle = \int dx \Psi(x)|x\rangle. \quad (5.0.1)$$

The coordinate operator \hat{x} is then represented by its eigenvalues x and the conjugate momentum is represented by a differential operator in such a way that the canonical commutation relations are preserved. The Hamiltonian then also becomes a differential operator and dynamics are recovered via the Schrödinger equation, which in this representation becomes a differential equation.

In quantum field theory we also have a Hamiltonian which is quantised using canonical commutation relations. In place of the position operator \hat{x} and momentum operator $\hat{\pi}$ we now have fields $\hat{\phi}(x)$ and $\hat{\pi}(x)$. The coordinate SRQFT is produced in the same manner as the Schrödinger representation of quantum mechanics. We essentially just need to substitute the word function with functional. The differential

operator representing the canonical momentum operator in quantum mechanics becomes a functional differential operator in field theory. Similarly the wavefunction of quantum mechanics becomes a wavefunctional and the differential Schrödinger equation becomes a functional differential equation.

In principle the SRQFT may be considered a more fundamental approach than the usual path integral or Heisenberg formalism. It is more closely connected to the initial principle upon which quantum mechanics was founded and has a more intuitive and conceptual connection to a physical interpretation.

In reality, however, the functional differential equations can be extremely difficult to solve. In addition Lorentz covariance is not explicit in the SR and this may be the reason why historically it has not been highly developed. Another problem with the SRQFT is the apparent difficulties in describing their renormalisation properties due to this apparent lack of Lorentz invariance. Indeed it was only in 1981 that Symanzik [3] first addressed these problems. Only at this point was it proved that the Schrödinger equation exists.

Despite the problems that the SRQFT has, it should not be completely ignored. Its fundamental formalism and similarity to quantum mechanics means that in principle problems solved in quantum mechanics can also be solved in quantum field theory. Quantum mechanical problems are considered relatively easy when compared to field theory problems although the word *relative* may be considered key here. Certainly a wide range of techniques have been developed in quantum mechanics and this work can in principle be recycled by using the SRQFT.

The aim of this chapter is to describe the basic principles of the SRQFT for scalar theories. Before doing so it will be necessary to describe some basic techniques in functional calculus. In particular the technique of computing functional Gaussian integrals will be of great importance in the next chapter. We shall pay particular attention to the scalar ϕ^4 theory as a toy model for illustrating some key concepts. It was shown by Mansfield [21] that for fields that vary slowly on the scale of the lightest mass, the logarithm of the vacuum wavefunctional can be expanded as a sum of local quantities. We shall illustrate some techniques in constructing this local expansion and show how it can be used to reconstruct the full vacuum functional.

5.1 Functional Calculus

The Schrödinger representation of quantum field theory is often known as the functional representation due to its dependence on functional calculus techniques. Therefore in developing and working with the Schrödinger representation it will be useful to develop various techniques for solving functional differential equations and evaluating functional integrals. We shall provide a brief summary of the key results and techniques of functional calculus; however first, we must define the concept of a functional. There are a number of texts that illustrate such techniques; however, [32] was particularly helpful in writing this section.

Consider functions of the form $\varphi : \mathbb{R}^n \rightarrow \mathbb{C}$, a mapping of space time points to the complex plane. The function space \mathcal{F} is defined to be the set of all such functions so that each point in \mathcal{F} is a function of the form φ . We then define a functional to be a mapping from the function space to the complex plane, $F : \mathcal{F} \rightarrow \mathbb{C}$ and use the notation $F[\varphi]$ to represent the mapping of $\varphi \in \mathcal{F}$ to $F[\varphi] \in \mathbb{C}$.

In analogy to the usual derivative of a function, the functional derivative is defined as

$$\frac{\delta F[\varphi]}{\delta \varphi} \equiv \lim_{\epsilon \rightarrow 0} \frac{F[\varphi + \epsilon \delta] - F[\varphi]}{\epsilon} \quad (5.1.1)$$

where the δ in $F[\varphi + \epsilon \delta]$ is the Dirac delta function. We think of this as the rate of change of the functional F as a result of a change in $\varphi(x)$ in the direction of the δ function. Whilst we do not always explicitly write the x dependence of φ (as is the case in (5.1.1)) we should note that we require the change in F as a result in the change of φ at the point x only. We could of course have defined our functional derivative in the direction of an alternate function, say $\lambda(x)$ by

$$\frac{\delta_\lambda F[\varphi]}{\delta_\lambda \varphi} \equiv \lim_{\epsilon \rightarrow 0} \frac{F[\varphi + \epsilon \lambda] - F[\varphi]}{\epsilon} \quad (5.1.2)$$

although such derivatives will not be required in our formalism of the Schrödinger representation.

The most basic functional derivative we might compute is

$$\frac{\delta \varphi(x)}{\delta \varphi(y)} = \delta(x - y), \quad (5.1.3)$$

which may be deduced directly from the definition (5.1.1). Many of the well known results from differentiation of functions, such as the product rule, continue to hold in the case of a functional derivative.

5.1.1 Functional Differential Equations

One technique used in solving functional differential equations is a form of separation of variables. For example, consider the following differential equation

$$\int_{-\infty}^{\infty} dx \frac{\delta}{\delta\varphi(x)} F[a] = -\mu F[\varphi]. \quad (5.1.4)$$

We can think of $F[\varphi]$ as an infinite-dimensional vector space with one element for each point x in space. The left-hand side of the equation is an infinite sum of uncoupled differential operators acting on $F[\varphi]$. We therefore write $F[\varphi]$ as an infinite product of solutions to the uncoupled differential equations. Each solution will satisfy a differential equation of the form

$$\frac{d}{dz} \mathcal{F}(z) = -f \mathcal{F}(z) \quad (5.1.5)$$

which has solution

$$\mathcal{F}(z) = \eta e^{-fz}. \quad (5.1.6)$$

So the solution to (5.1.4) is of the form

$$F[a] = \tilde{\eta} \prod_x e^{-f(x)\varphi(x)} = \tilde{\eta} \exp\left(-\int_{-\infty}^{\infty} dx f(x)\varphi(x)\right) \quad (5.1.7)$$

with $f(x)$ determined by substitution back into the original functional differential equation, so that

$$\mu = \int_{-\infty}^{\infty} dx f(x). \quad (5.1.8)$$

The normalisation constant $\tilde{\eta}$ is determined via initial or boundary value conditions placed on F .

The technique we will mostly be using is one of power counting, in which powers of φ on both sides of a functional differential equation are compared. For example

consider¹

$$\int dx \frac{\delta^2}{\delta\varphi(x)^2} F[\varphi] = \mu \int dx g(x)\varphi(x). \quad (5.1.9)$$

We note that the right-hand side involves one power of φ . For the left-hand side to also contain one power of φ we need $F[\varphi]$ to be cubic. The most general cubic that we can write is

$$F[\varphi] = \int dx dy dz f(x, y, z)\varphi(x)\varphi(y)\varphi(z). \quad (5.1.10)$$

Applying the left-hand side of the functional differential equation, (5.1.9) to this we find

$$\mu g(x) = 2 \int dy (f(x, y, y) + f(y, x, y) + f(y, y, x)). \quad (5.1.11)$$

It is not obvious how to proceed to find $f(x, y, z)$ in terms of $g(x)$; however, we note that (5.1.10) is invariant upon interchanging a pair of x, y or z in $f(x, y, z)$. So we could take $f(x, y, z)$ to be a symmetric function. Some additional information about the form of $f(x, y, z)$ is useful in determining the correct solution.

We should be careful about how we interpret equations of the form

$$\int dx dy f(x, y)\varphi(x)\varphi(y) = \int dx dy g(x, y)\varphi(x)\varphi(y). \quad (5.1.12)$$

In general it is not sufficient to state $f(x, y) = g(x, y)$ but we should deduce the correct relationship by functionally differentiating both sides of the differential equation with respect to, say, $\varphi(\tilde{x})$ and $\varphi(\tilde{y})$. Then

$$f(\tilde{x}, \tilde{y}) + f(\tilde{y}, \tilde{x}) = g(\tilde{x}, \tilde{y}) + g(\tilde{y}, \tilde{x}). \quad (5.1.13)$$

If $f(x, y)$ is symmetric then

$$f(x, y) = \frac{1}{2} (g(x, y) + g(y, x)). \quad (5.1.14)$$

In general an equation of the form

$$\begin{aligned} \int dx_1 \dots dx_n f(x_1, \dots, x_n)\varphi(x_1) \dots \varphi(x_n) \\ = \int dx_1 \dots dx_n g(x_1, \dots, x_n)\varphi(x_1) \dots \varphi(x_n) \end{aligned} \quad (5.1.15)$$

¹The integrals should contain $\pm\infty$ limits; however, we shall not explicitly include these limits from now on. Where a definite integral is implied we shall assume that we are integrating over the whole space.

with f symmetric in all of its parameters is solved by functionally differentiating with respect to φ evaluated at n different points. Then

$$f(x_1, \dots, x_n) = \mathcal{S}g(x_1, \dots, x_n) \quad (5.1.16)$$

where \mathcal{S} instructs us to symmetrise g by summing all $n!$ distinct $g(y_1, \dots, y_n)$ with $y_i \in \{x_i \mid y_i \neq y_j\}$ and dividing by the symmetry factor $n!$.

5.1.2 Functional Integration

A functional integral is an integral of a functional over a function space. That is where the integration measure $\mathcal{D}\varphi$ represents integration over each point $\varphi(x)$:

$$\mathcal{D}\varphi = \prod_x d\varphi(x). \quad (5.1.17)$$

There are few types of functional integrals that we are able to perform exactly. The easiest is probably

$$\int \mathcal{D}\varphi \delta[\varphi - a] F[\varphi] = F[a] \quad (5.1.18)$$

where the delta functional is defined by

$$\delta[\varphi - a] = \prod_x \delta(\varphi(x) - a(x)). \quad (5.1.19)$$

This is easily seen by applying definitions (5.1.17) and (5.1.19) to the functional integral (5.1.18). We can think of $\varphi(x)$ as an infinite dimensional vector with each x labelling a different element of the vector. The functional integration measure $\mathcal{D}\varphi$ essentially replaces each element of $\varphi(x)$ with the corresponding element $a(x)$.

The main type of functional integral that we will be interested in is that of the Gaussian form. The simplest type of Gaussian functional integral is

$$\begin{aligned} \int \mathcal{D}\varphi e^{-\int dx \varphi^2(x)} &= \prod_x \int d\varphi(x) e^{-\varphi^2(x)dx} \\ &= \eta \prod_x \sqrt{\pi}. \end{aligned} \quad (5.1.20)$$

Due to the divergence of $\prod_x \sqrt{\pi}$ functional integrals are not well defined and usually only make sense when combined with a normalisation factor. The factor η is usually omitted by absorption into this normalisation factor.

This result is easily generalised so that

$$\int \mathcal{D}\varphi e^{-\int dx f(x)\varphi^2(x)} = \prod_x \sqrt{\frac{\pi}{f(x)}}. \quad (5.1.21)$$

We may think of $f(x)$ as an infinite-dimensional diagonal matrix that acts on the vector $\varphi(x)$. We think of $f(x)$ as being the diagonal elements of a matrix with indices x and y , thus $f(x, y) = f(x)\delta(x - y)$. Since the product of the eigenvalues is also the determinant of a matrix the result (5.1.21) can then be expressed in a number of ways

$$\prod_x \sqrt{\frac{\pi}{f(x)}} = \det^{-\frac{1}{2}} \left(\frac{f}{\pi} \right) = \frac{(\sqrt{\pi})^\infty}{\sqrt{\det f}}. \quad (5.1.22)$$

This representation makes it more natural to generalise the result (when $f(x, y)$ is not necessarily diagonal) to

$$\int \mathcal{D}\varphi e^{-\int dx dy \varphi(x)f(x,y)\varphi(y)} = \frac{(\sqrt{\pi})^\infty}{\sqrt{\det f}}. \quad (5.1.23)$$

The Gaussian functional integral can be generalised further by introducing a source term so that

$$\int \mathcal{D}\varphi e^{F[\varphi, J]} \quad (5.1.24)$$

where

$$F[\varphi, J] = \int dx dy \varphi(x)f(x, y)\varphi(y) + \int dx J(x)\varphi(x). \quad (5.1.25)$$

In a usual (non-functional) Gaussian integral of this type we would complete the square so

$$\int_{-\infty}^{\infty} dx e^{-ax^2+bx} = \int_{-\infty}^{\infty} -dx e^{-a(x-\frac{b}{2a})^2+\frac{b^2}{4a}} = e^{\frac{b^2}{4a}} \sqrt{\frac{\pi}{a}}. \quad (5.1.26)$$

So we write

$$\int \mathcal{D}\varphi e^{-F[\varphi, J]} = \frac{(\sqrt{\pi})^\infty}{\sqrt{\det f}} \exp \left(\frac{1}{4} \int dx dy J(x)f^{-1}(x, y)J(y) \right) \quad (5.1.27)$$

where $f^{-1}(x, y)$ is the inverse of the symmetric matrix $f(x, y)$,

$$\int dz f^{-1}(x, z)f(z, y) = \delta(x - y). \quad (5.1.28)$$

We are now in a position to derive a key result for functional integrals. That is

$$\begin{aligned} \int \mathcal{D}\varphi \varphi(x_1) \cdots \varphi(x_n) \exp \left(- \int dx dy \varphi(x)f(x, y)\varphi(y) \right) \\ = \frac{\delta}{\delta J(x_1)} \cdots \frac{\delta}{\delta J(x_n)} \int \mathcal{D}\varphi e^{-F[\varphi, J]} \Big|_{J=0}. \end{aligned} \quad (5.1.29)$$

For n odd the right hand side is zero. With an even power of φ ,

$$\begin{aligned} \int \mathcal{D}\varphi \varphi(x_1) \cdots \varphi(x_{2n}) \exp\left(-\int dx dy \varphi(x) f(x, y) \varphi(y)\right) \\ = \frac{1}{n! 2^n} \frac{(\sqrt{\pi})^\infty}{\sqrt{\det f}} \sum_{\sigma \in S_{2n}} \prod_{i=1}^n f^{-1}(x_{\sigma(2i-1)}, x_{\sigma(2i)}) \end{aligned} \quad (5.1.30)$$

where S_{2n} is the permutation group, the group of all permutations of $2n$ elements.

5.2 Scalar Field Theory

We will introduce the Schrödinger representation of quantum field theory by considering a bosonic scalar field theory in $D + 1$ dimensions. Whilst this section is not explicitly based on any one particular text there are a number of useful introductions to the Schrödinger representation, in particular [32] [33] [34]. We start with the Lagrangian of a general scalar field theory

$$L = \int d^{D+1}x \mathcal{L} = \int d^{D+1}x (\partial^\mu \phi \partial_\mu \phi - V(\phi)). \quad (5.2.1)$$

The conjugate field momentum to ϕ is

$$\pi = \frac{\partial \mathcal{L}}{\partial(\partial_t \phi)} = \frac{\partial}{\partial t} \phi \quad (5.2.2)$$

and the Hamiltonian is defined by

$$\begin{aligned} H = \int d^D x \mathcal{H} &= \int d^D x (\pi \dot{\phi} - \mathcal{L}) \\ &= \int d^D x \left(\frac{1}{2} \dot{\phi}^2 + \frac{1}{2} (\nabla \phi)^2 + V(\phi) \right) \end{aligned} \quad (5.2.3)$$

where we have introduced the usual notation $\dot{\phi} \equiv \partial_t \phi$. For bosonic fields we will introduce the usual equal time canonical commutation relations²

$$\begin{aligned} [\hat{\phi}(\vec{x}, t), \hat{\pi}(\vec{y}, t)] &= i\delta^D(\vec{x} - \vec{y}) \\ [\hat{\phi}(\vec{x}, t), \hat{\phi}(\vec{y}, t)] &= 0 \\ [\hat{\pi}(\vec{x}, t), \hat{\pi}(\vec{y}, t)] &= 0. \end{aligned} \quad (5.2.4)$$

²We will adopt the \vec{x} notation to refer to the D dimensional spatial vector but not including the time component.

With the scalar field theory defined we introduce the coordinate Schrödinger representation of quantum field theory by considering the operator $\hat{\phi}(\vec{x})$ as a function of space only with no time dependence. This is achieved by choosing a fixed time hypersurface, say $t = 0$. We work with a Fock space, $\{|\varphi(\vec{x})\rangle\}$ in which $\hat{\phi}(\vec{x})$ is diagonal. That is

$$\hat{\phi}(\vec{x})|\varphi(\vec{x})\rangle = \varphi(\vec{x})|\varphi(\vec{x})\rangle \quad (5.2.5)$$

where $\varphi(\vec{x})$ is a scalar function and the eigenstates $|\varphi\rangle$ satisfy the usual orthonormality and completeness relations

$$\langle\varphi|\varphi'\rangle = \delta[\varphi - \varphi'] \quad (5.2.6)$$

$$\int \mathcal{D}\varphi |\varphi\rangle\langle\varphi| = \hat{1}. \quad (5.2.7)$$

The canonical commutation relations (5.2.4) are satisfied by the functional differential representations of the field and conjugate momentum operators as defined by

$$\begin{aligned} \hat{\phi} &\rightarrow \varphi(\vec{x}), \\ \hat{\pi} &\rightarrow -i \frac{\delta}{\delta\varphi(\vec{x})}. \end{aligned} \quad (5.2.8)$$

A general state $|\Psi\rangle$ can be represented by a wavefunctional $\Psi[\varphi]$ as seen by inserting (5.2.7) in front of the state so

$$|\Psi\rangle = \int \mathcal{D}\varphi |\varphi\rangle\langle\varphi|\Psi\rangle = \int \mathcal{D}\varphi |\varphi\rangle\Psi[\varphi] \quad (5.2.9)$$

where

$$\Psi[\varphi] = \langle\varphi|\Psi\rangle. \quad (5.2.10)$$

This leads to a functional integration definition of the inner product

$$\langle\Psi_1|\Psi_2\rangle = \int \mathcal{D}\varphi \Psi_1^*[\varphi]\Psi_2[\varphi]. \quad (5.2.11)$$

In quantum mechanics we interpret $|\Psi(x, t)|^2$ as the probability of finding a particle at a time t at the point x . In quantum field theory we interpret $|\Psi[\varphi]|^2$ as the probability that the field $\phi(\vec{x}, t)$ takes the value φ at $t = 0$. This is equivalent to finding $\hat{x}(t)$ diagonal in quantum mechanics or $\hat{\phi}$ diagonal in quantum field theory.

The action of a general operator $\hat{\mathcal{O}}(\hat{\phi}, \hat{\pi})$ on a state $|\Psi\rangle$ is represented by

$$\hat{\mathcal{O}}(\hat{\phi}, \hat{\pi})|\Psi\rangle \rightarrow \mathcal{O}\left(\varphi, -i\frac{\delta}{\delta\varphi}\right)\Psi[\varphi], \quad (5.2.12)$$

which allows us to recover the dynamical equation, the time-dependent functional Schrödinger equation

$$H\left(\varphi, -i\frac{\delta}{\delta\varphi}\right)\Psi[\varphi, t] = i\frac{\partial}{\partial t}\Psi[\varphi, t]. \quad (5.2.13)$$

For our time-independent Hamiltonian we explicitly separate out the time dependence of the wavefunctional

$$\Psi[\varphi, t] = e^{-iEt}\Psi[\varphi] \quad (5.2.14)$$

so that $\Psi[\varphi]$ satisfies the time-independent Schrödinger equation

$$\int d^{D+1}x \left(-\frac{1}{2}\frac{\delta^2}{\delta\varphi^2(\vec{x})} + \frac{1}{2}|\nabla\varphi|^2 + V(\varphi) \right) \Psi[\varphi] = E\Psi[\varphi]. \quad (5.2.15)$$

In addition to this operator-type formalism as discussed so far we may also express the wavefunctionals in terms of the generating functional of certain Feynman diagrams on the half plane $t \leq 0$. To see this, consider the Schrödinger functional which is defined by the matrix element

$$\langle\varphi|e^{-TH}|\varphi'\rangle = \int \mathcal{D}\tilde{\phi} e^{-S_E[\tilde{\phi}]} \quad (5.2.16)$$

where S_E is the Euclidean action for a $D+1$ dimensional volume bounded by space-like surfaces at time t apart and $\tilde{\phi}(\vec{x}, 0) = \varphi(\vec{x})$, $\tilde{\phi}(\vec{x}, -T) = \varphi'(\vec{x})$. A wavefunctional representation is recovered by inserting a complete set of eigenstates of the Hamiltonian, $\{|n\rangle\}$, so that

$$\begin{aligned} \langle\varphi|e^{-TH}|\varphi'\rangle &= \sum_{n=0}^{\infty} \sum_{m=0}^{\infty} \langle\varphi|n\rangle \langle n|e^{-TH}|m\rangle \langle m|\varphi'\rangle \\ &= \sum_{n=0}^{\infty} \langle\varphi|n\rangle e^{-TE_n} \langle n|\varphi'\rangle \\ &= \sum_{n=0}^{\infty} \Psi_n[\varphi] \Psi_n^*[\varphi'] e^{-TE_n} \end{aligned} \quad (5.2.17)$$

We can extract the vacuum wavefunctional by considering the limit $T \rightarrow \infty$

$$\langle\varphi|e^{-TH}|\varphi'\rangle \sim \Psi_0[\varphi] \Psi_0^*[\varphi'] e^{-TE_0}. \quad (5.2.18)$$

If we assume that φ' vanishes as $T \rightarrow \infty$ and normalise the vacuum energy so that $E_0 = 0$ then we have

$$\Psi_0[\varphi] = \int \mathcal{D}\tilde{\phi} e^{-S_E[\tilde{\phi}]} \quad (5.2.19)$$

where $\tilde{\phi}(t = 0) = \varphi$.

5.2.1 Massive Free Scalar Field Theory

In a quantum mechanical system the ground state has no nodes and may therefore be written as an exponential. In the same manner we will find the vacuum functional of the massive free ($V = \frac{1}{2}m^2\varphi^2$) scalar field theory by writing the vacuum functional as

$$\Psi_0[\varphi] = \eta e^{W[\varphi]}. \quad (5.2.20)$$

and solving the functional Schrödinger equation. Substituting this form of the vacuum functional into (5.2.15) we find the functional equation satisfied by $W[\varphi]$

$$\frac{1}{2} \int d^D x \left(-\frac{\delta^2 W[\varphi]}{\delta\varphi^2(\vec{x})} - \left(\frac{\delta W[\varphi]}{\delta\varphi(\vec{x})} \right)^2 + \varphi(\vec{x}) (-\nabla^2 + m^2) \varphi(\vec{x}) \right) = E_0. \quad (5.2.21)$$

By inspection, counting powers of φ we see that it is sufficient for $W[\varphi]$ to be quadratic in φ , so we write

$$W[\varphi] = \int d^D x d^D y \varphi(\vec{x}) \Gamma(\vec{x}, \vec{y}) \varphi(\vec{y}) \quad (5.2.22)$$

where $\Gamma(\vec{x}, \vec{y})$ is a scalar function. Without loss of generality, Γ is taken to be symmetric in \vec{x} and \vec{y} . We substitute this into (5.2.21) and compare powers of φ .

To zeroth order we have

$$E_0 = - \int d^D x \Gamma(\vec{x}, \vec{x}) \quad (5.2.23)$$

and to quadratic order

$$2 \int d^D x d^D y d^D z \varphi(\vec{z}) \Gamma(\vec{z}, \vec{x}) \Gamma(\vec{x}, \vec{y}) \varphi(\vec{y}) = \frac{1}{2} \int d^D x \varphi(\vec{x}) (-\nabla^2 + m^2) \varphi(\vec{x}). \quad (5.2.24)$$

To explicitly determine Γ we functionally differentiate both sides of (5.2.24) with respect to two independent variables, then

$$\int d^D x \Gamma(\vec{z}, \vec{x}) \Gamma(\vec{x}, \vec{y}) = \frac{1}{4} (-\nabla^2 + m^2) \delta^D(\vec{z} - \vec{y}). \quad (5.2.25)$$

This is much more naturally expressed when Γ is Fourier transformed into $\tilde{\Gamma}$ via

$$\Gamma(\vec{x}, \vec{y}) = \int \frac{d^D p}{(2\pi)^D} \tilde{\Gamma}(\vec{p}) e^{i\vec{p} \cdot (\vec{x} - \vec{y})} \quad (5.2.26)$$

when things become much simpler. In doing so we have assumed that $\Gamma(\vec{x}, \vec{y})$ is a function of $\vec{x} - \vec{y}$. Our justification for doing this is based upon (5.2.26), in which the right hand side is a function of $\vec{z} - \vec{y}$ only. Now

$$\tilde{\Gamma}(\vec{p}) = -\frac{1}{2} \sqrt{\vec{p}^2 + m^2} \equiv -\frac{\omega(\vec{p})}{2}. \quad (5.2.27)$$

and inverting the Fourier transform

$$\Gamma(\vec{x}, \vec{y}) = \frac{1}{2} \int \frac{d^D p}{(2\pi)^D} \omega(\vec{p}) e^{i\vec{p} \cdot (\vec{x} - \vec{y})}. \quad (5.2.28)$$

The ground-state eigenvalue is given by (5.2.23) as

$$E_0 = \frac{1}{2} \int d^D p \omega(\vec{p}) \delta^D(0) \quad (5.2.29)$$

where the $\delta^D(0)$ originates from the infinite volume $\int d^D x / (2\pi)^D$. The vacuum wavefunctional is most elegantly expressed in terms of the Fourier-transformed field $\tilde{\varphi}$

$$\Psi_0[\tilde{\varphi}] = \eta \exp \left(-\frac{1}{2} \int \frac{d^D p}{(2\pi)^D} \omega(\vec{p}) \tilde{\varphi}(\vec{p}) \tilde{\varphi}(-\vec{p}) \right). \quad (5.2.30)$$

The normalisation constant η can be determined by requiring a unit normalisation $\langle \Psi_0 | \Psi_0 \rangle = 1$. Using the Gaussian integral results of section 5.1.2 we find

$$\eta = \prod_{\vec{p}} \left(\frac{\omega(\vec{p})}{\pi} \right)^{\frac{1}{4}}. \quad (5.2.31)$$

One interesting property of $\Psi[\tilde{\varphi}]$ is that it is an infinite product of ordinary harmonic oscillator ground state wavefunctions, one for each \vec{p} . Given that the Hamiltonian is just a sum of massive free harmonic oscillator Hamiltonians this result is not very surprising. In fact the excited states could be constructed by replacing the ground state of one (or more) mode(s), say \vec{P} for its excited wavefunction, and would have energy $E_0 + \omega(\vec{P})$. For example

$$\Psi_1[\varphi] = \left(\frac{2\omega(\vec{P})}{(2\pi)^3} \right)^{\frac{1}{2}} \tilde{\varphi}(\vec{P}) \Psi_0[\tilde{\varphi}] \quad (5.2.32)$$

The momentum operator in quantum mechanics generates infinitesimal spacial displacements and in quantum field theory is represented by

$$P_j = - \int d^D x \phi(\vec{x}) \frac{\partial}{\partial x^j} \pi(\vec{x}). \quad (5.2.33)$$

In the Schrödinger representation this becomes the functional operator

$$P_j = i \int d^D x \varphi(\vec{x}) \partial_j \frac{\delta}{\delta \varphi(\vec{x})}. \quad (5.2.34)$$

We can explicitly verify that such an excited state has momentum \vec{P} and that it is indeed an eigenstate of H with energy $E_0 + \omega(\vec{P})$. Thus we can interpret this as a one-particle state. This reproduces the particle interpretation of quantum field theory.

An alternative and more formal method of finding multiple particle states is to apply the usual creation and annihilation operators associated with the harmonic oscillator. In the Schrödinger representation of quantum field theory these become

$$a(\vec{P}) = \int d^D x e^{i\vec{k}\cdot\vec{x}} \left(\omega(\vec{P})\varphi(\vec{x}) + \frac{\delta}{\delta \varphi(\vec{x})} \right) \quad (5.2.35)$$

$$a^\dagger(\vec{P}) = \int d^D x e^{-i\vec{k}\cdot\vec{x}} \left(\omega(\vec{P})\varphi(\vec{x}) - \frac{\delta}{\delta \varphi(\vec{x})} \right) \quad (5.2.36)$$

The a^\dagger operator is then applied to $\Psi_0[\varphi]$ multiple times to generate states with additional particles (up to some normalisation).

5.3 Renormalisability of the Schrödinger Equation

Renormalisation of a theory is essential to prove its existence and finiteness. This is usually carried out by power-counting methods in momentum space; however, in the case of the Schrödinger functional this is no longer possible, as translational invariance is lost in the time direction. Therefore we cannot rely on Lorentz invariance to renormalise a theory and it is no longer clear if a renormalisable quantum field theory remains renormalisable in the presence of a boundary. This problem was first studied by Symanzik for 3+1-dimensional ϕ^4 theory [3]; however, his arguments extend to other models. We will outline the key features based on [3] [4] [35].

Symanzik showed that the Schrödinger functional of ϕ^4 perturbation theory in 3+1 dimensions is finite as any cut-off is removed provided that in addition to the usual mass, coupling and field renormalisation additional counter terms to renormalise new ultraviolet divergences are introduced. These counter terms occur because of additional divergences resulting from the boundary conditions. Field operators which are diagonalisable in the Schrödinger representation differ from the usual renormalised field operators by (in the case of perturbation theory, logarithmically) divergent factors. That is, the relation (5.2.5) does not hold but instead we should have

$$\lim_{t \rightarrow 0} a(t) \phi(\vec{x}, t) \Psi[\varphi] = \varphi(\vec{x}) \Psi[\varphi] \quad (5.3.1)$$

where $a(t)$ is singular and given to first order by

$$a(t) = 1 - \frac{g}{54\pi^2} (\ln(\mu^2 t^2) + \ln(4\pi) - \Gamma'(1) + 2) + O(g^2) \quad (5.3.2)$$

and μ is the normalisation mass in the minimal subtraction scheme of dimensional regularisation.

Consequently φ , the boundary value of the scalar field must be renormalised

$$\phi(\vec{x}, 0) = Z\varphi(\vec{x}) \quad (5.3.3)$$

where Z is a new renormalisation constant required to cancel the extra ultraviolet divergences introduced by the boundary at $t = 0$. This was taken further in [36].

We shall mostly be working in ϕ^4 theory. This will be a convenient toy theory to develop our techniques; however, it should be possible to generalise the principles to other theories. Surface counter terms have been calculated in perturbation theory for ϕ^3 but since 3+1 dimensional ϕ^4 theory is not asymptotically free these are not reliable. We will therefore for simplicity be working in 1+1 dimensional ϕ^4 theory since it is super renormalisable with no further divergences associated with the boundary, in which case no extra field renormalisation is required.

In a super renormalisable theory the number of divergent diagrams is finite. In the case of ϕ^4 theory in 1 + 1 dimensions there is only one mass counterterm which is associated with the divergent tadpole diagram arising from the Laplacian in the Schrödinger equation. This Laplacian has two functional derivatives acting

on the same point and must be regulated. We will achieve this by introducing a momentum cut-off. The mass counterterm can be calculated in the framework of perturbation theory or equivalently by normal ordering. We will employ Wick's theorem to expand powers of the field in terms of normal-ordered contributions. This separates the convergent terms (with no contractions) from the divergent ones (with at least one contraction). These divergent contributions are the required counter terms and are dependent on the Laplacian's momentum cut-off.

We define the normal-ordered Hamiltonian for scalar ϕ^4 theory with finite M and vacuum energy density \mathcal{E} by

$$H = \int dx : \left(\frac{1}{2} \left(\hat{\pi}(x)^2 + \hat{\phi}'^2 + M^2 \hat{\phi}(x)^2 \right) + \frac{g}{4!} \hat{\phi}^4 \right) : . \quad (5.3.4)$$

A momentum cut-off is then introduced by defining

$$\hat{H}_\epsilon = \int dx \left(\frac{1}{2} \left(\hat{\pi}_\epsilon^2 + \hat{\phi}_\epsilon'^2 + M^2(\epsilon) \hat{\phi}_\epsilon^2 \right) + \frac{g}{4!} \hat{\phi}_\epsilon^4 - \mathcal{E}(\epsilon) \right) \quad (5.3.5)$$

where the cut-off fields are

$$\hat{\phi}_\epsilon(x) = \int dy \mathcal{G}_\epsilon(x, y) \hat{\phi}(y), \quad \hat{\pi}_\epsilon(x) = \int dy \mathcal{G}_\epsilon(x, y) \hat{\pi}(y) \quad (5.3.6)$$

and the kernel

$$\mathcal{G}_\epsilon(x, y) = \int_{p^2 < 1/\epsilon} \frac{dp}{2\pi} e^{ip(x-y)} \quad (5.3.7)$$

implements the momentum cut-off.

We relate $\hat{\phi}^2$ to the normal ordered $:\hat{\phi}^2:$ by

$$\hat{\phi}_\epsilon^2 = : \hat{\phi}_\epsilon^2 : + T_\epsilon \quad (5.3.8)$$

which is formally accomplished by considering the vacuum expectation value of $\hat{\phi}^2$, since the vacuum expectation value of $:\hat{\phi}^2:$ is zero. This corresponds to the logarithmically divergent tadpole diagram, the self contraction of the the field, corresponding to the Feynman diagram in which the ends of a propagator are contracted to the same point. Thus we have

$$T_\epsilon \equiv \langle 0 | \hat{\phi}_\epsilon(x) \hat{\phi}_\epsilon(x) | 0 \rangle = \frac{1}{2} \int_{p^2 < 1/\epsilon} \frac{dp}{2\pi} \frac{1}{\sqrt{p^2 + M^2}} \quad (5.3.9)$$

Applying Wick's theorem we relate $\hat{\phi}^4$ to the convergent $: \hat{\phi}^4 :$ (the term with no contractions)

$$\hat{\phi}^4 =: \hat{\phi}^4 : + 6T_\epsilon : \hat{\phi}^2 : + 3T_\epsilon^2. \quad (5.3.10)$$

By rewriting the momentum cut-off Hamiltonian as

$$\hat{H}_\epsilon = \hat{H}_\epsilon^0 + \int dx \left(\frac{1}{2} (M^2(\epsilon) - M^2) \hat{\phi}_\epsilon^2 + \frac{g}{4!} \hat{\phi}_\epsilon^4 - \mathcal{E}(\epsilon) \right) \quad (5.3.11)$$

where

$$\hat{H}_\epsilon^0 = \int dx \frac{1}{2} \left(\hat{\pi}_\epsilon^2 + \hat{\phi}_\epsilon'^2 + M^2 \hat{\phi}_\epsilon^2 \right) \quad (5.3.12)$$

we are able to calculate the divergent corrections to the normal ordered $: H_\epsilon :$. To do this we note that the normal-ordered free part has an infinite zero-point correction given by

$$\hat{H}_\epsilon^0 =: \hat{H}_\epsilon^0 : + \frac{1}{2} \int_{p^2 < 1/\epsilon} \frac{dp}{2\pi} \omega(p). \quad (5.3.13)$$

and apply (5.3.8), (5.3.9) and (5.3.10)

$$\begin{aligned} \hat{H}_\epsilon =: \hat{H}_\epsilon : + \int dx \left(\frac{1}{2} (M^2(\epsilon) - M^2 + \frac{g}{2} T_\epsilon) : \hat{\phi}^2 : \right. \\ \left. + \frac{g}{8} T_\epsilon^2 + \frac{T_\epsilon}{2} (M^2(\epsilon) - M^2) + \frac{1}{2} \int_{p^2 < 1/\epsilon} \frac{dp}{2\pi} \omega_p - \mathcal{E}(\epsilon) \right). \end{aligned} \quad (5.3.14)$$

Now we define the cut-off dependent quantities $M(\epsilon)$ and $\mathcal{E}(\epsilon)$

$$M^2(\epsilon) = M^2 + \hbar \delta M^2 - \hbar \frac{g}{4} \int_{p^2 < 1/\epsilon} \frac{dp}{2\pi} \frac{1}{\sqrt{p^2 + M^2}} \quad (5.3.15)$$

$$\begin{aligned} \mathcal{E}(\epsilon) = \delta \mathcal{E} + \frac{\hbar}{2} \int_{p^2 < 1/\epsilon} \frac{dp}{2\pi} \left(\sqrt{p^2 + M^2} + \frac{M^2(\epsilon) - M^2}{2\sqrt{p^2 + M^2}} \right) \\ + \frac{g\hbar^2}{32} \left(\int_{p^2 < 1/\epsilon} \frac{dp}{2\pi} \frac{1}{\sqrt{p^2 + M^2}} \right)^2 \end{aligned} \quad (5.3.16)$$

so that when the cut-off is removed M , \mathcal{E} , δM and $\delta \mathcal{E}$ remain finite. In these last equations we have explicitly introduced the \hbar dependence previously set to unity. This will be of importance later in this and the next chapter.

5.4 Locality of the Wavefunctional

In this section we will show that the vacuum functional is in general non local. If, however, the field φ varies slowly on the scale of $1/m$ then $W[\varphi] \equiv \log \Psi_0[\varphi]$ may be expanded as a sum of local terms [21]. We illustrate this in the case of the free scalar field theory and show how to extract the small distance behaviour from the large distance expansion of the vacuum functional and energy eigenvalue. This will be based on the Cauchy inspired modified Borel resummation techniques of chapters 3 and 4.

In section 5.2 we showed how to build a functional integral-representation of the vacuum functional $\Psi_0[\varphi]$ using Feynman's representation of the Schrödinger functional. We took φ to be the boundary value of the field at $t = 0$; however, it will become necessary for us to make the φ dependence more explicit. We shall therefore define a bra $\langle D|$ with Dirichlet boundary conditions and the property of being annihilated by $\hat{\phi}$

$$\langle D|\hat{\phi} = 0. \quad (5.4.1)$$

Then defining

$$\langle \varphi| = \langle D|e^{i \int d^D x \varphi(\vec{x}) \hat{\pi}(\vec{x})} \quad (5.4.2)$$

we have

$$\frac{\delta}{\delta \varphi(\vec{x})} \langle \varphi| = i \langle \varphi| \hat{\pi}(\vec{x}) \quad (5.4.3)$$

and using canonical commutation relations we recover $\langle \varphi|\hat{\phi}(\vec{x}) = \varphi(\vec{x})\langle \varphi|$. Now the Schrödinger functional is

$$\langle \varphi|e^{-T\hat{H}}|\varphi'\rangle = \langle D|e^{i \int d^D x \hat{\pi}(\vec{x}, 0)\varphi(\vec{x})} e^{-T\hat{H}} e^{-i \int d^D x \hat{\pi}(\vec{x}, -T)\varphi'(\vec{x})}|D\rangle. \quad (5.4.4)$$

Rotating into Euclidean space we write (5.4.4) as a functional integral

$$\int \mathcal{D}\phi \exp \left\{ -S_E + \int d^D x \dot{\phi}(\vec{x}, 0)\varphi(\vec{x}) - \int d^D x \dot{\phi}(\vec{x}, -T)\varphi'(\vec{x}) \right\} \quad (5.4.5)$$

where the variable ϕ is defined on the Euclidean semi-plane $t \leq 0$ and satisfies Dirichlet boundary conditions, $\phi(\vec{x}, 0) = \phi(\vec{x}, -T) = 0$. As before (section 5.2), we can insert a basis of Hamiltonian eigenstates and take the $T \rightarrow \infty$ limit. Assuming

that φ' vanishes in this limit we can obtain a functional integral representation of the vacuum functional on the Euclidean space time $t \leq 0$

$$\Psi_0[\varphi] = \int \mathcal{D}\phi e^{-S_E + \int d^D x \dot{\phi}(\vec{x})\varphi(\vec{x})} \quad (5.4.6)$$

hence the non-local nature of the wavefunctional. This also shows that in a semi-classical expansion $W[\varphi] \equiv \log \Psi_0[\varphi]$ is a sum of Euclidean connected Feynman diagrams in which φ is the source term for $\dot{\phi}$ on the boundary where ϕ vanishes [23] [37] (see [22] for Yang-Mills). Due to the non-local nature of the wavefunctional we should make an expansion of the form

$$W[\varphi] = \sum_{n=1}^{\infty} \int d^D x_1 \dots d^D x_n \Gamma_n(\vec{x}_1, \dots, \vec{x}_n) \varphi(\vec{x}_1) \dots \varphi(\vec{x}_n) \quad (5.4.7)$$

although as we shall show it is possible to write a local expansion provided the field φ varies slowly on the scale of $1/m$.

5.4.1 Massive Free Scalar Field Theory

We continue the discussion of the locality of the wavefunctional by considering the massive free scalar field theory. We show how W can be expanded as a local functional from which we can extract the vacuum energy density as an expansion in the momentum cut-off, ϵ . Whilst this expression does not appear to produce the correct result when the cut-off is removed we show how to analytically continue the vacuum energy into the complex ϵ plane and reproduce the correct behaviour when the cut-off is removed by applying a contour integral resummation technique along the lines of the one in chapter 3. In doing so we will largely be following the work of [21].

The unregulated Laplacian $\Delta = \int d^D x \delta^2 / \delta\varphi(\vec{x})$ in the Schrödinger equation (5.2.15) consists of two functional derivatives at the same space-time point, resulting in a divergent vacuum energy. This Laplacian can be regulated by introducing a momentum cut-off, $1/\epsilon$, by defining

$$\Delta_\epsilon = \int d^D x d^D y \int_{p^2 < \frac{1}{\epsilon}} \frac{d^D p}{(2\pi)^D} \frac{\delta^2}{\delta\varphi(\vec{x})\delta\varphi(\vec{y})} = \int_{p^2 < \frac{1}{\epsilon}} d^D p (2\pi)^D \frac{\delta^2}{\delta\tilde{\varphi}(\vec{p})\delta\tilde{\varphi}(-\vec{p})}. \quad (5.4.8)$$

where $\tilde{\varphi}(\vec{p}) = \int d^D x \varphi(\vec{x}) \exp(-i\vec{p} \cdot \vec{x})$. The vacuum energy density $\mathcal{E} = E/V$ is then well defined and diverges as the cut-off is removed,

$$\mathcal{E} = \frac{1}{2V} \Delta_\epsilon W = \frac{1}{2} \int_{p^2 < \frac{1}{\epsilon}} \frac{d^D p}{(2\pi)^D} \sqrt{p^2 + m^2} \sim \frac{k}{(D+1)\epsilon^{(D+1)/2}}, \quad (5.4.9)$$

where k is the area of the unit sphere in D dimensions divided by $2(2\pi)^D$.

If φ varies slowly on the scale of $1/m$ then $W[\varphi]$ may be expanded as a sum of local expressions by expanding

$$\sqrt{-\nabla^2 + m^2} = m - \frac{\nabla^2}{2m} - \frac{(-\nabla^2)^2}{8m^3} + \frac{(-\nabla^2)^3}{16m^5} - \frac{5(-\nabla^2)^4}{128m^7} + \dots \quad (5.4.10)$$

to give

$$W_{loc} = \int d^D x \left(-\frac{m}{2} \varphi^2 + \frac{1}{4m} (\nabla \varphi)^2 - \frac{1}{16m^2} (\nabla^2 \varphi)^2 + \dots \right). \quad (5.4.11)$$

We naively apply our regulated Laplacian (5.4.8) to obtain the energy density

$$\mathcal{E} = \frac{1}{2V} \Delta_\epsilon W_{loc} = \int_{p^2 < \frac{1}{\epsilon}} \frac{d^D p}{(2\pi)^D} \left(\frac{m}{2} - \frac{p^2}{4m} - \frac{(p^2)^2}{16m^3} + \dots \right) = \sum_{s=0}^{\infty} \frac{\alpha_n}{(m^2 s)^{n+D/2}} \quad (5.4.12)$$

where

$$\alpha_n = \frac{km^{D+1}\Gamma(\frac{3}{2})}{\Gamma(\frac{3}{2}-n)\Gamma(n+1)(D+2n)}. \quad (5.4.13)$$

This expression for the vacuum energy (5.4.12) appears to have divergences of increasing order as $\epsilon \rightarrow 0$ unlike the solution in (5.4.9) which gives the correct behaviour as the cut-off is removed. This is because the expansion of W_{loc} (5.4.11) is only valid for slowly varying fields, that is for $\tilde{\varphi}(p)$ in which $p^2 < m^2$ and hence $\epsilon m^2 > 1$. It therefore does not make sense to take the small ϵ limit in (5.4.12).

To overcome this issue we define an analytic continuation of the regulated vacuum energy from real $\epsilon > 0$ into the complex s plane by

$$\mathcal{E}(s) = \frac{1}{2s^{D/2}} \int_{p^2 < 1} \frac{d^D p}{(2\pi)^D} \sqrt{m^2 + \frac{p^2}{s}} \quad (5.4.14)$$

The integrand is analytic through the whole complex s plane with the exception of a cut generated by the square root, which we take to be along the negative real axis. For $|s|m^2 > 1$ it has a large- s expansion.

We define a contour C (figure 5.1) to be key-hole shaped, running just under the negative real axis from $s = -\infty$ up to $s = -s_0$, then round a circular contour centred

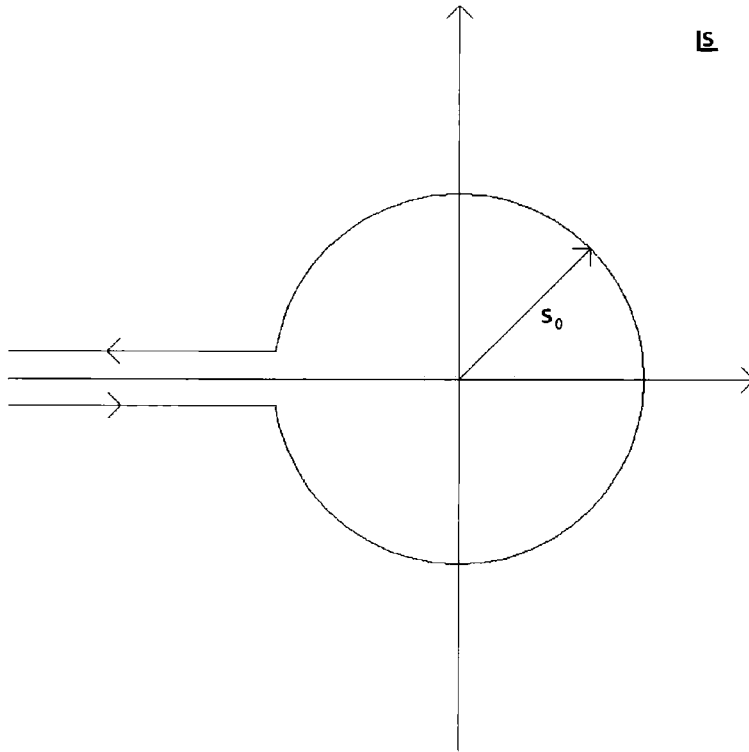


Figure 5.1: Key-hole shaped contour of integration

on the origin, stopping just above the negative real axis near $s = -s_0$, and back towards $s = -\infty$ remaining just above the negative real axis. Then for $s_0 > 1/m^2$ the integral

$$I(\lambda) = \frac{1}{2\pi i} \int_C \frac{ds}{s} \mathcal{E}(s) e^{\lambda s} \quad (5.4.15)$$

may be evaluated using the large s expansion so that

$$I(\lambda) = \sum_{n=0}^{\infty} \frac{\alpha_n}{\Gamma(n+1+D/2)} \left(\frac{\lambda}{m^2} \right)^{n+D/2}. \quad (5.4.16)$$

For large λ the exponential factor suppresses the cut contribution, and if $\mathcal{E}(0)$ were finite (5.4.16) would approximate $\mathcal{E}(0)$. In an interacting theory we would only be able to calculate (5.4.16) up to a finite number of terms truncated at order N . Since we have an alternating sign series the error in truncating (5.4.16) to order N is less than the absolute value of the $N+1$ term

$$\left| \frac{\alpha_{N+1} \lambda^{N+1+D/2}}{\Gamma(N+2+D/2) m^{2N+2+D}} \right| \quad (5.4.17)$$

which for large N behaves as $(e\lambda/m^2N)^{(N+1+D/2)}/N$. Since we want to take λ large we set $\lambda = N\mu^2$ where μ is an N independent parameter. The truncation error then goes to zero with large N provided μ is smaller than the mass m of the lightest particle. This shows that we can extract information about the high energy momentum cut-off by working to a finite order N despite the local expansion of the vacuum functional only being valid for slowly varying fields.

5.5 Reconstructing the Full Vacuum Functional

We have discovered that the vacuum functional is in general non-local; however, in the case of the free scale field theory we found a local expansion valid for fields which vary on the scale of the lightest mass. This local expansion can be used to extract the vacuum energy density. In this section we show that in 1+1 dimensional scalar field theories the full vacuum functional can also be reconstructed. A scaled field is defined $\varphi^s(x) = \varphi(x/\sqrt{s})$ and we will prove that $W[\varphi^s]$ extends to an analytic function in the complex s plane with singularities only on the negative real axis. For large s , $\varphi^s(x)$ varies slowly with x and so we may make a local expansion of $W[\varphi^s]$. Whilst we have done this explicitly for the free scalar field theory it should also be possible for a general interacting theory. Large s corresponds to small momenta and therefore we expect to be able to expand the Γ in our non-local expansion (5.4.7) in positive powers of the momenta. We shall show that this large- s local expansion for $W[\varphi^s]$ may be used to extract the $s = 1$ value via a contour integral method. This reproduces the correct vacuum functional $\exp(W[\varphi])$. We proceed again based on [21] but also with the help of [38].

We start by showing that $W[\varphi^s]$ extends to an analytic function in the complex s plane with singularities only on the negative s axis. In doing so we rotate coordinates in order to get a functional integral over the Euclidean space time $x \geq 0$, $-\infty \leq t \leq \infty$

$$e^{W[\varphi^s]} = \int \mathcal{D}\varphi e^{-S_E^r + \int dt \phi'(0,t)\varphi^s(t)} \quad (5.5.1)$$

where the prime indicates differentiation with respect to x and S_E^r is the Euclidean

action for rotated space time. This is the time ordered expectation value

$$T\langle 0^r | e^{\int dt \hat{\phi}'(0,t) \varphi^s(t)} | 0^r \rangle \quad (5.5.2)$$

where $\langle 0^r |$ is the ground state of the rotated Hamiltonian H^r . We expand the exponential in powers of φ^s and Fourier transform the sources

$$\begin{aligned} \sum_n \int_{-\infty}^{\infty} dt_n \int_{-\infty}^{t_n} dt_{n-1} \cdots \int_{-\infty}^{t_2} dt_1 \frac{1}{(2\pi)^n} \int dk_n \cdots dk_1 \exp(i \sum_i^n k_i t_i) \\ \times \tilde{\varphi}^s(k_n) \cdots \tilde{\varphi}^s(k_1) \langle 0^r | \hat{\phi}'(0) e^{-(t_n - t_{n-1}) \hat{H}^r} \hat{\phi}'(0) \\ \cdots e^{-(t_3 - t_2) \hat{H}^r} \hat{\phi}'(0) e^{-(t_2 - t_1) \hat{H}^r} \hat{\phi}'(0) | 0^r \rangle. \end{aligned} \quad (5.5.3)$$

We then calculate the time integrals, and after some algebra get

$$\begin{aligned} e^{W[\varphi^s]} = \sum_{n=0}^{\infty} \int dk_1 \cdots dk_n \tilde{\varphi}(k_n) \cdots \tilde{\varphi}(k_1) \delta(\sum_1^n k_i) \times \\ \sqrt{s}^n \langle 0^r | \hat{\phi}'(0) \frac{1}{\sqrt{s} \hat{H}^r + i(\sum_1^{n-1} k_i)} \hat{\phi}'(0) \cdots \hat{\phi}'(0) \frac{1}{\sqrt{s} \hat{H}^r + i k_1} \hat{\phi}'(0) | 0^r \rangle \end{aligned} \quad (5.5.4)$$

where we used $\tilde{\varphi}^s(k) = \sqrt{s} \tilde{\varphi}(\sqrt{s}k)$. The eigenvalues of the Hamiltonian H^r are real so singularities only occur when s is negative and real. The same holds for the connected part of $W[\varphi^s]$ as any additional singularities could not cancel between connected and disconnected pieces.

Given the analytic properties of $W[\varphi^s]$, we are able to reconstruct the the full vacuum functional from its local expansion only valid for slowly varying fields. Cauchy's theorem extracts the $s = 1$ value from the large s behaviour via

$$W[\varphi] = \lim_{\lambda \rightarrow \infty} \frac{1}{2\pi i} \int_C \frac{ds}{s-1} e^{\lambda(s-1)} W[\varphi^s] \quad (5.5.5)$$

where C is a large circular contour in the complex s plane centred on the negative real axis, beginning just below the negative real axis and ending just above. Cauchy's theorem tells us that the integral in (5.5.5) has a contribution from the $s = 1$ pole given by $W[\varphi]$ and a further contribution from the cut along the negative real axis. This cut is exponentially suppressed by λ and therefore approaches zero as $\lambda \rightarrow \infty$.

For large s , $\varphi^s(x)$ varies slowly with x and we can make a local expansion of W . Therefore we apply our local expansion of $W[\varphi^s]$ to (5.5.5) and let $|s| \rightarrow \infty$ in the contour C .

We illustrate this method for a massive free scalar field theory. The vacuum functional for the scaled field is

$$\Psi[\varphi^s] = e^{-\frac{1}{2} \int dx \varphi \sqrt{-\nabla^2 + sm^2} \varphi} \quad (5.5.6)$$

We can expand $W[\varphi^s]$ in inverse powers of $s - 1$ to get a local expansion

$$W[\varphi^s] = -\frac{m}{2} \sum_{n=0}^{\infty} \frac{\Gamma(3/2)}{\Gamma(n+1)\Gamma(3/2-n)} (s-1)^{1/2-n} \int dx \varphi \left(1 - \frac{\nabla^2}{m^2}\right)^n \varphi \quad (5.5.7)$$

Now we calculate the integral on the RHS of (5.5.5)

$$\begin{aligned} & \frac{m}{4\sqrt{\pi}} \sum_{n=0}^{\infty} \frac{(-1)^n \lambda^{n-1/2}}{n!(n-1/2)} \int dx \varphi \left(1 - \frac{\nabla^2}{m^2}\right)^n \varphi \\ &= -\frac{m}{2\sqrt{\pi}} \int dx \varphi \left(\frac{1}{\sqrt{\lambda}} e^{-\lambda(1-\nabla^2/m^2)} + \int_0^\lambda d\lambda \frac{1}{\sqrt{\lambda}} e^{-\lambda(1-\nabla^2/m^2)} \left(1 - \frac{\nabla^2}{m^2}\right) \right) \varphi \\ &= -\frac{1}{2} \int dx \varphi \sqrt{-\nabla^2 + m^2} \varphi + \frac{m}{4\sqrt{\pi}} \int dx \varphi \left(\int_\lambda^\infty d\lambda \frac{1}{\sqrt{\lambda^3}} e^{-\lambda(1-\nabla^2/m^2)} \right) \varphi. \end{aligned} \quad (5.5.8)$$

We note from the last line that we recover $W[\varphi]$ when $\lambda \rightarrow \infty$. The error in expressing $W[\varphi]$ is given by the last integral, which is exponentially suppressed. Therefore we have successfully reconstructed the vacuum functional from its large distance local expansion.

5.6 A Schrödinger Equation for the Local Expansion

So far we have seen that the logarithm of the vacuum functional, $W[\varphi]$ is in general a non-local quantity. If, however, the field φ varies slowly on the scale of the lightest mass then it may be expanded in terms of local functionals

$$W = \int dx \sum B_{j_0 \dots j_n} \varphi(x)^{j_0} \varphi'(x)^{j_1} \dots \varphi^{(n)}(x)^{j_n}. \quad (5.6.1)$$

We have shown that this local expansion can be used to construct $W[\varphi]$ for generic fields by relating the short-distance properties to the local large-distance behaviour. This local W does not satisfy the obvious form of the Schrödinger equation. The

Schrödinger equation depends on short-distance effects via a cut-off; however, the local expansion is only valid for fields characterised by large distance scales.

The Schrödinger equation with a momentum cut-off is $\lim_{\epsilon \rightarrow 0} F_\epsilon[\varphi] = 0$ where

$$F_\epsilon[\varphi] = -\frac{\hbar}{2}\Delta_\epsilon W + \int dx \left(\frac{1}{2} \left(-\left(\frac{\delta W}{\delta \varphi} \right) + \varphi'^2 + M^2(\epsilon)\varphi^2 \right) + \frac{g}{4!}\varphi^4 - \mathcal{E}(\epsilon) \right), \quad (5.6.2)$$

and the regulated Laplacian is given by

$$\Delta_\epsilon = \int dx dy \int_{p^2 < 1/\epsilon} \frac{dp}{2\pi} e^{ip(x-y)} \frac{\delta^2}{\delta \varphi(x)\varphi(y)} = \int_{|p| < 1/\epsilon} dp 2\pi \frac{\delta^2}{\delta \tilde{\varphi}(-p)\delta \tilde{\varphi}(p)} \quad (5.6.3)$$

with $\tilde{\varphi}(p) = \int dx \varphi(x) \exp(-ipx)$. The ϵ -dependence of $M(\epsilon)$ and $\mathcal{E}(\epsilon)$ was made explicit in section 5.3 in terms of the divergent tadpole diagrams and the finite M , \mathcal{E} , δM and $\delta \mathcal{E}$. If we evaluate $F_\epsilon[\varphi]$ for slowly-varying fields then it will be a sum of local functionals

$$F_\epsilon[\varphi] = \int dx \sum f_{j_0 \dots j_n}(\epsilon) \varphi(x)^{j_0} \varphi'(x)^{j_1} \dots \varphi^{(n)}(x)^{j_n}. \quad (5.6.4)$$

However, this is not the same as Δ_ϵ acting on the local W expansion, (5.6.1). The former, (5.6.4), includes differentiation with respect to the Fourier modes of φ in the range $M^2 < p^2 < 1/\epsilon$ which are absent from the latter. We therefore cannot naively take the local expansion (5.6.1) and substitute it into the Schrödinger equation (5.6.2) and take the limit in which the cut-off is removed, $\epsilon \rightarrow 0$. In this section we aim to construct the Schrödinger -type equation satisfied by the local expansion of W .

The solution to this problem is to scale the cut-off $\epsilon \rightarrow \epsilon s$ and the field $\varphi(x) \rightarrow \varphi^s(x) \equiv \varphi(x/\sqrt{s})$. Now $(\Delta_{s\epsilon} W)[\varphi_s]$, $M^2(s\epsilon)$ and $\mathcal{E}(s\epsilon)$ extend to analytic functions on the complex s plane with singularities lying only on the negative real axis. This statement is justified in the case of M and \mathcal{E} by their cut-off dependent expressions (5.3.15) and (5.3.16). In the case of the Laplacian a similar approach to deriving the analytic properties of $W[\varphi^s]$ in section 5.5 is used in [21]. Consequently the coefficients $f_{j_0 \dots j_n}$ also extend to analytic functions in the complex plane with singularities only on the negative real axis. For large $|s|$ the scaled field, φ^s varies slowly and the cut-off $1/(s\epsilon) < m_0$. So $\Delta_{s\epsilon} W[\varphi_s]$ can be calculated by acting with $\Delta_{s\epsilon}$ directly on the local W expansion. Since $s\epsilon$ now plays the role of the cut-off instead

of ϵ alone we will take ϵ to be finite, say $\epsilon = 1$. The coefficients in (5.6.1) now satisfy their own equation

$$\frac{1}{2\pi i} \int_{|s|=\infty} \frac{ds}{s} e^{\lambda s} F_s[\varphi^s] = 0 \quad (5.6.5)$$

where in $F_s[\varphi^s]$ we use the local form of W , (5.6.1).

In finding the coefficients of the local expansion (5.6.1) we should first note that integration by parts indicates that not all terms with a given number of fields and derivatives are unique. For example

$$\int dx \varphi \varphi'^2 \varphi'' = -\frac{1}{3} \int dx \varphi'^4. \quad (5.6.6)$$

We therefore define a set of independent local functionals. We will assume parity invariance, $\varphi \rightarrow -\varphi$, since this is an unbroken symmetry of the Lagrangian. This restricts both the number of fields ($j_0 + \dots + j_n$) and derivatives ($j_1 + 2j_2 + \dots + nj_n$) in a given term to be even. To ensure that our set of functions are not dependent through integration by parts (that is to ensure a linearly independent basis) we will restrict the power of the highest derivative to be at least two (i.e. $j_n \geq 2$). This requirement may be proved by induction [39]. So, for example $\int dx \varphi(x)(\varphi'(x))^2$ is not a basis vector since it violates parity invariance. $\int dx \varphi \varphi'^2 \varphi''$ is not a basis vector either, since the field of highest derivative φ'' does not have the required minimal power of two. This local functional is, however, linearly related to a basis element, $\int dx \varphi'^4$ via (5.6.6).

With these restrictions in place we proceed by substituting the local W , (5.6.1),

into its Schrödinger equation (5.6.5)

$$\begin{aligned}
& \int dx \left(2\bar{\mathcal{E}}(\lambda) + 2\mathcal{E} + \frac{\sqrt{\lambda}}{\sqrt{\pi}^3} \left(4B_2 + \frac{8B_{0,2}\lambda}{9} + \frac{16B_{0,0,2}\lambda^2}{75} + \dots \right) \right. \\
& + \varphi^2 \left(-\bar{M}^2(\lambda) + \frac{4B_2^2}{\sqrt{\pi}} + \frac{\sqrt{\lambda}}{\pi} \left(12B_4 + \frac{2B_{2,2}\lambda}{3} + \frac{B_{2,0,2}\lambda^2}{5} + \dots \right) \right) \\
& + \varphi^4 \left(-\frac{2g}{4!\sqrt{\pi}} + \frac{16B_4}{\sqrt{\pi}} + \frac{\sqrt{\lambda}}{\pi} \left(30B_6 + \frac{2B_{4,2}\lambda}{3} + \frac{B_{4,0,2}\lambda^2}{2} + \dots \right) \right) \\
& + \varphi'^2 \left(-\frac{2}{\sqrt{\pi}} + \frac{16B_2B_{0,2}}{\sqrt{\pi}} + \frac{\sqrt{\lambda}}{\pi} \left(2B_{2,2} + 2B_{0,4}\lambda + \frac{B_{2,0,2}\lambda}{3} + \frac{B_{0,2,2}\lambda^2}{3} - \dots \right) \right) \\
& + \varphi^2\varphi'^2 \left(\frac{32B_2B_{2,2} + 96B_{0,2}B_4}{\sqrt{\pi}} + \frac{12B_{4,2}\sqrt{\lambda}}{\pi} + \dots \right) \\
& + \varphi'^2 \left(\frac{32B_2B_{0,0,2} + 16B_{0,2}^2}{3\sqrt{\pi}} + \frac{\sqrt{\lambda}}{\pi} \left(B_{2,0,2} + \frac{B_{0,4}\lambda}{9} - \frac{B_{1,0,3}\lambda}{3} + \dots \right) \right) \\
& + \dots \left. \right) = 0
\end{aligned} \tag{5.6.7}$$

where

$$\bar{\mathcal{E}}(\lambda) = \frac{1}{2\pi i} \int_{|s|=\infty} \frac{ds}{s} e^{\lambda s} \mathcal{E}(s) \tag{5.6.8}$$

and

$$\bar{M}^2(\lambda) = \frac{1}{2\pi i} \int_{|s|=\infty} \frac{ds}{s} e^{\lambda s} M^2(s). \tag{5.6.9}$$

This equation can be solved in the usual semi-classical expansion [21] [23] by setting to zero the coefficients of the linearly-independent functionals. With the inclusion of an addition $\sqrt{\pi\lambda s}$ factor in the contour integral the resummation process can be improved, since the contribution from the origin becomes order $1/\lambda$ instead of $1/\sqrt{\lambda}$. It has been shown [23] that this approach correctly reproduces the short-distance properties of W .

For classically massless theories (e.g. Yang-Mills), the classical action does not have a local expansion. A semi-classical approach is therefore not viable, although the full action is believed to be massive [40]. An approximation scheme was proposed by Mansfield [21] in which the expansions in λ and the coefficients associated with the high orders were estimated. Whilst this would overcome the problem of finding

a local expansion in a classically massless theory it is believed that the solutions may be sensitive to the levels of truncation.

We will use an alternate approach [24] to construct the wavefunctional in the next chapter. In this approach we shall solve the coefficients of the vacuum functionals expansion as a power series in s . The limit $s \rightarrow 0$ is then taken using the contour-integral technique of resummation. [23].

5.7 Summary

We have shown how to formulate 1+1 dimensional ϕ^4 theory in the Schrödinger representation of quantum field theory. The problems of renormalisation have been addressed and the concept of a local expansion for the vacuum functional introduced. We have shown how to reconstruct the full vacuum functional from the large distance local expansion via the Cauchy-inspired resummation process developed in chapters 3 and 4. We have given limited attention to the methods that may be used to construct the local expansion of the vacuum wavefunctional and reserve the continuation of this discussion for the next chapter.

Finally, whilst we have restricted our attention to scalar ϕ^4 , theory we should be able to extend these techniques to other theories. Scalar field theories with other potentials should not require much additional work but we also highlight [41] [42] [22], in which these techniques have been extended to study the vacuum functional of Yang-Mills theory.

Chapter 6

A Large Distance Expansion of the S Matrix

The Schrödinger equation can be solved by a variety of methods not necessarily perturbative in the coupling or Planck's constant. In particular we shall follow [24], in which a local expansion for the logarithm of the vacuum wavefunctional is found without resorting to any truncation. The one-particle state in a zero-momentum frame has also been calculated using local expansion techniques. In this chapter we will show how to extend this solution to an arbitrary momentum frame of reference. We will also find a type of local expansion for a two-particle wavefunctional.

Such local functionals are of interest because they do not resort to an expansion in terms of the coupling or Planck's constant. These expansions will therefore continue to hold in classically massless theories such as Yang-Mills.

We are particularly motivated by a possible new method of constructing the S matrix. In principle a wavefunctional contains all information about a particular state. We therefore develop a method for extracting the S matrix from the wavefunctionals. When applied to a two-particle local expansion this offers the possibility of finding an S matrix that is not perturbative in either the coupling or Planck's constant. Our representation of the S matrix will not require any complicated integrals as is the case in the Feynman diagram expansion. The contour-integral techniques developed in chapters 3 and 4 can in principle be applied to this S matrix to extract the correct behaviour as the momentum cut-off is removed.

6.1 Finding a Semi-Classical Wavefunctional

It is possible to find a direct semi-classical expansion of the wavefunctional [23] [32] without resorting to the local expansion. This expansion is useful to illustrate some interesting features of the wavefunctional and will also be a good testing ground in recreating the usual Feynman diagram expansion of the S-matrix. We will create the ground state in a similar manner to [23] and then extend the technique to create first a one-particle state and then a two-particle state.

6.1.1 Ground State

We will introduce a momentum cut-off to regulate the divergence associated with the canonical momentum, $\hat{\pi} = -i\hbar\delta/\delta\varphi(x)$ acting twice at the same point in the kinetic term of the Hamiltonian. The Schrödinger equation for the vacuum state $\Psi_0[\varphi] = \exp(W[\varphi]/\hbar)$ is then given as $\lim_{l \rightarrow \infty} F_l[\varphi]$, where

$$F_l[\varphi] = -\frac{\hbar}{2}\Delta_l W + \int dx \left(\frac{1}{2} \left(-\left(\frac{\delta W}{\delta\varphi}\right) + \varphi'^2 + M^2(l)\varphi^2 \right) + \frac{g}{4!}\varphi^4 - \mathcal{E}(l) \right), \quad (6.1.1)$$

$$\Delta_l = \int dx dy \int_{|p|<l} \frac{dp}{2\pi} e^{ip(x-y)} \frac{\delta^2}{\delta\varphi(x)\varphi(y)} = \int_{|p|<l} dp 2\pi \frac{\delta^2}{\delta\tilde{\varphi}(-p)\delta\tilde{\varphi}(p)} \quad (6.1.2)$$

and $\tilde{\varphi}(p) = \int dx \varphi(x) \exp(-ipx)$. We have calculated the l dependence of the parameters in section 5.3

$$M^2(l) = M^2 + \hbar\delta M^2 - \hbar\frac{g}{4} \int_{|p|<l} \frac{dp}{2\pi} \frac{1}{\sqrt{p^2 + M^2}}, \quad (6.1.3)$$

$$\mathcal{E}(l) = \delta\mathcal{E} + \frac{\hbar}{2} \int_{|p|<l} \frac{dp}{2\pi} \left(\sqrt{p^2 + M^2} + \frac{M^2(l) - M^2}{2\sqrt{p^2 + M^2}} \right)^2 + \frac{g\hbar^2}{32} \left(\int_{|p|<l} \frac{dp}{2\pi} \frac{1}{\sqrt{p^2 + M^2}} \right)^2. \quad (6.1.4)$$

where M , \mathcal{E} , δM , $\delta\mathcal{E}$ remain finite as the cut-off is removed. $\delta\mathcal{E}$ and δM are resolved using renormalisation conditions.

We now make an expansion

$$W[\varphi] = \sum_{n=1}^{\infty} \int dp_1 \dots dp_{2n} \tilde{\varphi}(p_1) \dots \tilde{\varphi}(p_{2n}) \Gamma_{2n}(p_1, \dots, p_{2n}) \delta(p_1 + \dots + p_{2n}) \quad (6.1.5)$$

where the Γ are unknown quantities, then $F_l[\varphi]$ becomes

$$-\frac{\hbar}{2} \sum_{n=1}^{\infty} \Delta\Gamma_{2n} - \frac{1}{2} \sum_{n,m} \Gamma_{2n} \circ \Gamma_{2m} + \int dx \left(\frac{1}{2} \varphi'^2 + \frac{1}{2} M^2(l) \varphi^2 + \frac{1}{4!} \varphi^4 - \mathcal{E}(l) \right). \quad (6.1.6)$$

For convenience we have defined $\Delta\Gamma_{2n}$ by¹

$$\int_{|q|<l} 2\pi dq \int dp_3 \dots dp_{2n} 2n(2n-1) \tilde{\varphi}(p_3) \dots \tilde{\varphi}(p_{2n}) \\ \times \Gamma_{2n}(q, -q, p_3, \dots, p_{2n}) \delta(p_3 + \dots + p_{2n}) \quad (6.1.7)$$

and $\Gamma_{2n} \circ \Gamma_{2m}$ by

$$8nm\pi \int dp_2 \dots dp_{2n} dk_2 \dots dk_{2m} \tilde{\varphi}(p_2) \dots \tilde{\varphi}(p_{2n}) \tilde{\varphi}(k_2) \dots \tilde{\varphi}(k_{2m}) \\ \times \Gamma_{2n}(-(p_2 + \dots + p_{2n}), p_2, \dots, p_{2n}) \Gamma_{2m}(-(k_2 + \dots + k_{2m}), k_2, \dots, k_{2m}) \\ \times \delta(p_2 + \dots + p_{2n} + k_2 + \dots + k_{2m}). \quad (6.1.8)$$

The Γ are solved by expanding in positive powers of \hbar , $\Gamma_{2n} = \sum \hbar^m \Gamma_{2n}^{\hbar^m}$. We first compare the \hbar^0 and $\tilde{\varphi}^{2r}$ ($r > 0$) coefficients of (6.1.6) for each r then repeat for \hbar then \hbar^2 etc. So for example we start with coefficients of $\tilde{\varphi}^2$ and \hbar^0 in (6.1.6)

$$\Gamma_2^{\hbar^0}(p, -p) = -\frac{\sqrt{p^2 + M^2}}{4\pi} \equiv -\frac{\omega(p)}{4\pi}, \quad (6.1.9)$$

then $\tilde{\varphi}^4$ and \hbar^0

$$\Gamma_4^{\hbar^0}(p_1, \dots, p_4) = -\frac{g}{(2\pi)^3 (4!) (\omega(p_1) + \dots + \omega(p_4))}, \quad (6.1.10)$$

and continue to find the $\Gamma_{2r}^{\hbar^0}$ from each $\tilde{\varphi}^{2r}$, \hbar^0 coefficient. Now we look at the $\tilde{\varphi}^2$, \hbar^1 coefficient

$$\Gamma_2^{\hbar^1}(p, -p) = \frac{g}{32\pi^2} \int_0^l \frac{dq}{(\omega(q) + \omega(p))\omega(q)}. \quad (6.1.11)$$

then the $\tilde{\varphi}^4$, \hbar^1 etc. In the last equation it became natural to take $\delta M^2 = 0$. However, any choice of δM^2 could in principle be used in these calculations, although such terms would become increasingly complicated.

¹In the $n = 1$ case this should be interpreted as $\Delta\Gamma_2 = 4\pi \int_{|q|<l} dq \Gamma_2(q, -q) \delta(0)$.

The remaining $\Gamma_{2r}^{\hbar^k}$ ($r > 1$ or $r = 1$ with $k > 1$) are given by considering the φ^{2r} and \hbar^k coefficient in (6.1.6). Such terms are given by²

$$-\frac{1}{2} \sum_{n=1}^{\infty} \Delta \Gamma_{2r+2}^{\hbar^{k-1}} - \frac{1}{2} \sum_{n=1}^r \sum_{i=0}^k \Gamma_{2n}^{\hbar^i} \circ \Gamma_{2(r-n+1)}^{\hbar^{k-i}} = 0. \quad (6.1.12)$$

This gives the $\Gamma_{2r}^{\hbar^k}$ in terms of $\Gamma_{2r'}^{\hbar^{k'}}$ with $r' \leq r$, $k' \leq k$ or $r' = r + 1$, $k' = k - 1$. Explicitly,

$$\begin{aligned} \Gamma_{2r}^{\hbar^k}(p_1, \dots, p_{2r}) = & \\ & \frac{2\pi}{\sum_{i=1}^{2r} \omega(p_i)} \mathbf{S} \left\{ \int_{|q| < l} dq (r+1)(2r+1) \Gamma_{2r+2}^{\hbar^{k-1}}(q, -q, p_1, \dots, p_{2r}) \right. \\ & + \sum_{n=2}^{r-1} \sum_{i=0}^k (2 - \delta_{r1}) n(r-n+1) \Gamma_{2n}^{\hbar^i}(-p_1 + \dots + p_{2n-1}, p_1, \dots, p_{2n-1}) \\ & \quad \times \Gamma_{2(r-n+1)}^{\hbar^{k-i}}(-(p_{2n} + \dots + p_{2r}), p_{2n}, \dots, p_{2r}) \\ & \left. + \sum_{i=1}^k 2(2 - \delta_{r1}) r \Gamma_2^{\hbar^i}(-p_1, p_1) \Gamma_{2r}^{\hbar^{k-i}}(-(p_2 + \dots + p_{2r}), p_2, \dots, p_{2r}) \right\} \quad (6.1.13) \end{aligned}$$

where \mathbf{S} instructs us to symmetrise over the momenta p_1, \dots, p_{2r} as defined in section 5.1.1.

6.1.2 One-Particle State

We now construct the one-particle state in the form $\Psi_1[\varphi] = U[\varphi]\Psi_0[\varphi]$ where $U[\varphi]$ has external momentum P and satisfies

$$\frac{\hbar^2}{2} \Delta_l U + \hbar \int dx \frac{\delta W}{\delta \varphi(x)} \frac{\delta U}{\delta \varphi(x)} + E_1 U = 0 \quad (6.1.14)$$

where $E_0 + E_1$ is the one-particle energy and E_0 is the vacuum energy. We expand

$$U = \sum_{n,i=0}^{\infty} \int dp_1 \dots dp_n A_n^{\hbar^i}(p_1, \dots, p_n) \hbar^i \tilde{\varphi}(p_1) \dots \tilde{\varphi}(p_n) \delta(P - (p_1 + \dots + p_n)) \quad (6.1.15)$$

and

$$E_1 = \sum_{i=0}^{\infty} E_1^{\hbar^i} \hbar^i. \quad (6.1.16)$$

²We should regard $\Delta \Gamma_{2n}^{\hbar^{-1}} = 0$

Similarly to before we define ΔA_n by

$$\int_{|q|<l} 2\pi dq \int dp_3 \dots dp_n n(n-1) \tilde{\varphi}(p_3) \dots \tilde{\varphi}(p_n) \\ \times A_n(-q, q, p_3, \dots, p_n) \delta(P - (p_3 + \dots + p_n)) \quad (6.1.17)$$

and $A_n \circ \Gamma_{2m}$ by

$$\int dp_1 \dots p_{2m+n-2} 4\pi n m \tilde{\varphi}(p_1) \dots \tilde{\varphi}(p_{2m+n-2}) \\ \times A_n(p_n + \dots + p_{2m+n-2}, p_1, \dots, p_{n-1}) \\ \times \Gamma_{2m}(-(p_n + \dots + p_{2m+n-2}), p_n, \dots, p_{2m+n-2}) \\ \times \delta(P - (p_1 + \dots + p_{2m+n-2})). \quad (6.1.18)$$

so that the $\tilde{\varphi}^r, \hbar^k$ terms of (6.1.14) becomes

$$\frac{1}{2} \Delta A_{r+2}^{\hbar^{k-2}} + \sum_{\substack{n=0 \\ r-n \text{ even}}}^r \sum_{i=0}^{k-1} A_n^{\hbar^i} \circ \Gamma_{r-n+2}^{\hbar^{k-i-1}} + \sum_{i=0}^k E_1^{\hbar^i} A_r^{\hbar^{k-i}} = 0. \quad (6.1.19)$$

With $k=0$ in (6.1.19) we see that $E_1^{\hbar^0} = 0$ or $A_r^{\hbar^0} = 0 \forall r \geq 0$, the latter clearly violating our ability to choose the normalisation of the wavefunctional. We therefore take the former, which would also be required for the correct classical limit.

Now consider the $k=1$ case. With $r=0$ we have $A_1^{\hbar^0} = 0$ and as r is incremented we see at each stage that $A_r^{\hbar^0} = 0$ for all r unless $E_1^{\hbar^1} = \omega(P) \equiv \sqrt{P^2 + M^2}$. The latter is the correct classical limit and, as we have already stated, the former is undesirable. So we proceed with $E_1^{\hbar^1}$ determined. Since A_1 is non zero in the classical limit we will use our choice of normalisation to set $A_1 = 1$. That is, $A_1^{\hbar^0} = 1$ and $A_1^{\hbar^k} = 0$ for $k \geq 1$. Then with $r=2$ we find $A_2^{\hbar^0} = 0$. With $r=3$ we determine

$$A_3^{\hbar^0}(p_1, p_2, p_3) = \frac{1}{\pi^2 4!} \frac{g}{\omega(\sum_{i=1}^3 p_i)^2 - (\sum_{i=1}^3 \omega(p_i))^2}. \quad (6.1.20)$$

With $r=4$ we get $A_4^{\hbar^0} = 0$ and $r=5$ gives

$$A_5^{\hbar^0}(p_1, \dots, p_5) = \frac{1}{\sum_{i=1}^5 \omega(p_i) - \omega(\sum_{i=1}^5 p_i)} \left\{ 6\Gamma_6^{\hbar^0}(-(p_1 + \dots + p_5), p_1, \dots, p_5) \right. \\ \left. + 12\mathbf{S}A_3^{\hbar^0}(p_3 + p_4 + p_5, p_1, p_2) \Gamma_4^{\hbar^0}(-(p_3 + p_4 + p_5), p_3, p_4, p_5) \right\} \quad (6.1.21)$$

etc. In fact with r even we will inductively get $A_r^{\hbar^0} = 0$ and with r odd we get an expression for $A_r^{\hbar^0}$.

We continue the process of considering (6.1.19) for $k \geq 2$. With $r = 0$ we find each $A_0^{\hbar^{k-1}} = 0$. With $r = 1$ we get the coefficients in the energy expansion

$$E^{\hbar^k} = -6\pi \int_{|q|<l} dq A_3^{\hbar^{k-2}}(-q, q, P) - \sum_{i=0}^{k-1} 4\pi \Gamma_2^{\hbar^{k-i-1}}(-P, P). \quad (6.1.22)$$

For $r > 1$ we get the $A_r^{\hbar^k}$ in terms of the $A_{r'}^{\hbar^{k'}}$ for $r' \leq r$, $k' \leq k$ or $r' = r + 2$, $k' = k - 2$. Rearranging (6.1.19),

$$\begin{aligned} A_r^{\hbar^{k-1}}(p_1, \dots, p_r) = & \\ & \frac{1}{\sum_{i=1}^r \omega(p_i) - \omega(\sum_{i=1}^r p_i)} \mathbf{S} \left\{ \pi \int_{|q|<l} dq (r+2)(r+1) A_{r+2}^{\hbar^{k-2}}(q, -q, p_1, \dots, p_r) \right. \\ & + \sum_{\substack{n=1 \\ r-n \text{ even}}}^{r-1} \sum_{i=1}^{k-1} 2\pi n (r-n+2) A_n^{\hbar^i}(p_n + \dots + p_r, p_1, \dots, p_{n-1}) \\ & \quad \times \Gamma_{r-n+2}^{k-i-1}(-(p_n + \dots + p_r), p_n, \dots, p_r) \\ & \quad + \sum_{i=0}^{k-2} 4\pi r A_r^{\hbar^i}(p_1, \dots, p_r) \Gamma_2^{k-i-1}(-p_1, p_1) \\ & \quad \left. + \sum_{i=2}^k E^{\hbar^i} A_r^{\hbar^{k-i}}(p_1, \dots, p_r) \right\}. \quad (6.1.23) \end{aligned}$$

Note that this would recursively set all the $A_r = 0$ with r even. Therefore U should be expanded in odd powers of φ for the one-particle state, as we would expect.

6.1.3 Two-Particle State

We will construct the two-particle state with momenta P and Q in the form

$$\Psi_2(P, Q) = (U(P)U(Q) + R(P, Q))e^{W/\hbar} \quad (6.1.24)$$

with energy³ $E_0 + E_1(P) + E_1(Q)$. The R satisfies a Schrödinger -type equation

$$\begin{aligned} \frac{\hbar^2}{2} \Delta_l R(P, Q) + \int dx \left(\hbar^2 \frac{\delta U(P)}{\delta \varphi(x)} \frac{\delta U(Q)}{\delta \varphi(x)} + \hbar \frac{\delta R(P, Q)}{\delta \varphi(x)} \frac{\delta W}{\delta \varphi(x)} \right) \\ + (E_1(P) + E_1(Q))R(P, Q) = 0 \quad (6.1.25) \end{aligned}$$

³Although as we see in the next section we will require an additional $\pm i\epsilon$ term in the energy.

To solve this we make an expansion

$$R(P, Q) = \sum_{n,i=0}^{\infty} \int dp_1 \dots dp_n \tilde{\varphi}(p_1) \dots \tilde{\varphi}(p_n) \\ \times \hbar^i B_n^{\hbar^i}(p_1, \dots, p_n) \delta(P + Q - (p_1 + \dots + p_n)) \quad (6.1.26)$$

where the B_n are symmetric in p_1, \dots, p_n . The collated $\tilde{\varphi}^r \hbar^k$ terms in (6.1.25) are

$$\frac{1}{2} \Delta B_{r+2}^{\hbar^{k-2}} + \sum_{n=1}^r \sum_{i=0}^{k-2} A_n^{\hbar^i} \circ A_{r-n+1}^{\hbar^{k-i-2}} + \sum_{\substack{n=1 \\ r-n \text{ even}}}^r \sum_{i=0}^{k-1} B_n^{\hbar^i} \circ W_{r-n+1}^{\hbar^{k-i-1}} + (\omega(P) + \omega(Q)) B_r^{\hbar^{k-1}} = 0 \quad (6.1.27)$$

with the definitions of ΔB_n , $A_n \circ A_m$ and $B_n \circ W_m$ hopefully clear from the previous sections.

With $k = 1$, sequentially incrementing r we see that $B_r^{\hbar^0} = 0$ for all r . The $r = 0$ case reveals

$$B_0^{\hbar^1} = -\frac{2\pi \delta(P + Q)}{\omega(P) + \omega(Q)} \quad (6.1.28)$$

and the remaining $B_0^{\hbar^k} = 0$. We continue the process of examining each coefficient, first incrementing each r for a given k , then incrementing k . A recurrence relation for the remaining $B_r^{\hbar^k}$ can be found from

$$B_r^{\hbar^{k-1}}(p_1, \dots, p_r) = \frac{2\pi}{\sum_{n=1}^r \omega(p_n) - \omega(P) - \omega(Q)} \\ \mathbf{S} \left\{ \sum_{n=1}^{r+1} \sum_{i=0}^{k-2} n(r-n+2) A_n^{\hbar^i}(P - (p_1 + \dots + p_{n-1}), p_1, \dots, p_{n-1}) \right. \\ \times A_{r-n+2}^{\hbar^{k-i-2}}(Q - (p_n + \dots + p_r), p_n, \dots, p_r) \\ + \frac{r(r-1)}{2} B_{r+2}^{\hbar^{k-2}}(p_1, \dots, p_r) \delta(p_1 + p_2) \\ + \sum_{\substack{n=1 \\ r-n \text{ even}}}^r \sum_{i=0}^{k-2} n(r-n+2) B_n^{\hbar^i}(p_n + \dots + p_r, p_1, \dots, p_{n-1}) \\ \times \Gamma_{r-n+2}^{\hbar^{k-i-1}}(-(p_n + \dots + p_r), p_n, \dots, p_r) \\ + \sum_{\substack{n=1 \\ r-n \text{ even}}}^{r-1} n(r-n+2) B_n^{\hbar^{k-1}}(p_n + \dots + p_r, p_1, \dots, p_{n-1}) \\ \left. \times \Gamma_{r-n+2}^{\hbar^0}(-(p_n + \dots + p_r), p_n, \dots, p_r) \right\}. \quad (6.1.29)$$

for $k \geq 2$ and $r \geq 1$. Again, we have the B_r^{hk} in terms of the $B_{r'}^{hk'}$, with $r' \leq r$, $k' \leq k$ or $r' = r + 2$, $k' = k - 2$. The recursion relation immediately tells us that $B_r = 0$ for odd r .

The solutions for the coefficients in the vacuum state (6.1.13) are defined for all p_i subject to being able to compute the integrals. Similarly the quantities in the one-particle state (6.1.23) are equally valid for any choice of momentum. Whilst having a denominator $\omega(\sum_i p_i) - \sum_i \omega(p_i)$, the integral (6.1.15) includes a delta function that restricts $\sum_i p_i = P$. In a zero momentum-frame it is easy to see that this denominator is always non-zero; however, in the 2 particle case we are not so lucky. The denominator in (6.1.29), $\omega(P) + \omega(Q) - \sum_i \omega(p_i)$ is potentially zero when $r = 2$. For example, one part of $R(P, Q)$ will be (with $r = 2$, $k = 2$)

$$6\pi \int dp_1 dp_2 \tilde{\varphi}(p_1) \tilde{\varphi}(p_2) \frac{A_3(-P, p_1, p_2) + A_3(-Q, p_1, p_2)}{\omega(p_1) + \omega(p_2) - \omega(P) - \omega(Q)} \delta(P + Q - p_1 - p_2). \quad (6.1.30)$$

Such denominators will also iteratively find their way into terms with $r > 2$ via (6.1.29). The question now is how do we define integrals such as (6.1.30)? The answer to this question is related to the time-independent definition of the S Matrix as developed by Lippmann and Schwinger [44], as outlined in the next section.

6.2 Generating the S Matrix

We shall work in the interaction picture of quantum mechanics, in which wavefunctions $\Psi'(t)$ are replaced via a unitary transformation so that

$$\Psi'(t) = \exp^{-iH_0 t/\hbar} \Psi(t) \quad (6.2.1)$$

where H_0 is the massive free Hamiltonian and H_1 the interacting part, both time independent. The Schrödinger equation in this picture is

$$i\hbar \frac{\partial \Psi(t)}{\partial t} = H_1(t) \Psi(t) \quad (6.2.2)$$

with

$$H_1(t) = e^{iH_0 t/\hbar} H_1 e^{-iH_0 t/\hbar}. \quad (6.2.3)$$

We are interested in the evolution of an “in” state at $t = -\infty$ into an “out” state at $t = \infty$. This defines the S matrix⁴

$$\Psi(-\infty) = S\Psi(\infty), \quad (6.2.4)$$

$$S_{ba} = (\Psi_b(-\infty), S\Psi_a(\infty)). \quad (6.2.5)$$

We can eliminate the need for in and out states by defining the unitary operator that describes time evolution according to

$$\Psi(t) = U_+(t)\Psi(-\infty), \quad (6.2.6)$$

$$\Psi(t) = U_-(t)\Psi(\infty) \quad (6.2.7)$$

U_+ and U_- satisfy the differential equations

$$i\hbar \frac{\partial U_+(t)}{\partial t} = H_1(t)U_+(t), \quad (6.2.8)$$

$$i\hbar \frac{\partial U_-(t)}{\partial t} = H_1(t)U_-(t), \quad (6.2.9)$$

as can be explicitly checked through use of their definitions and the Schrödinger equation. These differential equations have solutions (satisfying boundary conditions determined by (6.2.6) and (6.2.7))

$$U_+(t) = 1 - \frac{i}{\hbar} \int_{-\infty}^t H_1(t')U_+(t')dt', \quad (6.2.10)$$

$$U_-(t) = 1 + \frac{i}{\hbar} \int_t^{\infty} H_1(t')U_-(t')dt'. \quad (6.2.11)$$

Since $S = U_+(\infty) = U_-(-\infty)$,

$$S = 1 - \frac{i}{\hbar} \int_{-\infty}^{\infty} H_1(t)U_+(t)dt \quad (6.2.12)$$

$$= 1 + \frac{i}{\hbar} \int_{-\infty}^{\infty} H_1(t)U_-(t)dt. \quad (6.2.13)$$

Using this form of the S matrix and the definition of $H_1(t)$, (6.2.3) we can write the T ($\equiv S - 1$) matrix as

$$T_{ba} = \mp \frac{i}{\hbar} \int_{-\infty}^{\infty} dt (\Psi_b, e^{iH_0t/\hbar} H_1 e^{-iH_0t/\hbar} U_{\pm}(t) \Psi_a) \quad (6.2.14)$$

⁴The notation (A,B) is used to indicate the inner product. In the case of the Schrödinger representation of quantum field theory this corresponds to functional integration (5.2.11).

Whist $\Psi_{a,b}$ are supposed to represent non-interacting wavefunctions at fixed time $\pm\infty$, they are not exact eigenfunctions of H_0 . To overcome this we represent the cessation of interaction at $t = \pm\infty$ by introducing a factor $\exp(-\epsilon|t|/\hbar)$ in front of H_1 . With ϵ arbitrarily small we reproduce the original Hamiltonian. We can now introduce eigenstates Φ_a and Φ_b of H_0 with eigenvalues E_a, E_b so that the T matrix is given by

$$T_{ba} = \mp \frac{i}{\hbar} \int_{-\infty}^{\infty} dt (\Phi_b, e^{iE_b t/\hbar} e^{-\epsilon|t|/\hbar} H_1 e^{-iH_0 t/\hbar} U_{\pm}(t) \Phi_a). \quad (6.2.15)$$

The form of the T matrix is simplified by defining

$$\Psi_a^{\pm}(E) = \int_{-\infty}^{\infty} dt e^{i(E-H_0)t/\hbar} e^{-\epsilon|t|/\hbar} U_{\pm} \Phi_a \quad (6.2.16)$$

so that

$$T_{ba} = -\frac{i}{\hbar} (\Phi_b, H_1 \Psi_a^+(E_b)) \quad (6.2.17)$$

$$= -\frac{i}{\hbar} (\Psi_b^-(E_b), H_1 \Phi_a). \quad (6.2.18)$$

Energy conservation in Ψ_a^{\pm} can be made explicit with some algebra. First substitute expressions for U_{\pm} as given by (6.2.10) and (6.2.11) into Ψ_a^{\pm} . Then with $\tau = |t - t'|$,

$$\begin{aligned} \Psi_a^{\pm}(E) &= \int_{-\infty}^{\infty} dt e^{i(E-E_a)t/\hbar} e^{-\epsilon|t|/\hbar} \Phi_a \mp \frac{i}{\hbar} \int_0^{\infty} d\tau e^{\pm i(E-H_0)\tau/\hbar} e^{-\epsilon\tau/\hbar} H_1 \Psi_a^{\pm}(E) \\ &= 2\pi\hbar\delta(E - E_a)\Phi_a + \frac{1}{E \pm i\epsilon - H_0} H_1 \Psi_a^{\pm}(E) \\ &= 2\pi\hbar\delta(E - E_a)\Psi_a^{\pm} \end{aligned} \quad (6.2.19)$$

where

$$\Psi_a^{\pm} = \Phi_a + \frac{1}{E_a \pm i\epsilon - H_0} H_1 \Psi_a^{\pm}. \quad (6.2.20)$$

This leads to a useful definition of the T matrix as given by Lippmann and Schwinger [44],

$$T_{ba} = -2\pi i \delta(E_a - E_b) (\Phi_b, H_1 \Psi_a^+) \quad (6.2.21)$$

$$= -2\pi i \delta(E_a - E_b) (\Psi_b^-, H_1 \Phi_a) \quad (6.2.22)$$

To see how this fits in with the problem of regulating the integrals in the semi-classical expansion of the two-particle states, compare (6.2.19) and (6.2.16). Using the integral representation of the delta function

$$2\pi\hbar\delta(E - E_a) = \int dt e^{i(E-E_a)t/\hbar} \quad (6.2.23)$$

we have

$$e^{-iH_0t/\hbar} e^{-\epsilon|t|/\hbar} U_{\pm}(t) \Phi_a = e^{-iE_a t/\hbar} \Psi_a^{\pm}. \quad (6.2.24)$$

With $t = 0$ this relation is simply

$$\Psi_a^{\pm} = U_{\pm}(0) \Phi_a. \quad (6.2.25)$$

Returning to the definition of the S matrix (6.2.5) and U_{\pm} (6.2.6),(6.2.7), we have

$$S = (\Phi_a, U_-(t)^\dagger U_+(t) \Phi_b) \quad (6.2.26)$$

which at $t = 0$ gives

$$S = (\Psi_a^-, \Psi_b^+). \quad (6.2.27)$$

Also note that (6.2.20) implies that Ψ^{\pm} is an eigenstate of the full Hamiltonian with an addition $\pm i\epsilon$ energy term.

The introduction of an additional $\pm i\epsilon$ to the energy helps define terms such as (6.1.30), and indeed all terms in the semi-classical solution of the two-particle state, (6.1.29). We also have a method of extracting the S matrix via (6.2.26), which also gives a physical interpretation of the $\pm i\epsilon$ term. The $\pm i\epsilon$ term appears to tell us something about the history or future of the state. Without such an additional term it is not clear how to correctly write the wavefunction.

Via the Schrödinger representation of quantum field theory we are now in a position to extract the S matrix from the wavefunctional. In particular this approach to the S matrix is nice to have due to the time independence of the definition. Whilst (6.2.26) is a particularly elegant definition we will find that (6.2.21), (6.2.22) considerably reduces the combinatoric complexity of the calculation.

6.2.1 A Tree-Level Example

The two-particle state with momenta P_1, P_2 and the additional $i\epsilon$ energy term may be calculated as a perturbative expansion in the coupling multiplied by a Gaussian-

type exponential. This is achieved by expanding the exponential terms where appropriate. We have

$$\begin{aligned} \Psi^+[\tilde{\varphi}] = & \left(\tilde{\varphi}(P_1)\tilde{\varphi}(P_2) - \hbar \frac{2\pi\delta(P_1 + P_2)}{\omega(P_1) + \omega(P_2) + i\epsilon} + \mathcal{O}(g) \right) \\ & \times \exp \left(\frac{1}{\hbar} \int dq_1 dq_2 \tilde{\varphi}(q_1)\tilde{\varphi}(q_2)\Gamma_2^{\hbar^0}(q_1, q_2)\delta(q_1 + q_2) \right) \end{aligned} \quad (6.2.28)$$

which is the solution to the free theory (with the extra $i\epsilon$) plus higher order corrections. The interacting part of the Hamiltonian is given by

$$H_1 = \frac{g}{4!(2\pi)^3} \int dq_1 \dots dq_4 \tilde{\varphi}(q_1) \dots \tilde{\varphi}(q_4)\delta(q_1 + \dots + q_4). \quad (6.2.29)$$

We shall take the free solution Φ to have momenta P_3 and P_4 . It will look like (6.2.28) with $\epsilon = 0$ and the momenta P_1, P_2 exchanged for P_3 and P_4 .

We proceed to apply the definition (6.2.21) to calculate the tree-level part of the S matrix. This reduces the problem of finding the S matrix to that of performing Gaussian functional integrals as developed in section 5.1.2. Schematically we require a term of the form

$$\begin{aligned} \int \mathcal{D}\varphi \int dq_1, \dots, dq_4 \tilde{\varphi}(P_1)\tilde{\varphi}(P_2)\tilde{\varphi}(-P_3)\tilde{\varphi}(-P_4)\tilde{\varphi}(q_1) \dots \tilde{\varphi}(q_4)\delta(q_1 + \dots + q_4) \\ \times \exp \left(\frac{2}{\hbar} \int dr_1 dr_2 \tilde{\varphi}(r_1)\tilde{\varphi}(r_2)\Gamma_2^{\hbar^0}(r_1, r_2)\delta(r_1 + r_2) \right). \end{aligned} \quad (6.2.30)$$

The Gaussian functional integral is calculated using the result (5.1.30) where

$$f^{-1}(p, q) = -\frac{2\pi\hbar}{\omega(p)}\delta(p + q). \quad (6.2.31)$$

We are required to pair the field momenta in all possible combinations. Each pairing of momenta then contributes a product of $f^{-1}(p, q)$ terms, where p and q are the paired momenta. We could pair the eight different fields in 105 different ways. We do, however, have a number of simplifications which result in a significant reduction in the combinatorics. The first is due to the symmetry between the interchange of q_1, \dots, q_4 in (6.2.30). This reduces the number of distinct pairings to 10. For simplicity we shall ignore disconnected diagrams and restrict ourselves purely to the connected terms. These terms will have an overall momentum conservation delta function $\delta(P_1 + P_2 - P_3 - P_4)$ but no factors such as $\delta(P_1 - P_3)\delta(P_2 - P_4)$ which

would result in a disconnected diagram. This further reduces the number of terms we require to one. That is the term in which each P_i is paired with q_i . So the only connected term in (6.2.30) is

$$\int dq_1 \dots dq_4 f^{-1}(P_1, q_1) f^{-1}(P_2, q_2) f^{-1}(-P_3, q_3) f^{-1}(-P_4, q_4) \\ = \frac{\sqrt{\pi}^\infty}{\sqrt{\det f}} \frac{(2\pi)^{4!}}{2^4} \hbar^4 \frac{\delta(P_1 + P_2 - P_3 - P_4)}{\omega(P_1)\omega(P_2)\omega(P_3)\omega(P_4)} \quad (6.2.32)$$

where the $4!$ term is due to the different ways that the P_i may be paired with the q_i each generating an equivalent term.

Terms other than (6.2.30) will not produce a connected Feynman diagram and therefore from (6.2.21) we have the tree-level term of the S matrix

$$\eta g \frac{\sqrt{\pi}^\infty}{\sqrt{\det f}} \frac{(2\pi)^{2i}}{2^4} \hbar^4 \frac{\delta^2(P_1 + P_2 - P_3 - P_4)}{\omega(P_1)\omega(P_2)\omega(P_3)\omega(P_4)} \quad (6.2.33)$$

where the parameter η comes from the normalisation of the wavefunctionals. With

$$\eta = 16\omega(P_1)\omega(P_2)\omega(P_3)\omega(P_4) \frac{\sqrt{\det f}}{\sqrt{\pi}^\infty} \quad (6.2.34)$$

we reproduce the correct Feynman diagram term

$$-ig(2\pi)^2 \delta^2(P_1 + P_2 - P_3 - P_4). \quad (6.2.35)$$

Having used the the tree-level Feynman diagram term to calculate η we can remove it from higher order terms in the S matrix.

We shall also apply the alternate definition of the S matrix (6.2.26) to fully understand the role of the ϵ parameter. Again we shall expand the interacting portion of the ground-state exponential. The term of order g in the two-particle wavefunctional (6.1.24) has a number of contributions which we shall write excluding the free exponential for convenience. The first arrives from the order- g portion of R (recall R was defined in (6.1.24))

$$6\pi\hbar \int dq_1 dq_2 \tilde{\varphi}(q_1) \tilde{\varphi}(q_2) \frac{A_3(-P_1, q_1, q_2) + A_3(-P_2, q_1, q_2)}{\omega(q_1) + \omega(q_2) - \omega(P_1) - \omega(P_2) \mp i\epsilon} \delta(P_1 + P_2 - q_1 - q_2) \quad (6.2.36)$$

another from the product $U(P_1)U(P_2)$

$$\int dq_1 dq_2 dq_3 \tilde{\varphi}(q_1) \tilde{\varphi}(q_2) \tilde{\varphi}(q_3) A_3^{\hbar^0}(q_1, q_2, q_3) \\ \times (\tilde{\varphi}(P_1) \delta(P_2 - q_1 - q_2 - q_3) + \tilde{\varphi}(P_2) \delta(P_1 - q_1 - q_2 - q_3)) \quad (6.2.37)$$

and lastly from the order- g term in the ground-state wavefunctional

$$\frac{2}{\hbar} \left(\int dq_1 dq_2 \tilde{\varphi}(q_1) \tilde{\varphi}(q_2) \Gamma_2^{\hbar^1}(q_1, q_2) + \int dq_1 \dots dq_4 \tilde{\varphi}(q_1) \dots \tilde{\varphi}(q_4) \Gamma_4^{\hbar^0}(q_1, \dots, q_4) \right) \times \left(\tilde{\varphi}(P_1) \tilde{\varphi}(P_2) - \hbar \frac{3\pi \delta(P_1 + P_2)}{\omega(P_1) + \omega(P_2)} \right). \quad (6.2.38)$$

The zeroth order in the coupling is somewhat trivial so we will immediately go to the tree-level term. Again we will restrict our attention to the connected terms only and omit the infinite $\sqrt{\pi^\infty}/\sqrt{\det f}$ term. The first term originates from a $\tilde{\varphi}^4$ Gaussian integral

$$\frac{3(2\pi)^3 \hbar^3}{2} \frac{A_3(-P_3, P_1, P_2) + A_3(-P_4, P_1, P_2)}{\omega(P_1) + \omega(P_2) - \omega(P_3) - \omega(P_4) + i\epsilon} \frac{\delta(P_1 + P_2 - P_3 - P_4)}{\omega(P_1)\omega(P_2)} + [(P_1, P_2) \leftrightarrow (P_2, P_3)] \quad (6.2.39)$$

the second is from a $\tilde{\varphi}^8$ term generated using the $\tilde{\varphi}^2$ portion of W

$$\frac{3(2\pi)^3 \hbar^3 A_3(P_1, P_2, -P_4)}{4\omega(P_1)\omega(P_2)\omega(P_4)} \delta(P_1 + P_2 - P_3 - P_4) + [(P_1, P_2) \leftrightarrow (P_2, P_3)] \quad (6.2.40)$$

and the last is also a $\tilde{\varphi}^8$ Gaussian integral

$$3\hbar^3 (2\pi)^4 \frac{\Gamma_4^{\hbar^0}(P_1, P_2, -P_3, -P_4)}{\omega(P_1)\omega(P_2)\omega(P_3)\omega(P_4)} \delta(P_1 + P_2 - P_3 - P_4). \quad (6.2.41)$$

This last $\tilde{\varphi}^8$ integral comes from the $\tilde{\varphi}^4$ portion of W .

We add these terms together and multiply by the normalisation factor η (6.2.34) to get

$$4\pi \hbar^3 g \frac{\omega(P_3) + \omega(P_4)}{\omega(P_1) + \omega(P_2) + \omega(P_3)\omega(P_4)} \frac{-2i\epsilon}{(\omega(P_1) + \omega(P_2) - \omega(P_3) - \omega(P_4))^2 + \epsilon^2} + \mathcal{O}(\epsilon). \quad (6.2.42)$$

Using the well-known limit

$$\lim_{\epsilon \rightarrow 0} \frac{i\epsilon}{x^2 + \epsilon^2} = \pi \delta(x) \quad (6.2.43)$$

we reproduce the tree-level S matrix term exactly, (6.2.35).

For the tree-level terms in the S matrix, in the definition (6.2.21) the ϵ parameter does not play a vital role and is essentially taken to be zero. In the second definition, (6.2.26) the ϵ parameter plays the role of producing the energy-momentum-conserving delta function. Higher-order terms will become increasingly complicated.

The energy conserving delta function is part of the definition (6.2.21), whereas in (6.2.26) this delta function can only come from the $\epsilon \rightarrow 0$ limit given the form of the ground state prefactor. Higher-order Feynman diagrams themselves, however, also require a limiting process to be implemented. For example the 1-loop Feynman diagram

$$-\frac{g^2}{2}\delta^2(P_1 + P_2 - P_3 - P_4) \int d^2k \frac{1}{(k^2 - m^2)(P_1 + P_2 - k)^2 - m^2 + i\tilde{\epsilon}} \quad (6.2.44)$$

will require the limit $\tilde{\epsilon} \rightarrow 0$ to be taken. This process is also encoded in both definitions, (6.2.21) and (6.2.26). We should note, however, that the expressions we expect to get before taking the limit may differ in that $\epsilon = \tilde{\epsilon}$ is not necessarily correct. Having taken the limit, however, our definitions should reproduce the correct S matrix as given by the Feynman diagram expansion.

6.3 The Local Field Expansion

Instead of using the semi-classical expansion described in section 6.1 we will adopt a local field expansion in the Schrödinger representation as outlined in [24] and further developed here. This will have the advantage of avoiding the loop integrals obtained in the semi-classical expansion and will also provide an expansion in powers of the momentum cut-off instead of the coupling. We have a technique which allows us to numerically evaluate asymptotic expansions in the cut-off for the limit in which it is removed. Again this is as prescribed by [24] and the resummation technique examined further in chapter 3. Since we no longer expand in \hbar we shall set it to unity for the remainder of this section.

6.3.1 Ground State

In this approach we multiplicatively renormalise the bare field, φ_0 in the Hamiltonian so that $\varphi_0 = \sqrt{Z}\varphi$ and again impose the momentum cutoff $|p| < l$ via (6.1.2),

$$\Delta_l = \int dx dy \int_{|p|<l} \frac{dp}{2\pi} e^{ip(x-y)} \frac{\delta^2}{\delta\varphi(x)\delta\varphi(y)}. \quad (6.3.1)$$

The ground state, $\Psi_0 = e^W$, satisfies the Schrödinger equation,

$$\Delta_l W + \int dx \left(\left(\frac{\delta W}{\delta \varphi} \right)^2 - Z^2 \varphi'^2 - m_0^2 Z^2 \varphi^2 - \frac{g_0}{12} Z^3 \varphi^4 \right) + 2ZE_0 = 0 \quad (6.3.2)$$

in the limit $l \rightarrow \infty$. Symanzik's Theorem [4] tells us that if we make such a multiplicative renormalisation and tune the bare quantities m_0 and g_0 accordingly then W should be finite apart from a local term proportional to $\int dx \varphi^2$.

We now make a local expansion in the form of (5.6.1). However we introduce new notation for the coefficients in such a way that it will become easier to code the process of solving the coefficients in Maple. Explicitly we write

$$\begin{aligned} W = \int dx & (b_2 \varphi^2 + b_{2,2} \varphi'^2 + b_{2,4} \varphi''^2 + b_{2,6,1} \varphi'''^2 \dots \\ & + b_4 \varphi^4 + b_{4,2} \varphi'^2 \varphi^2 + b_{4,4,1} \varphi''^2 \varphi^2 + b_{4,4,2} \varphi'^4 + \dots \\ & + b_6 \varphi^6 + b_{6,2} \varphi'^2 \varphi^4 + b_{6,4,1} \varphi''^2 \varphi^4 + b_{6,4,2} \varphi'^4 \varphi'^2 + \dots \\ & + b_8 \varphi^8 + b_{8,2} \varphi'^2 \varphi^6 + b_{8,4,1} \varphi''^2 \varphi^4 + b_{8,4,2} \varphi'^6 \varphi'^2 + \dots) \end{aligned} \quad (6.3.3)$$

where the labels on the coefficients, b , represent firstly the number of fields, then the total number of derivatives and lastly a label to distinguish between terms with the same number of fields and derivatives⁵. As outlined in section 5.6, we restrict the local terms to a set of basis elements determined by requiring the power of the field with highest number of derivatives to be greater than one. Other local terms will be linearly related to these basis elements through integration by parts.

The regulated Laplacian acts on the local expansion to generate another local expansion. For example,

$$\Delta_l \int dy \varphi^2 \varphi'^2 = \int dx \left(\frac{2l}{\pi} \varphi'^2 + \frac{2l^3}{3\pi} \varphi^2 \right). \quad (6.3.4)$$

We substitute (6.3.3) into the Schrödinger equation (6.3.2) and obtain an equation

⁵Sometimes only one label is required to identify a coefficient, e.g. b_2 as the φ^2 coefficient. In this case we should regard $b_2 = b_{2,0,1}$ etc. where necessary.

of the form

$$\begin{aligned}
& \int dx \left(\frac{1}{\pi} \left[\left(2b_2 l + \frac{2}{3} b_{2,2} l^3 + \dots \right) + \varphi^2 \left(12b_4 l + \frac{2}{3} b_{4,2} l^3 + \dots \right) \right. \right. \\
& \quad + \varphi'^2 \left(2b_{4,2} l + b_{4,4,1} l^3 + \frac{8}{3} b_{4,4,2} l^3 + \dots \right) + \varphi^4 \left(30b_6 l + \frac{2}{3} b_{6,2} l^3 + \dots \right) \\
& \quad \left. \left. + \varphi^6 \left(56b_8 l + \frac{2}{3} l^3 + \dots \right) + \varphi^2 \varphi'^2 \left(12b_{6,2} l + 16b_{6,4,2} l^3 + \dots \right) \right] \right. \\
& \quad + \left[\varphi^2 4b_2^2 + \varphi'^2 8b_2 b_{2,2} + \varphi^4 b_2 b_4 + \varphi^6 (24b_2 b_6 + 16b_4^2) \right. \\
& \quad \left. + \varphi^2 \varphi'^2 (16b_2 b_{4,2} + 48b_{2,2} b_4 + \dots) \right. \\
& \quad \left. - Z^2 \varphi'^2 - m_0^2 Z^2 \varphi^2 - \frac{g_0}{12} Z^3 \varphi^4 \right) + 2ZE_0 = 0. \quad (6.3.5)
\end{aligned}$$

Equating the coefficients of the basis functionals we obtain an infinite set of algebraic equations relating the coefficients. The equations obtained from the coefficients of 1, φ^2 , φ'^2 and φ^4 ,

$$\frac{2b_2}{\pi} l + \frac{2b_{2,2}}{3\pi} l^3 + \dots + 2ZE_0 = 0 \quad (6.3.6)$$

$$\frac{12b_4}{\pi} l + \frac{2b_{4,2}}{3\pi} l^3 + \dots + b_2^2 - m_0^2 Z^2 = 0 \quad (6.3.7)$$

$$\frac{2b_{4,2}}{\pi} l + \frac{4b_{4,4,2}}{3\pi} l^3 + \dots + 8b_2 b_{2,2} - Z^2 = 0 \quad (6.3.8)$$

$$\frac{30b_6}{\pi} l + \frac{2b_{6,2}}{3\pi} l^3 + \dots + 16b_2 b_4 - \frac{g_0}{12} Z^3 = 0 \quad (6.3.9)$$

involve the bare quantities m_0 , g_0 , E_0 and the multiplicative renormalisation factor Z . The remaining basis functional coefficients relate the various $b_{i,j,k}$ coefficients.

For example,

$$\frac{56b_8}{\pi} l + \frac{2b_{8,2}}{3\pi} l^3 + \dots + 24b_2 b_6 + 16b_4^2 = 0 \quad (6.3.10)$$

$$\frac{12b_{6,2}}{\pi} l + \dots + 16b_2 b_{4,2} + 48 \frac{b_{2,2}}{b_4} = 0 \quad (6.3.11)$$

⋮

These equations need to be solved in conjunction with renormalisation conditions. Since Symanzik's theorem [3] states that all of the $b_{i,j,k}$ coefficients remain finite as the cut-off is removed with the possible exception of b_2 , we will choose renormalisa-

tion conditions

$$b_4 = -\frac{g\mu}{8} \quad (6.3.12)$$

$$b_{2,2} = -\frac{1}{4\mu} \quad (6.3.13)$$

where μ is a finite mass scale and g plays the role of the renormalised coupling.

We solve the $b_{i,j,k}$ with the exception of b_2 , $b_{2,2}$ and b_4 by making an expansion in positive powers of l ,

$$b_{i,j,k} = \sum_{r=0}^{\infty} b_{i,j,k}^r l^r \quad (6.3.14)$$

and equating coefficients in powers of l to zero in (6.3.10), (6.3.11) etc. It is possible to determine each $b_{i,j,k}^r$ in terms of b_2 , $b_{2,2}$ and b_4 . To explain this process we consider the coefficient of a basis functional with F fields and D derivatives in (6.3.5). In turn we consider the equation obtained from equating the l^p coefficient of this term to zero. We note that such an equation has the form

$$\begin{aligned} \sum_{D'=D}^{D+p-1} A_{F,D,r}^{p,D',r'} b_{F+2,D',r'}^{p-1+D-D'} + b_2 b_{F,D,r}^p \\ + \sum_{\substack{D''=D, F'=F-4, p'=p \\ D''=0, F'=4, p'=0, r'=r''}} C_{F,D,r}^{p,D'',F',p',r',r''} b_{F',D'',r'}^{p'} b_{F+2-F',D-D'',r''}^{p-p'} = 0 \end{aligned} \quad (6.3.15)$$

where the A and C are known coefficients. This can be solved for $b_{F,D,r}^p$ in terms of the coefficients $b_{F',D',r'}^{p'}$ where $F' + 2D' + 2p' \leq F + 2D + 2p \equiv Q$ and either $F' = F + 2$, $p' < p$ or $F' < F$, $p' \leq p$, $D' \leq D$.

We build a set of solutions by starting with $p = 0$ and solving the $\{b_{F',D'}^0\}$ for $F' + 2D' \leq Q$. For example the l^0 coefficient of (6.3.10) gives

$$24b_2 + \frac{(g\mu)^2}{4} = 0 \implies b_6^0 = -\frac{(g\mu)^2}{96b_2} \quad (6.3.16)$$

and (6.3.11) gives

$$16b_2 b_{4,2}^0 + \frac{3g}{2} = 0 \implies b_{4,2}^0 = -\frac{3g}{32b_2} \quad (6.3.17)$$

etc. Next we examine the p^1 coefficients, substituting in our known solutions to obtain the $\{b_{F',D'}^1\}$ for $F' + 2D' + 2 \leq Q$. We continue the process, incrementing p each time so that we find the $\{b_{F',D'}^2\}$ then $\{b_{F',D'}^3\}$, and in general finding the

$\{b_{F',D'}^{2p}\}$ for $F' + 2D' + 2p \leq Q$ where we have sequentially considered p ranging from 0 to p' .

All of the coefficients up to some truncated order are solved exactly in terms of unknown quantities m_0 , g_0 and b_2 and known quantities μ and g . We now return to (6.3.6)-(6.3.9) and substitute in the solutions. First we find Z via (6.3.8) then substitute this into (6.3.7) and (6.3.9) to obtain m_0 and g_0 respectively, again as a power series in l . Now b_2 is the only unknown quantity, with everything else expressed in terms of this and the quantities μ and g .

6.3.2 One-Particle State

We now outline how to generate a one-particle local wavefunctional. This was done in [24] for a particle of energy μ , that is a particle in a zero momentum frame. We extend this solution by introducing a particle of arbitrary momentum P and energy $E_0 + E_1$ where $E_1 = \omega(P) \equiv \sqrt{P^2 + m^2}$. We look for a Hamiltonian eigenstate of the form $\Psi_1 = U\Psi_0$, as was the case in the semi-classical expansion. The local expansion of U consists of a sum of terms with an odd number of fields. That is,

$$U[\varphi] = \int dx e^{iPx} (\varphi + c_3\varphi^3 + c_4\varphi^5 + \dots + c_{3,2}\varphi\varphi'^2 + c_{3,4}\varphi\varphi''^2 + \dots) \quad (6.3.18)$$

where again the subscripts of the c coefficients represent first the number of fields, then the total number of derivatives and finally a label to distinguish between basis functionals with the same number of fields and derivatives (if appropriate).

Again we restrict our attention to a basis of local terms which are linearly independent upon integration by parts. These relations are different in a non-zero centre of momentum frame since contributions will come from differentiation of the $\exp(iPx)$ term in (6.3.18). For example

$$\int dx e^{iPx} \varphi\varphi'\varphi''' = \int dx e^{iPx} \left(-\varphi\varphi''^2 + \frac{iP}{3}\varphi'^3 - \frac{iP}{2}(-\varphi'^3 - iP\varphi\varphi'^2) \right). \quad (6.3.19)$$

In the centre of momentum frame, $P = 0$ the total number of derivatives in each term (e.g. 0+1+3 in the LHS of (6.3.19)) is conserved. Now we also have terms where one or more derivatives may be substituted for factors of P . Basis elements should therefore be of the form

$$\varphi^{r_0} \dots \varphi^{(n)r_n} P^{r_{n+1}} \quad (6.3.20)$$

with $r_n > 1$. For terms with $r_n = 1$ we use integration by parts to write them as a linear combination of basis elements. In each local quantity we should consider the total number of derivatives to be defined by $D \equiv r_1 + 2r_2 + \dots + nr_n$ so that $T = D + r_{n+1}$ is conserved upon integration by parts. It should be noted that $r_1 + \dots + nr_n$ must no longer be restricted to even numbers; however, T will necessarily be even. This can be seen by considering an expansion of the coefficients in the semi-classical expansion. We need not make this assumption; however, we would expect this to be reflected upon solving the Schrödinger equation. To include the need to consider powers of P in the basis elements we introduce another index to the c coefficients so that c_{F,D_1,m,D_2} is the coefficient of a basis element comprising of F fields with $D_1 = r_1 + \dots + nr_n$ and $D_2 = r_{n+1}$. The local expansion of U is therefore

$$U[\varphi] = \int dx e^{iPx} \left(\varphi + \sum_{d=0}^{\infty} P^d \left(c_{3,0,1,d} \varphi^3 + c_{4,0,1,d} \varphi^5 + \dots \right. \right. \\ \left. \left. + c_{3,2,1,d} \varphi \varphi'^2 + c_{3,3,1,d} \varphi'^3 + \dots \right) \right). \quad (6.3.21)$$

The $P^d \varphi$ coefficients, $c_{1,0,1,d}$ are fixed by choosing a normalisation of the wavefunctional. In the above we have chosen $c_{1,0,1,d} = \delta_{0d}$.

The differential equation satisfied by U is

$$\Delta_l U + 2 \int dx \left(\frac{\delta W}{\delta \varphi} \frac{\delta U}{\delta \varphi} + E_1 Z U \right) = 0. \quad (6.3.22)$$

Substituting the local expansion (6.3.21) into this differential equation we get

$$\sum_{d=0}^{\infty} P^d \int dx e^{iPx} \left(\left[\varphi \left(6c_{3,0,1,d} l^d + \left(\frac{2}{3} c_{3,2,1,d} - 2iP c_{3,3,1,d} + \frac{4}{3} c_{3,4,1,d} P^2 \right) l^3 + \dots \right) \right. \right. \\ \left. \left. + \varphi \varphi'^2 \left(6c_{5,2,1,d} l^d + \left(4c_{5,4,1,d} + 8c_{5,4,2,d} + \frac{4}{3} iP c_{5,5,2,d} \right) l^3 + \dots \right) + \dots \right] \right. \\ \left. + 2 \left[\varphi (b_{2,0,1} + 2b_{2,2,1} P^2 + \dots) \right. \right. \\ \left. \left. + \varphi \varphi'^2 \left((2b_{4,2,1} + 12c_{3,0,1,d} b_{4,2,1}) + (4b_{4,4,2} + \dots) P^2 + \dots \right) \right] \right. \\ \left. + 2E_1 Z (c_{3,0,1,d} \varphi^3 + c_{3,2,1,d} \varphi \varphi'^2 + \dots) \right) + 2 \int dx e^{iPx} E_1 Z \varphi = 0. \quad (6.3.23)$$

Again we collate coefficients of basis elements and equate them to zero. For example the coefficients of φ and $P^d\varphi\varphi'^2$ are

$$6c_{3,0,1,d}l + \left(\frac{2}{3}c_{3,2,1,d} - 2iPc_{3,3,1,d} + \frac{4}{3}c_{3,4,1,d-2}P^2 \right) l^3 + \cdots + 2E_1Z = 0 \quad (6.3.24)$$

$$\left(6c_{5,2,1,d}l + \left(4c_{5,4,1,d} + 8c_{5,4,2,d} + \frac{4}{3}iPc_{5,5,2,d-1} \right) l^3 + \cdots \right) + 2E_1Zc_{3,2,1,d} = 0. \quad (6.3.25)$$

It can be seen from (6.3.24) that E_1Z itself must be a power series in P and l . Z is independent of P , as seen from calculating the ground state, and it is already known that $E_1 = \omega(P)$ is l independent. On the other hand, the form of E_1Z can be solved for via the Schrödinger equation. We shall achieve this by expanding

$$E_1Z = \sum_{n=0}^{\infty} \sum_{m=0}^{\infty} a_n^m P^n l^m. \quad (6.3.26)$$

The c coefficients themselves may also be solved as a power series in l

$$c_{F,D,n} = \sum_{m=0}^{\infty} c_{F,D,n}^m l^m. \quad (6.3.27)$$

The equations (6.3.24)(6.3.25) etc. may now be solved by equating coefficient of l^p .

In general we have an equation of the form

$$\begin{aligned} & \sum_{D_1=D, D_2=0}^{D_1=D+p-1, D_2=D_1} B_{F,D,r}^{p,D_1,r',D_2} c_{F+2,D_1,r',d+D_2-D_1}^{p-1+D-D_2} + \sum_{p'=0}^p \sum_{d'=0}^d c_{F,D,n,d'}^{p'} a_{d-d'}^{p-p'} \\ & + \sum_{F'=2, p'=0, r'=r'', D_1=0, D_2=D-D_1}^{F'=F+1, p'=p, D_1=D, D_2=d+D-D_1} D_{F,D,r}^{p,D'',F',p',r',r''} b_{F',D_1,r'}^{p'} c_{F+2-F',D_2,r'',d+D-D_1-D_2}^{p-p'} = 0 \end{aligned} \quad (6.3.28)$$

where B and D are unknown coefficients. This is solved for $c_{F,D,n,d}^p$ in terms of $c_{F',D',n',d'}^{p'}$ with $F' + 2D' + 2d' + 2p' \leq F + 2D + 2d + 2p$ and either $F' = F + 2$ with $p' < p$ or $F' < F$ and $D' + d' < D + d$. The $F = 1$ (6.3.24) case is, however, special. In this case we compare coefficients of l^p and look at the basis elements $P^d\varphi$. Since the $c_{1,0,1,d} = \delta_{0d}$ are known quantities we solve instead for a_p^r .

All of the b , c and a coefficients are now determined in terms of μ , g and the unknown quantity b_2 . However, as we know the form of $E_1 = \omega(P)$ and Z as a power series in l we may invert (6.3.24) to determine b_2 . This can then be substituted

back into the other coefficients and quantities including Z . This does not, however, uniquely determine Z . For example Z should be the P^0 coefficient of $E_1 Z/\mu$, the P^2 coefficient of $2\mu E_1 Z$ and the P^4 coefficient of $-8\mu^2 E_1 Z$ etc. In reality each of these quantities has a different power series expansion in l . This is because the energy eigenvalue $\omega(P)$ is determined by relativistic principles. In the Schrödinger representation of quantum field theory Lorentz covariance is not explicitly manifested. Only when the limit $l \rightarrow \infty$ is taken can we expect to recover this. So whilst Z and b_2 can be found as a power series expansion in l in multiple ways each solution should be equivalent in the $l \rightarrow \infty$ limit.

As we intend to take the $l \rightarrow \infty$ limit it should not matter which expansion we use. The approach we outlined solved Z and b_2 by considering the P^0 coefficient of $E_1 Z$. We chose this expansion because the coefficients are solved with $F + 2D + 2d + 2p < Q$, where Q is some predefined level of truncation. This choice of solution allows us to extract a maximal numbers of terms in the l series expansion.

6.3.3 Two-Particle State

The two-particle state is generated in the form $(U(P)U(Q) + R(P, Q))\Psi_0$. R satisfies its own functional differential equation as determined by the Schrödinger equation

$$\Delta_l R(P, Q) + 2 \int dx \left(\frac{\delta U(P)}{\delta \varphi} \frac{\delta U(Q)}{\delta \varphi} + \frac{\delta W}{\delta \varphi} \frac{\delta R(P, Q)}{\delta \varphi} \right) + 2Z(E_1(P) + E_1(Q) + i\epsilon)R(P, Q) = 0. \quad (6.3.29)$$

In principle we could make a local expansion, with the number of fields in each term even:

$$R(P, Q) = \int dx e^{i(P+Q)x} \left(\sum_{s_1=0}^{\infty} \sum_{s_2=0}^{\infty} P^{s_1} Q^{s_2} \left(d_{0,0,1,s_1,s_2} + d_{2,0,1,s_1,s_2} \varphi^2 + \dots + d_{2,2,1,s_1,s_2} \varphi'^2 + d_{4,3,1,s_1,s_2} \varphi \varphi'^3 + \dots \right) \right). \quad (6.3.30)$$

Instead we shall work in a centre of momentum frame in which $Q = -P$. This simplifies the complexity of calculation. The local expansion for R is therefore

$$R(P, Q) = \int dx \left(\sum_{s=0} P^s \left(d_{0,0,1,s} + d_{2,0,1,s} \varphi^2 + \dots \right. \right. \\ \left. \left. + d_{2,2,1,s} \varphi'^2 + d_{4,3,1,s} \varphi \varphi'^3 + \dots \right) \right). \quad (6.3.31)$$

In this momentum frame there is no $\exp(iPx)$ term in the integrand. Therefore the linear dependencies due to integration by parts of local terms will be the same as we had for W . The basis elements will necessarily have an even number of derivatives and even powers of P . This is again seen from an expansion of the semi-classical solution. It may also be seen by noting that the contribution from U in the differential equation (6.3.29) is even in P . and therefore in the number of derivatives. The number of derivatives in the W contribution are even, as are the powers of P in the energy contribution.

The next step is to solve the d coefficients as a power series expansion in l . Our approach so far has, however, been naive, since in making a local expansion we reproduce the problem of defining the two-particle state that we saw in the semi-classical expansion. For example, comparing the φ^2 terms in (6.3.29) to zeroth order in l and P :

$$12c_{3,0,1,0}^0 + 8b_2^0 d_{2,0,1,0}^0 + (4a_0^0 + 2i\epsilon) d_{2,0,1,0}^0 = 0. \quad (6.3.32)$$

Since $b_{2,0,1}^0 = -\mu/2$ and $a_0^0 = \mu$ this reduces to

$$12c_{3,0,1,0}^0 + 2i\epsilon d_{2,0,1,0}^0 = 0. \quad (6.3.33)$$

This suggests, however, that $d_{3,0,1,0}^0$ is undefined in the $\epsilon \rightarrow 0$ limit. This will also be true of some other coefficients. In the semi-classical expansion we discovered that the two-particle state makes little sense without the additional $\pm i\epsilon$ energy term corresponding to the selection of a past or future boundary condition. The local expansion, however, does not make sense in the $\epsilon \rightarrow 0$ limit when made in inverse powers of the mass. For $\epsilon > 0$, however, the local expansion does make sense. We therefore propose two methods of writing the local expansion

- Equations such as (6.3.33) can naively be solved in terms of ϵ . In general the d coefficients will be a power series in negative powers of ϵ . The $\epsilon \rightarrow 0$ limit could be found by using a contour integral method of resummation. The semi-classical solution implies that when ϵ is analytically continued into the complex plane it will have singularities along the imaginary axis. Singularities may therefore need rotating into the left-half complex plane by the usual trick of substituting $\epsilon \rightarrow \epsilon^\alpha$ and taking $\alpha < 1$.
- Instead of expanding $E_1 Z$ in powers of l as calculated from (6.3.24) it may be more appropriate to evaluate E_1 exactly and then use a separate power series for Z in the differential equation (6.3.29). Equations such as (6.3.33) will then have a solution

$$d_{3,0,1} = \frac{12c_3}{4\mu - 4\omega(P) - i\epsilon} \quad (6.3.34)$$

which is valid in the limit $\epsilon \rightarrow 0$ provided $P \neq 0$.

6.4 Computing the S Matrix: Functional Integration

Here we explain how to compute the S-Matrix from the local functional expansion using the time-independent definition (6.2.21). Having computed the local expansion of Ψ^+ we have already found the expansion of Φ , the latter just being Ψ^+ when $g = 0$. So we need to calculate

$$\int \mathcal{D}\varphi (U(P)U(-P))|_{g=0} (U(P)U(-P) + R(P, -P)) H_1 e^{W+W|_{g=0}}. \quad (6.4.1)$$

The $W|_{g=0}$ term in the semi-classical solution is simply the term corresponding to Γ_2 . In the local expansion this is the same as restricting W to the $b_{2,D,n}$ terms.

We know how to compute Gaussian functional integrals from section 5.1.2; therefore we write (6.4.1) in this format. This is achieved by expanding the vacuum

wavefunctional

$$\begin{aligned}
& \exp(W + W|_{g=0}) \\
&= \exp\left(\int dx (2b_2\varphi^2 + 2b_{2,2}\varphi'^2 + \dots + b_4\varphi^4 + \dots + b_6\varphi^6 + \dots)\right) \\
&= \left[1 + \left(\int dx (2b_{2,2}\varphi'^2 + \dots + b_4\varphi^4 + \dots + b_6\varphi^6 + \dots)\right)\right. \\
&\quad \left. + \frac{1}{2!} \left(\int dx (2b_{2,2}\varphi'^2 + \dots + b_4\varphi^4 + \dots + b_6\varphi^6 + \dots)\right)^2 + \dots\right] \exp\left(2 \int dx b_2\varphi^2\right)
\end{aligned} \tag{6.4.2}$$

Now (6.4.1) is a sum of Gaussian integrals of the form

$$\int \mathcal{D}\varphi \left(\int dx_1 e^{iP_r x_1} \varphi^{r_0} \dots (\varphi^{(n)})^{r_n} \right) \dots \left(\int dx_2 e^{iP_s x_2} \varphi^{s_0} \dots (\varphi^{(m)})^{s_m} \right) \times \exp\left(2 \int dy b_2 \varphi^2\right). \tag{6.4.3}$$

The Fourier transform of the φ fields will be needed to reduce this to the Gaussian form as in (5.1.30). All possible pairings of fields outside the exponential will be required. A typical pairing of two fields will be of the form

$$\begin{aligned}
& \int \mathcal{D}\varphi \left(\int dx_1 e^{iP_r x_1} \varphi^{r_0} \dots (\varphi^{(i)})^{r_i} \dots (\varphi^{(j)})^{r_j} \dots (\varphi^{(n)})^{r_n} \right) \\
&\quad \times \dots \left(\int dx_2 e^{iP_s x_2} \varphi^{s_0} \dots (\varphi^{(m)})^{s_m} \right) \exp\left(2 \int dy b_2 \varphi^2\right) \\
&= \frac{\pi}{b_2} \frac{l^{i+j+1}}{i+j+1} \int \mathcal{D}\varphi \left(\int dx_1 e^{iP_r x_1} \varphi^{r_0} \dots (\varphi^{(i)})^{r_i-1} \dots (\varphi^{(j)})^{r_j-1} \dots (\varphi^{(n)})^{r_n} \right) \\
&\quad \times \dots \left(\int dx_2 e^{iP_s x_2} \varphi^{s_0} \dots (\varphi^{(m)})^{s_m} \right) \exp\left(2 \int dy b_2 \varphi^2\right)
\end{aligned} \tag{6.4.4}$$

provided $r_i, r_j \geq 1$. Where fields with different arguments (e.g. $\varphi(x_1)$ and $\varphi(x_2)$) are paired the two local expansions are combined. For example

$$\begin{aligned}
& \int \mathcal{D}\varphi \left(\int dx_1 e^{iP_r x_1} \dots (\varphi^{(i)})^{r_i} \dots \right) \dots \left(\int dx_2 e^{iP_s x_2} \dots (\varphi^{(j)})^{s_j} \dots \right) \\
&\quad \times \exp\left(2 \int dy b_2 \varphi^2\right) \\
&= \frac{\pi}{b_2} \frac{l^{i+j+1}}{i+j+1} \int \mathcal{D}\varphi \exp\left(2 \int dy b_2 \varphi^2\right) \\
&\quad \times \dots \left(\int dx e^{i(P_r+P_s)x} \varphi^{r_0+s_0} \dots (\varphi^{(i)})^{r_i+s_i-1} \dots (\varphi^{(j)})^{r_j+s_j-1} \dots (\varphi^{(n)})^{r_n+s_n} \right)
\end{aligned} \tag{6.4.5}$$

provided $i \neq j$.

This produces some combinatorial problems, since with $2n$ fields there would be $(2n)!/n!/2^n$ distinct ways of pairing them. Clearly this becomes very large very quickly. In reality the $2n$ fields will not be distinct and many of the individual terms will cancel.

Whilst the exponential's prefactor is normally a product of local functionals, the case where only one such local term exists may be simplified. This is done by introducing an orthonormal basis $\{\Psi^{(n)}\}$, with

$$\Psi^{(n)} = c_{n,n}\varphi^{(n)} + c_{n,n-1}\varphi^{n-1} + \dots + c_{n,0}\varphi. \quad (6.4.6)$$

The inner product is defined by

$$\underbrace{\varphi^{(n)}\varphi^{(m)}} = \begin{cases} \frac{n+m+1}{n+m+1}i^{n+m} & \text{if } n+m \text{ odd} \\ 0 & \text{if } n+m \text{ even} \end{cases} \quad (6.4.7)$$

and the $c_{n,m}$ coefficients determined via a Gram-Schmidt orthonormalisation procedure. Now the problem is reduced to finding a sum of terms of the form

$$\int \mathcal{D}\varphi \left(\int dx e^{iPx} \Psi^{r_1} \dots (\Psi^{(n)})^{r_n} \right) \exp \left(2 \int dy b_2 \varphi^2 \right). \quad (6.4.8)$$

This is evaluated by pairing the Ψ terms in all possible combinations. Only the pairing of $\Psi^{(n)}$ with another $\Psi^{(n)}$ term will give a non-zero contribution. This means that only if all of the r_i are even do we get a non zero contribution.

By inserting the power series expansion of the b , c and d coefficients obtained in section 6.3 we produce a power series expansion of the T matrix in the momentum cut-off l . The idea is then to remove the cut-off by using the contour integral techniques of chapters 3 and 4.

6.5 The Computer Program

Solving the coefficients for a local expansion of the wavefunctionals to a high order in the momentum cut-off is a considerable task when done manually. It therefore makes sense that, having developed the relevant mathematics, we should try to automate the procedure.



Computer code for generating the local expansion of the various wavefunctionals is given in appendix A, where a schematic explanation is provided of how these programs work. The computer package used to do this is MAPLE. This is a high-level programming language ideal for the purpose of developing mathematical procedures and techniques. We note, however, that a final implementation of a procedure is likely to be more suitable in a lower-level programming language. We develop the relevant procedures using modest computing facilities; however, in general an implementation involving parallel-processing technology would considerably increase the speed and achievable order of truncation that we may realistically work with.

One of the most demanding parts of our procedure from a computer resources point of view is the initial setup of required structures needed before solving the Schrödinger equation. These structures are needed to describe the basis functionals and the linear dependencies of non basis functionals. The effect of the Laplacian and other functional differential operators must first be determined. These structures, whilst simple to calculate, do require many levels of recursion. We have been successful in generating and executing the procedures relevant to the vacuum, one and two-particle states up to a truncation with $F + 2D + 2p \leq 38$.

We have been slightly less successful in producing the S matrix to such a high order due to the considerable combinatorial problems involved. We have generated the S matrix up to 8 orders in the momentum cut-off l , however, this is insufficient to be successfully apply the modified Borel resummation technique. A more appropriate programming language may be the answer, or a more efficient way of constructing the S matrix from the wavefunctional may be found.

6.6 Summary

We have developed both a semi-classical and local expansion of the one-particle and two-particle state wavefunctionals in the Schrödinger representation. A method of extracting the S Matrix from a wavefunctional has been introduced and applied to the local expansion. The procedure has been automated in MAPLE. We have been unable to extract the S matrix to high orders. In the case of producing the wave-

functional we believe that this is mostly attributable to the choice of programming language. Further research into methods of reducing the combinatorial difficulty would greatly benefit the calculation of the S matrix.

We note, however, that there are some advantages of our technique. The most demanding parts of our procedure are in solving the linear dependencies and constructing the effect of functional differential operators such as the Laplacian on local functionals. We note, however, that these portions of the code are not dependent on the potential of any particular theory. Therefore, having completed the process once, the results may be used to calculate a two-particle state for any scalar field theory, either with a different potential term or different physical parameters. Additionally our procedures do not contain any difficult mathematics such as in the loop integrals in a Feynman diagram approach. In fact all our calculations are based on linear equations.

Chapter 7

Conclusions and Further Research

There are still many technical difficulties outstanding in computing physical quantities in quantum mechanics. These may largely be attributed to the inability of perturbation theory to describe some phenomena and the divergence of these perturbative expansions. For example, in double-well anharmonic oscillators instanton effect become dominant in some domain of the physical parameters of the potential.

Our arsenal of non-perturbative techniques to deal with these problems is limited. Resummation techniques are not usually exact and often do not even provide an error estimate. With the introduction of the modified Borel summation technique discussed in chapter 2 we now have another technique at our disposal. We have refined the technique and produced a method of finding some of the dominant sources of error which in turn may be subtracted from the original estimate to produce a better approximation. With confidence in the accuracy and behaviour of this technique we are in a better position to apply it to theories which are less well understood in the hope of extracting useful information.

We also showed how the analytic structure of an asymptotic series can be used to extract very accurate results. In chapter 4 we showed how to produce energy eigenvalues by resumming the large x behaviour of the wavefunction and tuning the solution until the correct boundary condition is observed. In this approach the exact value of the resummed large- x behaviour was irrelevant. It is the analytic properties of the solution that we look at. As the analytic structure of the solution to the differential equation exhibits discontinuous behaviour it was easy to identify

the solution corresponding to the correct boundary condition.

The analytic structure of quantum mechanical wavefunctions has been of increasing interest lately in \mathcal{PT} -symmetric quantum mechanics. In these theories it is necessary to analytically continue x into the complex plane so that the differential equation is defined along some contour. For example

$$-\frac{d^2\Psi}{dx^2} + x^2\Psi - gx^4\Psi = E\Psi \quad (7.0.1)$$

with $g > 0$ is at first sight a Hermitian theory defined along the real x axis and therefore has real energy eigenvalues. This is actually incorrect, as the boundary condition $\lim_{|x|\rightarrow\infty} \Psi$ does not make sense for real x . Instead the boundary condition is defined so that $\Psi \rightarrow 0$ when $|x| \rightarrow \infty$ within the complex plain with $-\pi/3 < \arg(x) < 0$ and $\pi < \arg(x) < 4\pi/3$. In a Hermitian theory, the n th excited wavefunction has n nodes along the real axis. It is proposed that this is also true for a \mathcal{PT} -symmetric theory, but the nodes now lie on a contour between the turning points of the potential [43]. The exact analytic structure of nodes in the complex plane for both Hermitian and \mathcal{PT} -symmetric theories is clearly of interest and in need of further study. Indeed we hope that our technique of tuning for the correct boundary condition might be adapted to work with these types of theories.

Whilst quantum field theory has been incredibly successful as a mathematical language for the description of physics at its most fundamental level we still have few tools for extracting meaningful observables from its rich mathematical structure. The Schrödinger representation of quantum field theory offers the ability to use the lessons learnt in quantum mechanics. With an additional technique in non-perturbative and divergent quantum mechanical expansions we are slightly closer to understanding these quantum field theory problems.

Whilst we do not claim credit for the semi-classical expansion of the vacuum ϕ^4 field theory wavefunctional, we have managed to extend the technique to produce a one-particle and two-particle wavefunctional. The definition of the two-particle wavefunctional is not clear without the introduction of an additional $\pm i\epsilon$ term to the energy. This is also linked to the time-independent definition of the S matrix. We have explicitly shown that this time-independent definition of the S matrix correctly reproduces the Feynman diagram expansion at low orders.

Mansfield [24] originally found a method of producing a local expansion of the logarithm of the vacuum functional for fields that varied slowly on the scale of the lightest mass. Use of a modified Borel summation technique allows the full wavefunctional to be reconstructed from the local expansion. Mansfield also produced a type of local expansion for the one-particle wavefunctional in a centre of momentum frame. We have extended this technique to produce a one-particle state in an arbitrary momentum frame. We have also shown how to produce a type of local expansion for a two-particle state.

We have produced MAPLE code to automate the solution of the two-particle wavefunctional. We have also coded the functional integration required to produce the S matrix. It is not clear how best to write the local two-particle wavefunctional. There are a number of suggested ways of doing this; however, a numerical study needs to be undertaken to determine the best approach.

Before numerical results may be extracted from the large distance expansion of the S matrix we first need to be able to complete the procedure up to a higher order of truncation. This may be achieved in a number of ways

- Use of a lower level programming language
- Parallelising the procedure
- Use of a less demanding combinatorial approach to the S matrix

We remain confident that study of a local expansion of the S matrix is worth continued study. Should we be able to achieve sufficient orders in the expansion we should be able to find a good approximation to the exact S matrix. Our approach has the advantage of only requiring the solution of linear equations, as opposed to the tricky loop integrals in the Feynman diagram approach. Also, having setup the required linear dependencies between basis elements etc. we will have completed most of the work needed to produce the S matrix for different theories. We see no reason why this technique cannot be extended to non scalar theories such as Yang Mills.

Appendix A

Computer Programs: Large Distance Expansions

In what follows we describe the basic principles behind coding the solution of the Schrödinger equation and computing the S matrix. We also include the relevant MAPLE code for completing each task.

A.1 Generating the Basis Elements

We have seen how basis elements can be represented by three numbers F , D and n where F represents the total number of fields, D the total number of derivatives and n an index to differentiate between different elements with the same number of fields and derivatives. Where an external momentum is required (such as in the one-particle state) then an additional parameter will be required to represent powers of P . We temporarily ignore this, however, as these powers of P are easily reinstated later.

In solving the Schrödinger equation it will be necessary to know the exact structure of each element. This is done by generating an array in MAPLE, be $[F, D, n, r]$ which for each r represents the power of the field with r derivatives. For example, the basis element represented by $[F, D, n] = [4, 10, 4]$ is

$$\int dx e^{iPx} \varphi \varphi'' (\varphi^{(4)})^2 \tag{A.1.1}$$

and $\text{be}[4,10,4,r]$ will be 1,0,1,0,2 for $r = 0,1,2,3,4$ respectively. The highest possible value of r for a given functional is represented by the matrix element $\text{be}[F,D,n,-1]$, so in the above example $\text{be}[4,10,4,-1]=4$. It will also be necessary to know the range that n may take for a given F and D . An array $\text{track}[F,D]$ represents the highest possible value of n . Whilst F and D may take on any non negative integer we must realistically truncate the expansion and therefore specify an upper limit on F and D by G and H .

Another piece of information that will be helpful later is a representation of the local functionals by a number unique to that particular element. The above functional for example would be represented as 20101 in base $G+2$ but stored as a base 10 number in $\text{be}[F,D,n,-2]$. In general

$$\text{be}[F,D,n,-2] = \sum_{r=0}^{\text{be}[F,D,n,-1]} \text{be}[F,D,n,r](G+2)^r. \quad (\text{A.1.2})$$

The basis elements are assigned the identifier n in such a way that they are ordered by the base $G+2$ representation. That is $\text{be}[F,D,n1,-2] < \text{be}[F,D,n2,-2]$ provided $n1 < n2$.

Upon functionally differentiating basis elements we may get a non basis local functional. These reduce to a sum of basis elements using linear dependencies determined through differentiation by parts. We should therefore generate a list of all possible local functionals and will need to find the linear relations. The above structures are therefore produced for all local functionals not necessarily restricted to basis elements. These arrays are labelled $\text{ntrack}[F,D]$ and $\text{nbe}[F,D,n,r]$ whereas the previous arrays strictly contain the basis elements. They will contain the relevant information to describe all local functionals with a given number of fields and derivatives. Some of these functionals will be basis elements; however, some will not. Note that the index n in $\text{nbe}[F,D,n,r]$ will not necessarily correspond with the same index in $\text{be}[F,D,n,r]$. Also, in reality it is the nbe and ntrack arrays that are calculated first. The basis elements are then found by selecting only those local functionals with $\text{nbe}[F,D,n,r] > 1$ when $r = \text{nbe}[F,D,n,-1]$.

The procedure that produces the structures outlined so far is called via the command $\text{basis}[G,H]$. The relevant MAPLE code is given below. Credit for this

procedure belongs to Paul Mansfield.

```

basis:=proc(fields,dimension)
global be,track;
for G from 0 by 1 to fields do
for H from 0 by 1 to dimension do
track[0,H]:=0:track[1,H]:=0:
basis1(G,H,fields):
number:=0:
for n from 1 by 1 to numb do
if nbe[G,H,n,nbe[G,H,n,-1]]>1 then
number:=number+1:
for nn from -2 by 1 to nbe[G,H,n,-1] do
be[G,H,number,nn]:=nbe[G,H,n,nn]: od:
track[G,H]:=number:
fi:od:
od:od:
be[0,0,1,-2]:=0: track[0,0]:=1:track[1,0]:=1:
end:

basis1:=proc(G,H,fields)
global numb,nbe,ntrack;
numb:=0:
j:=array(0..24):
n25:=G:
for n24 from n25 by -1 to n25-iquo(H,24) do
j[24]:=n25-n24: dim24:=j[24]*24:
for n23 from n24 by -1 to n24-iquo(H-dim24,23) do
j[23]:=n24-n23: dim23:=dim24+j[23]*23:
for n22 from n23 by -1 to n23-iquo(H-dim23,22) do
j[22]:=n23-n22: dim22:=dim23+j[22]*22:
for n21 from n22 by -1 to n22-iquo(H-dim22,21) do

```

```

j[21]:=n22-n21: dim21:=dim22+j[21]*21:
for n20 from n21 by -1 to n21-iquo(H-dim21,20) do
  j[20]:=n21-n20: dim20:=dim21+j[20]*20:
for n19 from n20 by -1 to n20-iquo(H-dim20,19) do
  j[19]:=n20-n19: dim19:=dim20+j[19]*19:
for n18 from n19 by -1 to n19-iquo(H-dim19,18) do
  j[18]:=n19-n18: dim18:=dim19+j[18]*18:
for n17 from n18 by -1 to n18-iquo(H-dim18,17) do
  j[17]:=n18-n17: dim17:=dim18+j[17]*17:
for n16 from n17 by -1 to n17-iquo(H-dim17,16) do
  j[16]:=n17-n16: dim16:=dim17+j[16]*16:
for n15 from n16 by -1 to n16-iquo(H-dim16,15) do
  j[15]:=n16-n15: dim15:=dim16+j[15]*15:
for n14 from n15 by -1 to n15-iquo(H-dim15,14) do
  j[14]:=n15-n14: dim14:=dim15+j[14]*14:
for n13 from n14 by -1 to n14-iquo(H-dim14,13) do
  j[13]:=n14-n13: dim13:=dim14+j[13]*13:
for n12 from n13 by -1 to n13-iquo(H-dim13,12) do
  j[12]:=n13-n12: dim12:=dim13+j[12]*12:
for n11 from n12 by -1 to n12-iquo(H-dim12,11) do
  j[11]:=n12-n11: dim11:=dim12+j[11]*11:
for n10 from n11 by -1 to n11-iquo(H-dim11,10) do
  j[10]:=n11-n10: dim10:=dim11+j[10]*10:
for n9 from n10 by -1 to n10-iquo(H-dim10,9) do
  j[9]:=n10-n9: dim9:=dim10+j[9]*9:
for n8 from n9 by -1 to n9-iquo(H-dim9,8) do
  j[8]:=n9-n8: dim8:=dim9+j[8]*8:
for n7 from n8 by -1 to n8-iquo(H-dim8,7) do
  j[7]:=n8-n7: dim7:=dim8+j[7]*7:\
for n6 from n7 by -1 to n7-iquo(H-dim7,6) do
  j[6]:=n7-n6: dim6:=dim7+j[6]*6:

```


A.2 Setting up the Problem

Before solving for the relevant coefficients in the local expansions of the wavefunctionals it is necessary to set up certain structures. It will be important to know the linear dependencies of local functionals on a set of basis elements. Also, we will need to know the effect of the various functional differential operators such as the Laplacian. This will be necessary in order to compare the coefficients of basis functionals in the Schrödinger equation. From the point of view of automating the procedure in MAPLE this will be the most challenging task, both in terms of the code required and the processor time needed to complete the computations. The procedure that does this is called via the command `pSetupsimp(p)` where p sets the level of truncation by considering basis elements with $F + 2D \leq 2p + 2$. The procedure itself is reproduced at the end of this section.

The MAPLE code was originally written by Paul Mansfield for the purpose of setting up structures needed to solve the vacuum and one-particle wavefunctionals in a centre of momentum frame. Since then, the procedure has been significantly modified and extended. The structures required for the one-particle state have been altered to include an external momentum. This required modifying the linear dependencies between the local functionals. The procedure has also been altered to include provision for the two-particle state.

In what follows the procedure is broken down to explain briefly how each task is automated. The MAPLE variables used and output are described.

Solving the Linear Dependencies

We need to solve the linear dependencies between local functionals. In MAPLE the basis elements are represented by `ER[F,D,n]` and non-basis functionals in a centre of momentum frame by `EE[F,D,n]`. The `EE` are therefore expressed as a linear combination of the `ER`. Consider the example (5.6.6)

$$\int dx \varphi \varphi'^2 \varphi'' = -\frac{1}{3} \int dx \varphi'^4. \quad (\text{A.2.1})$$

In MAPLE, this relationship is expressed $EE[4,4,2] = -ER[4,4,1]/3$. If an external momentum is introduced the relation changes to

$$\int dx e^{iPx} \varphi \varphi'^2 \varphi'' = -\frac{1}{3} \int dx e^{iPx} \varphi'^4 - IP \int dx e^{iPx} \varphi \varphi'^3. \quad (A.2.2)$$

The additional term is stored by the variable $EP[4,4,2]$ as $-I*P*ER[4,3,1]/3$. The momentum dependence is stored separately and may be included depending on whether it is required.

To reduce a non-basis functional to a sum of basis elements we apply functional differentiation. In a centre of momentum frame of reference

$$\begin{aligned} \int dx \varphi^{r_0} (\varphi')^{r_1} \dots (\varphi^{(m-1)})^{r_{m-1}} \varphi^{(m)} = \\ - \int dx \varphi^{(m-1)} \partial_x \left(\varphi^{r_0} (\varphi')^{r_1} \dots (\varphi^{(m-1)})^{r_{m-1}} \right). \end{aligned} \quad (A.2.3)$$

Upon completing the differentiation, the right hand side is a sum of local functionals. The unique identifier $nbe[F,D,n,-2]$ for each term on the right hand side will be less than or equal to that corresponding to the original functional. This is because the decrease in the identifier for each term will be

$$\begin{aligned} (G+2)^m - (G+2)^{m-1} + (G+2)^{p-1} - (G+2)^p \\ = (G+1)(G+2)^{m-1} - (G+1)(G+2)^{p-1} \geq 0 \end{aligned} \quad (A.2.4)$$

for $p = 0 \dots m$. The basis elements are ordered to ensure that when $n1 < n2$, $nbe[F,D,n1,-2] < nbe[F,D,n1,-2]$. The linear dependencies may therefore be calculated by expressing $EE[F,D,n2]$ linearly in terms of the $EE[F,D,n1]$ with $n1 < n2$ and coefficients determined by the r_i .

In a non zero centre of momentum frame we require an additional $EP[F,D,n]$ to represent the contribution due to the spatial derivative acting on the $\exp(iPx)$ factor as given by

$$-iP \int dx e^{iPx} \varphi_0^r (\varphi')^{r_1} \dots (\varphi^{(m-1)})^{r_{m-1}+1}. \quad (A.2.5)$$

This contribution is $-iP$ times a local functional with $D-1$ derivatives. Therefore $EP[F,D,n]$ may be recursively written in terms of the $EE[F,D,p] + EP[F,D-1,p]$.

The Laplacians: $\Delta_l W$, $\Delta_l U$ and $\Delta_l R$

The Laplacian of a general local functional is given by

$$\begin{aligned} \pi \Delta_l \int dx e^{iPx} \varphi^{r_0} (\varphi')^{r_1} \dots (\varphi^{(m)})^{r_m} \\ = \sum_{i \neq j} \frac{r_i r_j}{i+j+1} l^{i+j+1} \int dx e^{iPx} \varphi^{r_0} (\varphi')^{r_1} \dots (\varphi^i)^{r_i-1} \dots (\varphi^j)^{r_j-1} \dots (\varphi^{(m)})^{r_m} \\ + \sum_{i|r_i \geq 2} \frac{r_i(r_i-1)}{2i+1} l^{2i+1} \int dx e^{iPx} \varphi^{r_0} (\varphi')^{r_1} \dots (\varphi^i)^{r_i-2} \dots (\varphi^{(m)})^{r_m}. \end{aligned} \quad (\text{A.2.6})$$

The terms on the right hand side are not necessarily basis functionals; however, the linear dependencies already calculated can be used to reduce these terms to a sum of basis elements. In the case of $\Delta_l W$ and $\Delta_l R$ we work in a centre of momentum frame. The linear dependencies are therefore given by EE. For $\Delta_l U$ an external momentum contribution should be included, so the dependencies are given by EE+EP. The exponential term in (A.2.6) is not relevant from the point of view of calculating the Laplacians other than to remind us to use the correct linear dependencies. The overall π factor is ignored when calculating the structure of the Laplacian as this is easily reinstated later.

The MAPLE variables `lapW`, `lapU`, `lapR` represent a sum of the Laplacian acting upon all basis elements which have either an odd or even number of fields as appropriate. Each term would be represented by a coefficient multiplied by a basis element and a power of l , e.g. `B[F,D1,n1]*ER[F-2,D2,n2]*l^p`. We shall use the array variables `B`, `C` and `D` to represent the coefficients in the W , U and R functionals. The arrays `lapmW[F,D,n]`, `lapmU[F,D,n]`, `lapmR[F,D,n]` represent coefficient of basis elements in `lapW` etc. when collated.

Products of Functional Derivatives

Here we explain how to calculate the following products of functional derivatives

$$\int dx \left(\frac{\delta W}{\delta \varphi} \right)^2, \quad \int dx \frac{\delta W}{\delta \varphi} \frac{\delta U(P)}{\delta \varphi}, \quad \int dx \frac{\delta U(P)}{\delta \varphi} \frac{\delta U(-P)}{\delta \varphi}, \quad \int dx \frac{\delta W}{\delta \varphi} \frac{\delta R}{\delta \varphi}. \quad (\text{A.2.7})$$

For a general functional

$$\begin{aligned} \frac{\delta}{\delta\varphi(x)} \int dy e^{iPy} \varphi^{r_0} \dots (\varphi^{(m)})^{r_m} \\ = \sum_i r_i (-1)^i \frac{\partial}{\partial x^i} \left(e^{iPx} \varphi^{r_0} \dots (\varphi^{(i)})^{r_{i-1}} \dots (\varphi^{(m)})^{r_m} \right). \end{aligned} \quad (\text{A.2.8})$$

We start in a centre of momentum frame of reference in which case all i derivatives are acting directly on a local functional and not on the $\exp(iPx)$. Suppose this functional is represented by the numbers $[F, D, n]$ where n refers to an index in $\text{nbe}[F, D, n, r]$ (not necessarily a basis element). The i th derivative will be a linear combination of basis elements with F fields and $D + i$ derivatives. In MAPLE $\text{dp}[i, F, D+i, n1, F, D, n]$ is the coefficient of the local functional described by the $n1$ index. For example

$$\frac{\partial}{\partial x} (\varphi^2 \varphi') = 2\varphi (\varphi')^2 + \varphi^2 \varphi''. \quad (\text{A.2.9})$$

The functional differentiated is represented by $[3, 1, 1]$ and the functionals on the right hand side are represented by $[3, 2, 2]$ and $[3, 2, 1]$. The result of this differentiation is specified in MAPLE by $\text{dp}[1, 3, 2, 1, 3, 1, 1]=1$ and $\text{dp}[1, 3, 2, 2, 3, 1, 1]=2$.

Using this information we can generate an array $\text{ddp}[F, D, n]$ to represent contributions from the functional derivative of W which result in a term proportional to a $[F, D, n]$ local functional. This will be a linear combination of the coefficients $\text{B}[F+1, D, n1]$. Similarly the array $\text{ddpR}[F, D, n]$ collates terms relevant to the functional derivative of R .

For the functional derivative of U it is necessary to include the contribution due to some of the i spatial derivatives acting on the $\exp(iPx)$ factor. The structure dp can again be used and the relevant number of iP factors inserted. These additional contributions are stored in the array $\text{ddpPU}[F, D, n]$ with $\text{ddpU}[F, D, n]$ representing the zero-momentum contribution.

To calculate the products of these functional derivatives as in (A.2.7) we simply multiply the ddp , ddpU and ddpR terms and apply the relevant linear dependencies to the functionals. Initially the products are calculated as a sum of all relevant terms and stored in the MAPLE variables class , prodUW , prodUU and prodWR . Terms are then collated with coefficients of basis elements stored in the arrays $\text{classm}[F, D, n]$, $\text{prodUWm}[F, D, n]$, $\text{prodUUm}[F, D, n]$ and $\text{prodWRm}[F, D, n]$.

The Procedure

```
pSetupsimp:=proc(ph)
global be,track,nbe,ntrack,classm,lapm,B,C,lapUm,prodUWm,lapRm,
prodRWm,prodUUm,P,EE,EP,ddpU,ddp,dpU,ddpPU,lapU,prodUW;
FF:=2*ph+2:Fields:=FF:Dimension:=ph:
basis(Fields,ph):
```

This part solves the linear dependencies between the local expansion functionals.

```
for F from 1 by 1 to Fields do
  EE[F,1,1]:=0:EP[F,1,1]:=-I*P*ER[F,0,1]/F:
od:
for DD from 1 by 1 to ph-1/2+1 do
  EE[1,DD,1]:=0:EP[1,DD,1]:=-I*P*(EE[1,DD-1,1]+EP[1,DD-1,1]):
od:
for F from 2 by 1 to Fields do
  for DD from 2 by 1 to ph-F/2+1 do
    for n from 1 by 1 to ntrack[F,DD] do
      hi:=nbe[F,DD,n,-1]:
      if nbe[F,DD,n,hi]=1 then
        EE[F,DD,n]:=0:
        EP[F,DD,n]:=0:
        for p from 0 by 1 to hi-2 do
          if nbe[F,DD,n,p]>0 then
            nn:=0: m:=1:
            while nn=0 do
              if nbe[F,DD,m,-2]=nbe[F,DD,n,-2]+(FF+2)^(hi-1)-(FF+2)^hi
+(FF+2)^(p+1)-(FF+2)^p then nn:=m: fi:
              m:=m+1:
            od:
            EE[F,DD,n]:=EE[F,DD,n]-EE[F,DD,nn]*nbe[F,DD,n,p]
/(nbe[F,DD,n,hi-1]+1):
```

```

      EP[F,DD,n] :=EP[F,DD,n]-EP[F,DD,nn]*nbe[F,DD,n,p]
/(nbe[F,DD,n,hi-1]+1):
  fi:
  od:
  nn:=0: m:=1:
  while nn=0 do
    if nbe[F,DD-1,m,-2]=nbe[F,DD,n,-2]+(FF+2)^(hi-1)-(FF+2)^hi then
      nn:=m:
      fi:
      m:=m+1:
    od:
    EP[F,DD,n] :=EP[F,DD,n]-I*P*(EE[F,DD-1,nn]+EP[F,DD-1,nn])
/(nbe[F,DD,n,hi-1]+1):
  else
    nn:=0: m:=1:
    while nn=0 do
      if be[F,DD,m,-2]=nbe[F,DD,n,-2] then nn:=m: fi:
      m:=m+1:
    od:
    EE[F,DD,n] :=ER[F,DD,nn]:
    EP[F,DD,n] :=0:
  fi:
  od:
od:
od:
for F from 0 by 1 to Fields do EE[F,0,1] :=ER[F,0,1]:EP[F,0,1] :=0:od:

```

This part calculates the Laplacian applied to W and R .

```

lap:=0:
lapR:=0:
for F from 2 by 2 to Fields do
  for DD from 0 by 2 to ph-F/2+1 do

```

```

for n from 1 by 1 to track[F,DD] do
  hi:=be[F,DD,n,-1]:
  for p from 0 by 1 to hi do
    if be[F,DD,n,p]>1 then
      nn:=0:  m:=1:
      while nn=0 do
        if nbe[F-2,DD-2*p,m,-2]=be[F,DD,n,-2]-2*(FF+2)^p then
          nn:=m:
          fi:
          m:=m+1:
        od:
        lapR:=lapR+D[F,DD,n]*be[F,DD,n,p]*(be[F,DD,n,p]-1)
*EE[F-2,DD-2*p,nn]*1^(2*p+1)/((2*p+1)):
        lap:=lap+B[F,DD,n]*be[F,DD,n,p]*(be[F,DD,n,p]-1)
*EE[F-2,DD-2*p,nn]*1^(2*p+1)/((2*p+1)):
        fi:
      if p>0 then
        for q from 0 by 1 to p-1 do
          if be[F,DD,n,p]*be[F,DD,n,q]>0 then
            if 2*iquo(p,q,2)=p+q then
              nn:=0:  m:=1:
              while nn=0 do
                if nbe[F-2,DD-p-q,m,-2]=be[F,DD,n,-2]-(FF+2)^p-(FF+2)^q then
                  nn:=m:
                  fi:
                  m:=m+1:
                od:
                lap:=lap+2*(-1)^((p-q)/2)*B[F,DD,n]*be[F,DD,n,p]*be[F,DD,n,q]
*EE[F-2,DD-p-q,nn]*1^(p+q+1)/((p+q+1)):
                lapR:=lapR+2*(-1)^((p-q)/2)*D[F,DD,n]*be[F,DD,n,p]
*be[F,DD,n,q]*EE[F-2,DD-p-q,nn]*1^(p+q+1)/((p+q+1)):

```

```

    fi:
  fi:
od:
fi:
od:
od:
od:
od:
od:

```

This part calculates the Laplacian applied to U .

```

lapU:=0:
for F from 3 by 2 to Fields do
  for DD from 0 by 1 to ph-F/2+1 do
    if DD<>1 then
      for n from 1 by 1 to track[F,DD] do
        hi:=be[F,DD,n,-1]:
        for p from 0 by 1 to hi do
          if be[F,DD,n,p]>1 then
            nn:=0:  m:=1:
            while nn=0 do
              if nbe[F-2,DD-2*p,m,-2]=be[F,DD,n,-2]-2*(FF+2)^p then
                nn:=m:
              fi:
              m:=m+1:
            od:
            lapU:=lapU+C[F,DD,n]*be[F,DD,n,p]*(be[F,DD,n,p]-1)
            *(EE[F-2,DD-2*p,nn]+EP[F-2,DD-2*p,nn])*1^(2*p+1)/((2*p+1)):
          fi:
          if p>0 then
            for q from 0 by 1 to p-1 do
              if be[F,DD,n,p]*be[F,DD,n,q]>0 then
                if 2*iquo(p+q,2)=p+q then

```

```

nn:=0: m:=1:
while nn=0 do
  if nbe[F-2,DD-p-q,m,-2]=be[F,DD,n,-2]-(FF+2)^p-(FF+2)^q
then nn:=m: fi:
  m:=m+1:
od:
lapU:=lapU+2*(-1)^((p-q)/2)*C[F,DD,n]*be[F,DD,n,p]
*be[F,DD,n,q]*(EE[F-2,DD-p-q,nn]+EP[F-2,DD-p-q,nn])
*l^(p+q+1)/((p+q+1)):
  fi:
  fi:
od:
  fi:
od:
od:
  fi:
od:
od:

```

This part calculates the functional derivative of W and R .

```

check:=array(0..Fields-1,0..Dimension,0..ntrack[Fields,Dimension]
,0..Dimension,0..ntrack[Fields,Dimension],sparse);
dp:=array(0..Dimension,0..Fields-1,0..Dimension
,0..ntrack[Fields,Dimension],0..Fields-1,0..Dimension
,0..ntrack[Fields-1,Dimension],sparse):
ddp:=array(0..Fields-1,0..Dimension
,0..ntrack[Fields,Dimension],sparse);
ddpR:=array(0..Fields-1,0..Dimension
,0..ntrack[Fields,Dimension],sparse);
ddp[1,0,1]:=2*B[2,0,1]:
ddpR[1,0,1]:=2*D[2,0,1]:
for F from 1 by 2 to Fields-1 do

```

```

for DD from 0 by 1 to ph-F/2+1 do
  for n from 1 by 1 to ntrack[F,DD] do
    hi:=nbe[F,DD,n,-1]:
    dp[0,F,DD,n,F,DD,n]:=1:
    if nbe[F,DD,n,hi]>1 and 2*iquo(DD,2)=DD then
      nn:=0:  m:=1:
      while nn=0 do
        if be[F+1,DD,m,-2]=nbe[F,DD,n,-2]+1 then nn:=m:  fi:
        m:=m+1:
      od:
      ddpR[F,DD,n]:=ddpR[F,DD,n]+be[F+1,DD,nn,0]*D[F+1,DD,nn]:
      ddp[F,DD,n]:=ddp[F,DD,n]+be[F+1,DD,nn,0]*B[F+1,DD,nn]:
    fi:
    NM:=1:  count[F,DD,n,0,1]:=n:
    for lie from 1 by 1 to min(hi,Dimension-DD) do
      N:=0:
      for r from 1 by 1 to NM do
        mm:=count[F,DD,n,lie-1,r]:
        for p from 0 by 1 to nbe[F,DD+lie-1,mm,-1] do
          if nbe[F,DD+lie-1,mm,p] >0 then
            nn:=0:  m:=1:
            while nn=0 do
              if nbe[F,DD+lie,m,-2]=nbe[F,DD+lie-1,mm,-2]+(FF+2)^(p+1)
-(FF+2)^p then nn:=m:  fi:
              m:=m+1:
            od:
            if check[F,DD,n,lie,nn]=0 then
              N:=N+1:
              count[F,DD,n,lie,N]:=nn:
              check[F,DD,n,lie,nn]:=1:
            fi:
          fi:
        fi:
      fi:
    fi:
  fi:
end do

```

```

    dp[lie,F,DD+lie,nn,F,DD,n]:=dp[lie,F,DD+lie,nn,F,DD,n]
+nbe[F,DD+lie-1,mm,p]*dp[lie-1,F,DD+lie-1,mm,F,DD,n]:
    tot:=lie+DD:
    if (2*iquo(tot,2)=tot) and (nbe[F,DD,n,hi]>1 or
(nbe[F,DD,n,hi]=1 and lie=hi)) then
        nuu:=0:  muu:=1:
        while nuu=0 do
            if be[F+1,DD+lie,muu,-2]=nbe[F,DD,n,-2]+(FF+2)^lie then
                nuu:=muu:
                fi:
                muu:=muu+1:
            od:
            ddp[F,DD+lie,nn]:=ddp[F,DD+lie,nn]+(-1)^lie
*nbe[F,DD+lie-1,mm,p]*(nbe[F,DD,n,lie]+1)
*dp[lie-1,F,DD+lie-1,mm,F,DD,n]*B[F+1,DD+lie,nuu]:
            ddpR[F,DD+lie,nn]:=ddpR[F,DD+lie,nn]+(-1)^lie
*nbe[F,DD+lie-1,mm,p]*(nbe[F,DD,n,lie]+1)
*dp[lie-1,F,DD+lie-1,mm,F,DD,n]*D[F+1,DD+lie,nuu]:
                fi:
                NM:=N:
                fi:
            od:
        od:
    od:
    od:
    od:
    od:
    od:
    od:
    od:

```

This part calculates the functional derivative of U.

```

check:=array(0..Fields-1,0..Dimension,0..ntrack[Fields,Dimension]
,0..Dimension,0..ntrack[Fields,Dimension],sparse);
dpU:=array(0..Dimension,0..Fields-1,0..Dimension

```

```

,0..ntrack[Fields,Dimension],0..Fields-1,0..Dimension
,0..ntrack[Fields-1,Dimension],sparse):
ddpU:=array(0..Fields-1,0..Dimension,0..ntrack[Fields,Dimension]
,sparse);
ddpU[0,0,1]:=C[1,0,1]:
for F from 2 by 2 to Fields-2 do
  for DD from 0 by 1 to ph-F/2+1 do
    for n from 1 by 1 to ntrack[F,DD] do
      hi:=nbe[F,DD,n,-1]:
      dpU[0,F,DD,n,F,DD,n]:=1:
      if nbe[F,DD,n,hi]>1 and 2*iquo(DD,2)=DD then
        nn:=0: m:=1:
        while nn=0 do
          if be[F+1,DD,m,-2]=nbe[F,DD,n,-2]+1 then nn:=m: fi:
          m:=m+1:
        od:
        ddpU[F,DD,n]:=ddpU[F,DD,n]+be[F+1,DD,nn,0]*C[F+1,DD,nn]: fi:
        NM:=1: count[F,DD,n,0,1]:=n:
        for lie from 1 by 1 to min(hi,Dimension-DD) do
          N:=0:
          for r from 1 by 1 to NM do
            mm:=count[F,DD,n,lie-1,r]:
            for p from 0 by 1 to nbe[F,DD+lie-1,mm,-1] do
              if nbe[F,DD+lie-1,mm,p] >0 then
                nn:=0: m:=1:
                while nn=0 do
                  if nbe[F,DD+lie,m,-2]=nbe[F,DD+lie-1,mm,-2]+(FF+2)^(p+1)
-(FF+2)^p then nn:=m: fi:
                  m:=m+1:
                od:
                if check[F,DD,n,lie,nn]=0 then

```

```

    N:=N+1:
    count[F,DD,n,lie,N]:=nn:
    check[F,DD,n,lie,nn]:=1:
    fi:
    dpU[lie,F,DD+lie,nn,F,DD,n]:=dpU[lie,F,DD+lie,nn,F,DD,n]
+nbe[F,DD+lie-1,mm,p]*dpU[lie-1,F,DD+lie-1,mm,F,DD,n]:
    tot:=lie+DD:
    if (nbe[F,DD,n,hi]>1 or (nbe[F,DD,n,hi]=1 and lie=hi)) then
        nuu:=0: muu:=1:
        while nuu=0 do
            if be[F+1,DD+lie,muu,-2]=nbe[F,DD,n,-2]+(FF+2)^lie then
                nuu:=muu:
            fi:
            muu:=muu+1:
        od:
        ddpU[F,DD+lie,nn]:=ddpU[F,DD+lie,nn]+(-1)^lie
*nbe[F,DD+lie-1,mm,p]*(nbe[F,DD,n,lie]+1)
*dpU[lie-1,F,DD+lie-1,mm,F,DD,n]*C[F+1,DD+lie,nuu]:
    fi:
    NM:=N:
    fi:
    od:
    od:
    od:
    od:
    od:
    od:
    od:
    ddpPU:=array(0..Fields-1,0..Dimension
,0..ntrack[Fields,Dimension],sparse);
for F from 2 by 2 to Fields-2 do
    for DD from 0 by 1 to ph-F/2+1 do

```

```

for n from 1 to ntrack[F,DD] do
  hi:=nbe[F,DD,n,-1]:
  for lie from 1 to min(hi,Dimension-DD) do
    for nnP from 1 to lie do
      for nnf from 1 to ntrack[F,DD+lie-nnP] do
tot:=lie+DD:
      if nbe[F,DD,n,hi]>1 or (nbe[F,DD,n,hi]=1 and lie=hi) then
        nuu:=0: muu:=1:
        while nuu=0 do
          if be[F+1,DD+lie,muu,-2]=nbe[F,DD,n,-2]+(FF+2)^lie then
            nuu:=muu:
            fi:
            muu:=muu+1:
          od:
          ddpPU[F,DD+lie-nnP,nnf]:=ddpPU[F,DD+lie-nnP,nnf]+(-1)^lie
*C[F+1,DD+lie,nuu]*(I*P)^nnP*lie!/nnP!/(lie-nnP)!
*dpU[lie-nnP,F,DD+lie-nnP,nnf,F,DD,n]*(nbe[F,DD,n,lie]+1):
          fi:
        od:
      od:
    od:
  od:
od:

```

This part calculates the product of the functional derivatives of W and R .

```

class:=0:
prodRW:=0:
for F from 2 by 2 to Fields do
  for DD from 0 by 2 to ph-F/2+1 do
    for F1 from 1 by 2 to F do
      for D1 from 0 by 2 to DD do

```

```

for n1 from 1 by 1 to ntrack[F1,D1] do
  for n2 from 1 by 1 to ntrack[F-F1,DD-D1] do
    h:=0: n:=0:
    while h=0 do
      n:=n+1: hk:=0:
      for p from 0 by 1 to max( nbe[F,DD,n,-1],nbe[F1,D1,n1,-1]
,nbe[F-F1,DD-D1,n2,-1]) do
        if p<nbe[F1,D1,n1,-1]+1 then
          su1:=nbe[F1,D1,n1,p]:
        else
          su1:=0:
        fi:
        if p<nbe[F-F1,DD-D1,n2,-1]+1 then
          su2:=nbe[F-F1,DD-D1,n2,p]:
        else
          su2:=0:
        fi:
        if nbe[F,DD,n,p]=su1+su2 then hk:=hk+1: fi:
      od:
      if hk=1+max( nbe[F,DD,n,-1],nbe[F1,D1,n1,-1]
,nbe[F-F1,DD-D1,n2,-1]) then h:=1: fi:
    od:
    class:=class+EE[F,DD,n]*ddp[F1,D1,n1]*ddp[F-F1,DD-D1,n2]:
    prodRW:=prodRW+EE[F,DD,n]*ddpR[F1,D1,n1]*ddp[F-F1,DD-D1,n2]:
  od:
od:
od:
od:
od:
od:
od:
od:

```

This part calculates the product of the functional derivatives of U and of W .

```

prodUW:=0:
for F from 1 by 2 to Fields do
  for DD from 0 by 1 to ph-F/2+1 do
    for F1 from 0 by 2 to F do
      if is(DD,odd) then stD1:=1; else stD1:=0: fi:
      for D1 from stD1 by 2 to DD do
        for n1 from 1 by 1 to ntrack[F1,D1] do
          for n2 from 1 by 1 to ntrack[F-F1,DD-D1] do
            h:=0: n:=0:
            while h=0 do
              n:=n+1:hk:=0:
              for p from 0 by 1 to max( nbe[F,DD,n,-1]
,nbe[F1,D1,n1,-1],nbe[F-F1,DD-D1,n2,-1]) do
                if p<nbe[F1,D1,n1,-1]+1 then
                  su1:=nbe[F1,D1,n1,p]:
                else
                  su1:=0:
                fi:
                if p<nbe[F-F1,DD-D1,n2,-1]+1 then
                  su2:=nbe[F-F1,DD-D1,n2,p]:
                else
                  su2:=0:
                fi:
                if nbe[F,DD,n,p]=su1+su2 then hk:=hk+1:fi:
              od:
              if hk=1+max( nbe[F,DD,n,-1],nbe[F1,D1,n1,-1]
,nbe[F-F1,DD-D1,n2,-1]) then h:=1: fi:
            od:
            prodUW:=prodUW+(EE[F,DD,n]+EP[F,DD,n])*(ddpU[F1,D1,n1]
+ddpPU[F1,D1,n1])*ddp[F-F1,DD-D1,n2]:
          od:
        od:
      od:
    od:
  od:
end for

```

```

od:
od:
od:
od:
od:

```

This part calculates the square of the functional derivative of U .

```

prodUU:=0:
for F from 0 by 2 to Fields-1 do
  for DD from 0 by 1 to ph-F/2 do
    for F1 from 0 by 2 to F do
      for D1 from 0 by 1 to DD do
        for n1 from 1 by 1 to ntrack[F1,D1] do
          for n2 from 1 by 1 to ntrack[F-F1,DD-D1] do
            h:=0: n:=0:
            while h=0 do
              n:=n+1:hk:=0:
              for p from 0 by 1 to max( nbe[F,DD,n,-1],nbe[F1,D1,n1,-1]
,nbe[F-F1,DD-D1,n2,-1]) do
                if p<nbe[F1,D1,n1,-1]+1 then
                  su1:=nbe[F1,D1,n1,p]:
                else
                  su1:=0:
                fi:
                if p<nbe[F-F1,DD-D1,n2,-1]+1 then
                  su2:=nbe[F-F1,DD-D1,n2,p]:
                else
                  su2:=0:
                fi:
                if nbe[F,DD,n,p]=su1+su2 then hk:=hk+1:fi:
              od:
            if hk=1+max( nbe[F,DD,n,-1],nbe[F1,D1,n1,-1]

```

```
,nbe[F-F1,DD-D1,n2,-1]) then h:=1: fi:
    od:
    prodUU:=prodUU+(EE[F,DD,n]+0*EP[F,DD,n])*ddpU[F1,D1,n1]
*subs(P=-P,ddpU[F-F1,DD-D1,n2]):
    od:
    od:
    od:
    od:
    od:
od:
```

This converts above results into tabular format (coefficients of ER).

```
for F from 1 by 2 to Fields do
  for DD from 0 by 1 to ph-F/2+1 do
    if DD<>1 then
      for n from 1 by 1 to track[F,DD] do
        prodUWm[F,DD,n]:=coeff(collect(prodUW,ER[F,DD,n]),ER[F,DD,n]):
        lapUm[F,DD,n]:=coeff(collect(lapU,ER[F,DD,n]),ER[F,DD,n]):
      od:
    fi;
  od:
od:
for F from 0 by 2 to Fields do
  for DD from 0 by 1 to ph-F/2 do
    if DD<>1 and not(F=2 and is(DD,odd)) then
      for n from 1 by 1 to track[F,DD] do
        prodUUm[F,DD,n]:=coeff(collect(prodUU,ER[F,DD,n]),ER[F,DD,n]):
      od:
    fi:
  od:
od:
for F from 0 by 2 to Fields do
```

```

for DD from 0 by 2 to ph-F/2+1 do
  for n from 1 by 1 to track[F,DD] do
    classm[F,DD,n]:=coeff(collect(class,ER[F,DD,n]),ER[F,DD,n]):
    prodRWm[F,DD,n]:=coeff(collect(prodRW,ER[F,DD,n]),ER[F,DD,n]):
    lapm[F,DD,n]:=coeff(collect(lap,ER[F,DD,n]),ER[F,DD,n]):
    lapRm[F,DD,n]:=coeff(collect(lapR,ER[F,DD,n]),ER[F,DD,n]):
  od:
od:
od:
end:

```

A.3 Solving the Schrödinger Equation

Having set up the structures in sections A.1 and A.2, solving the Schrödinger equation becomes relatively easy. In this section we will briefly outline the procedures required to find the vacuum, one-particle and two-particle states.

A.3.1 Ground State

The ground-state wavefunction is solved by expanding the $B[F,D,n]$ coefficients in powers of l

$$B[F,D,n] := \sum_j BL[F,D,n,j] * l^j. \quad (\text{A.3.1})$$

A list containing the expanded form of the $B[F,D,n]$ is stored using the variable B_{exp} . The coefficient $B[2,0,1]$ is set equal to k in this list alongside the chosen renormalisation conditions in which the physical mass μ is more simply represented m . The coefficient of the basis functional represented by $[F,D,n]$ in the Schrödinger equation is now simply

$$\text{lapm}[F,D,n] |/\text{Pi} + \text{classm}[F,D,n] = 0$$

for all but the initial values of F and D . Solving the Schrödinger equation is therefore reduced to cycling through F, D, n in the correct sequence and at each stage

substituting in `Bexp`, the power series expansion in l , and comparing the coefficients of powers of l .

The variable `solo` is a list of solutions for the BL[F,D,n,j]. As we cycle through the F , D , n and j solving the coefficients, we add to the list `solo` and substitute these solutions into `Bexp`. The coding below for solving the vacuum state was produced by Paul Mansfield. The procedure is called via the command `iter(p)` and solves coefficients with $F + 2D + 2j \leq 2p + 2$.

```
iter:=proc(p)global sol,solo,newv,m,g,rho,Bexp:
Bexp:={}:
for F from 2 by 2 to 2*p+2 do
  for DD from 0 by 2 to p-F/2+1 do
    for n from 1 by 1 to track[F,DD] do
      if (F>4 or DD>2) or (F=4 and DD=2) or (F=6) then
        Bexp:=Bexp union {B[F,DD,n]=sum(BL[F,DD,n,j]*l^j
,j=0..p-DD-F/2+2)}:
        fi:
      od:
    od:
  od:
solo:={B[2,0,1]=k,B[2,2,1]=-1/(4*m),B[4,0,1]=-g*m/(8)}:
for JJ from 0 by 1 to p do
  for F from 2 by 2 to 2*p+2 do
    for DD from 0 by 2 to p-F/2+1 do if JJ+DD+F/2<p+3 then
      auxi1:={}: auxi2:={}:
      for n from 1 by 1 to track[F,DD] do
        if (F>4 or DD>2) or (F=4 and DD=2) or (F=6) then
          Bexp:=subs(solo,Bexp):
          lapmu[F,DD,n]:=sum(coeff(lapm[F,DD,n],l,ni)*l^(ni)
,ni=1..p+1-DD-F/2):
          auxi1:=auxi1 union {coeff(subs(solo union
Bexp,lapmu[F,DD,n]/Pi+classm[F,DD,n]),1,JJ)=0}:

```

```

    auxi2:=auxi2 union {BL[F,DD,n,JJ]}:
  fi:
od:
  solo:=solo union solve(auxi1,auxi2):fi:
od:
od:
od:
end:

```

A.3.2 One-Particle State

The one-particle state is solved in the same manner to that used in the ground state. This time the coefficients are expanded in powers of the momenta P as well as the momentum cut-off l . Similarly the variable E_1Z which in MAPLE is represented with the single variable E is also expanded in powers of l and P . The expansions are stored as a list in `Cexp` and individual solutions to the CLP and ELP are stored in `solospec`. The coefficients of a $[F, D, n]$ functional in the Schrödinger equation for the one-particle state is

$$\text{lapUm}[F, \text{DDD}, n] / 2 / \text{Pi} + \text{prodUWm}[F, \text{DDD}, n] + E * C[F, \text{DDD}, n] = 0$$

Substituting in `Cexp` we then further select the exact basis functional we require by comparing powers of P . The coefficient of this basis functional is then determined by simultaneously comparing powers of l . The procedure is called via the command `iterspectrum(p)`.

```

iterspectrum:=proc(p)
global sol,solo,newv,m,g,rho,Bexp,Cexp,solospec,P:
Cexp:={E=sum(sum(ELP[j,PP]*l^j*P^PP,PP=0..p-j),j=0..p)}:
for F from 3 by 2 to 2*p+2 do
  for DD from 0 by 1 to p-F/2+2 do
    if DD<>1 then
      for n from 1 by 1 to track[F,DD] do
        Cexp:=Cexp union {C[F,DD,n]=sum(sum(CLP[F,DD,n,j,k]*l^j*P^k

```

```

,j=0..p-DD-k-F/2+1),k=0..(p+1-F/2-DD)}:
  od:
  fi:
  od:
od:
solospec:={C[1,0,1]=1}:
for JJ from 0 by 1 to p do
  for F from 1 by 2 to 2*p+2 do
    for DD from 0 by 1 to p-F/2+1 do
      if JJ+DD+F/2<p+2 then
        auxi1:={}: auxi2:={}:
        for DDD from 0 to DD do
          if DDD<>1 then
            for n from 1 by 1 to track[F,DDD] do
              Cexp:=subs(solospec,Cexp):
              auxi1:=auxi1 union {coeff(coeff(subs(solo union Bexp union
solospec union Cexp,lapUm[F,DDD,n])/2/Pi+prodUWm[F,DDD,n]
+E*C[F,DDD,n]),P,DD-DDD),1,JJ)=0}:
              if F=1 then
                auxi2:={ELP[JJ,DD-DDD]}:
              else
                auxi2:=auxi2 union {seq(CLP[F,DDDD,n,JJ,DD-DDDD]
,DDDD=0..DD)}:
              fi:
            od:
          fi:
        od:
        solospec:=solospec union solve(auxi1,auxi2):
      fi:
    od:
  od:
od:

```

od:

end:

A.3.3 Z and b_2

To find b_2 ($B[2,0,1]$ or k in the MAPLE code) and Z there are a sequence of three programs to be run in the following order: `ziter(p)`, `kiter(p)` then `zeval(p)`. These procedures are reproduced below.

`ziter`

The first procedure, `ziter(p)` produces a power series expansion of Z in l that is also dependent on k . The variable `Zexp` is the power series expansion with coefficients of l^i denoted `ZL[i]`. The value of Z is found using the φ'^2 coefficient in the Schrödinger equation:

$$\text{lapm}[2,2,1]/\text{Pi} + \text{classm}[2,2,1] - \text{Zexp}^2 = 0$$

As each `ZL[i]` is found, the solutions are stored as a list in `Zsolo`.

```
ziter:=proc(p)
global Zsolo:
Zexp:=sum(ZL[j]*l^j,j=0..p-2):
Zsolo:={ZL[0]=sqrt(-2*k/m)}:
for JJ from 1 by 1 to p-2 doZexp:=subs(Zsolo,Zexp):
  auxi1:={}: auxi2:={}:
  auxi1:=auxi1 union {coeff(subs(solo union Bexp,lapm[2,2,1]/Pie
+classm[2,2,1]-Zexp^2),1,JJ)=0}:
  auxi2:=auxi2 union {ZL[JJ]}:
  Zsolo:=Zsolo union solve(auxi1,auxi2):
od:
end:
```

kiter

This procedure finds $1/k$ as a power series expansion in l . The variable `kexp` represents this power series expansion with coefficients of l^i represented by `kl[i]`. As each `kl[i]` is solved, the solutions are stored in the list `ksol`.

The scheme used to find $1/k$ is to examine the P^0 coefficient of the MAPLE variable `E`. This should be mZ . We compare this expression of Z to that obtained from `ziter(p)` and invert the series to find $1/k$.

```
kiter:=proc(L)
global ksol,LHS,RHS;
kexp:=sum(kl[i]*l^i,i=0..L-2);
LHS:=expand(coeff(subs(Cexp,E/k),P,0));
RHS:=expand(subs(Zsolo,sum(ZL[i]*sqrt(-2*k/m)*l^i/k,i=0..L-2)*m));
for EEL from 1 to 2*L do
  exp:=convert(series(sum(kl[i]*l^i,i=0..L-2)^EEL,1,L-1),polynom);
  LHS:=subs(1/k^EEL=exp,expand(LHS));
  RHS:=subs(1/k^EEL=exp,expand(RHS));
od;
RHS:=convert(series(RHS/sqrt(-2/kexp/m),1,L-1),polynom);
ksol:={};
for LL from 0 to L-2 do
  ksol:=ksol union {kl[LL]=solve(coeff(LHS-RHS,1,LL)=0,kl[LL])};
  LHS:=subs(ksol,LHS);
  RHS:=subs(ksol,RHS);
od;
end;
```

evalz

With k determined we can evaluate Z by simply substituting the power series expansion of $1/k$ back into the solution for Z as determined by `ziter`.

```
evalz:=proc(L)
```

```

global zout;
kexp:=subs(ksol,sum(kl[i]*1^i,i=0..L-2));
RHS:=subs(Zsolo,sum(ZL[i]*sqrt(-2*k/m)*1^i,i=0..L-2));
for ZZL from 1 to 2*L-3 do
  exp:=convert(series(sum(kl[i]*1^i,i=0..L-2)^ZZL,1,L-1),polynom);
  RHS:=series(subs(ksol,subs(1/k^ZZL=exp,expand(RHS))),1,L-1);
od;
zout:=RHS/sqrt(-2/kexp/m);
zout:=convert(series(zout,1,L-1),polynom);
zout:=series(subs(k=1/kexp,zout),1,L-1);
end:

```

A.3.4 Two-Particle State

This procedure finds the coefficients of the two-particle local expansion in terms of the energy $E_1 Z + i\epsilon Z$, which is represented in MAPLE by EZ. This is done by expanding the coefficients $D[F,DD,n]$ in powers of l and P with the coefficients given by DLP. The variable Dexp is a list of these expansions with Dspec the list of solutions for the individual DLP.

```

Dseries:=proc(p)
global solo,m,g,Bexp,Cexp,solospec,Dexp,Dspec:
Dexp:={}:
for F from 0 by 2 to 2*p+2 do
  for DD from 0 by 2 to p-F/2+1 do
    for n from 1 by 1 to track[F,DD] do
      Dexp:=Dexp union {D[F,DD,n]=sum(sum(DLP[F,DD,n,j,2*PP]*1^j
*P^(2*PP),j=0..p+1-F/2-DD-2*PP),PP=0..(p+1-F/2-DD)/2)}:
    od:
  od:
od:
Dspec:={}:
for JJ from 0 by 1 to p do

```

```

for F from 0 by 2 to 2*p+2 do
  for DD from 0 by 2 to p-F/2+1 do
    if JJ+DD+F/2<p+2 then
      auxi1:={}: auxi2:={}:
      for DDD from 0 by 2 to DD do
        if DDD<>1 then
          for n from 1 by 1 to track[F,DDD] do
            Dexp:=subs(Dspec,Dexp):
            Dspec union Dexp,lapRm[F,DDD,n]/2/Pi+prodUUm[F,DDD,n]
+prodRWm[F,DDD,n]+2*ZE*D[F,DDD,n]),1, JJ+1),polynom),1, JJ));
            auxi1:=auxi1 union {coeff(coeff(convert(series(subs(k=1/kinv
,subs(solo union solospec union Bexp union Cexp union Dspec union
Dexp,lapRm[F,DDD,n]/2/Pi+prodUUm[F,DDD,n]+prodRWm[F,DDD,n]
+2*ZE*D[F,DDD,n])),1, JJ+1),polynom),P,DD-DDD),1, JJ)=0};
            auxi2:=auxi2 union {DLP[F,DDD,n, JJ,DD-DDD]}:
          od:
        fi:
      od:
      Dspec:=Dspec union solve(auxi1,auxi2):
    fi:
  od:
od:
od:
end:

```

A.4 Findind the S Matrix

Finding the S matrix is split into two key parts, the procedure itself which generates the various terms to be calculated and the dependent procedures required to complete the functional integration of each term. Throughout this section we will assume the existence of a global variable `Psetup` which should assume the value

of p used in `pSetupsimp(p)`. This will be necessary as it tells us which base the information in `be[F,D,n,-2]` is encoded.

A.4.1 Functional Integration

Completing the functional integration of a particular Gaussian type integral is split into multiple tasks which we shall address individually as follows. Local functionals represented by $[F, D, n]$ in all of the procedures relating to functional integration are not necessarily basis functionals. Thus n should be in the range $0..ntrack[F,D]$.

Orthonormal Basis

An orthonormal basis is generated via a Gram-Schmidt orthonormalisation procedure. We represent the orthonormal $\Psi^{(n)}$ as `EN[n]` and the $\varphi^{(n)}$ as `EP[n]`. We then expand

$$EN[n] = \sum (EN[i] * N[n,i], i=0..n-1) * N[n,-1] + EP[n] * N[n,-1]$$

The individual `N[n,i]` coefficients are determined by calculating the inner product of `EN[n]` with `EP[i]`. The overall normalisation `N[n,-1]` is then found using the inner product of `EN[n]` with itself. The variable `orthbasis` is a list of the solutions for the `N` coefficients and is generated using the procedure `orth(p)`.

```
orth:=proc(p)
global orthbasis;
orthbasis:={N[0,-1]=1/sqrt(1)};
orthexp:={EN[0]=N[0,-1]*EP[0]};
for cur from 1 to p do
  orthexp:=orthexp union {EN[cur]=subs(orthexp,sum(EN[i]*N[cur,i],
,i=0..cur-1)*N[cur,-1])+EP[cur]*N[cur,-1]};
  for coef from 0 to cur-1 do
    orthbasis:=orthbasis union {N[cur,coef]=-subs(orthbasis,sum(
coeff(subs(orthexp,EN[coef]),EP[i],round(evalf(sin(i)^2+cos(i)^2)))
*1^(cur+i+1)/(cur+i+1)*I^(cur+i)*(1+(-1)^(cur+i))/2,i=0..coef))};
```

```

od;
  orthbasis:=orthbasis union {N[cur,-1]=1/sqrt(-subs(orthbasis,sum(
N[cur,coeff2]^2,coeff2=0..cur-1))+I^(2*cur)*1^(2*cur+1)/(2*cur+1))};
od;
end:

```

Having found the orthonormal basis it is useful to know the EP in terms of the EN. This is accomplished via the procedure `invorth(p)`. The solutions for EP as a linear combination of the EN are stored in the list `invsol`.

```

invorth:=proc(p)
global invsol;
invsol:={};
for cur from 0 to p do
  invsol:=invsol union {EP[cur]=subs(orthbasis,EN[cur]/N[cur,-1]
-sum(EN[n]*N[cur,n],n=0..cur-1))};
od;
end:

```

Functional Integration - The Easiest Case

In general the functional integral we are trying to compute will be a product of local terms multiplied by $\exp(\int \varphi^2)$. The most simple example of this is when the exponential only has one local term in the prefactor. This prefactor is represented by $[F, D, n]$, not necessarily a basis element. The input variable `term` will be of the form `term[1,1]=[F,D,n]`. The reason for specifying `term` as a two-dimensional array becomes apparent in the more general case with multiple local expansions in the functional integral. The output of `fint2` is the result of this functional integration. This procedure uses the orthonormal basis in achieving this by writing the $[F, D, n]$ functional in terms of the $\Psi^{(n)}$. Only local terms in which all of the $\Psi^{(n)}$ have an even power are selected. Other terms will automatically be zero.

```

fint2:=proc(term)
tot:=1;

```

```

for n from 0 to nbe[op(term[1,1]),-1] do
  tot:=tot*EP[n]^nbe[op(term[1,1]),n];
od;
tot:=subs(invsol,tot);
for n from 0 to nbe[op(term[1,1]),-1] do
  tot:=(tot+subs(EN[n]=-EN[n],tot))/2;
od;
tot:=expand(tot);
for n from 0 to nbe[op(term[1,1]),-1] do
  for m from 2 by 2 to nbe[op(term[1,1]),-1]-n do
    tot:=subs(EN[n]^m=m!/((m/2)!)/(m^(m/2))*EN[n]^m,tot)
  od;
  tot:=subs(EN[n]=sqrt(1/8/Pi/k),tot);
od;
tot:=tot*2*Pi;
tot;
end:

```

Differentiating Local Functionals

When computing a more general functional integral it will be necessary to find the derivative of some local functionals. The procedure `diffsetup(p)` produces an array `diffn[F,D,n,nn]` which represents the coefficient of a `[F,D+1,nn]` term in the derivative of a `[F,D,n]` local functional.

```

diffsetup:=proc(p)
global diffn;
for F from 1 to 2*p+2 do
  for D from 0 to p do
    for n from 1 to ntrack[F,D] do
      for nnn from 1 to ntrack[F,D+1] do
        diffn[F,D,n,nnn]:=0;
      od;
    od;
  od;
end;

```

```

for DD from 0 to nbe[F,D,n,-1] do
  for nn from 1 to ntrack[F,D+1] do
    if nbe[F,D+1,nn,-2]=nbe[F,D,n,-2]-(2*Psetup+4)^DD
+(2*Psetup+4)^(DD+1) then
      diffn[F,D,n,nn]:=diffn[F,D,n,nn]+nbe[F,D,n,DD];
      fi;
    od;
  od;
od;
od;
end:

```

In general we will want to differentiate functionals multiple times as specified by the integer `derivs`. The procedure `diffn` differentiates a linear combination of functionals with F fields, D derivatives and the coefficients given by `fun[n]` where $n=1..ntrack[F,D]$. The output of the differentiation is given by an array `funout[nn]` where $nn=1..ntrack[F,D+derivs]$.

```

diffn:=proc(F,D,fun,derivs)
DD:=D;
funout:=fun;
for k from 1 to derivs do
  newfun:=[seq(0,i=1..ntrack[F,DD+1])];
  for n from 1 to ntrack[F,DD] do
    for nn from 1 to ntrack[F,DD+1] do
      newfun[nn]:=newfun[nn]+diffn[F,DD,n,nn]*funout[n];
    od;
  od;
  funout:=newfun;
  DD:=DD+1;
od;
funout;

```

end:

Functional Integration - The Main Procedure

A general term in the S matrix will be generated by a product of n_{term} different local functionals multiplied by $\exp(\int \varphi^2)$. The format of each term will be specified by an array $\text{term}[i,j]$ where $i=1..n_{\text{term}}$. Each $\text{term}[i,1]$ will be of the form $[F,D,n]$. The overall multiplicative factor of each term is specified by $\text{term}[i,2]$ and the external momenta in each case is given by $\text{term}[i,3]$.

The procedure works by pairing a field in the first local expansion with a field in another local expansion labelled by sec . We always take the field in the first expansion with lowest number of derivatives which is determined and labled firD . This field is paired in all possible ways with other fields. When two fields from two different local expansions are combined we require the use of the `diffR` procedure to integrate by parts. The number of local functionals in the exponential prefactor is now reduced by one. The procedure is then recursively called until there is only one local expansion. This is then evaluated using `fint2`.

```
fint:=proc(nterm,term)
global be;
tot:=0;
for sec from 2 to nterm do
  for firD from 0 to nbe[op(term[1,1]),-1]
  while nbe[op(term[1,1]),firD]=0 do od;
  for secD from 0 to nbe[op(term[sec,1]),-1] do
    if firD+secD<>0 then
      fun:=[seq(0,i=1..ntrack[term[1,1][1]-1,term[1,1][2]-firD])];
      for n from 1 to ntrack[term[1,1][1]-1,term[1,1][2]-firD] do
        if nbe[op(term[1,1]),-2]-(2*Psetup+4)^firD=nbe[term[1,1][1]-1
,term[1,1][2]-firD,n,-2] then
          fun[n]:=1;
          fi;
        od;
      od;
    fi;
  od;
od;
```

```

if term[1,3]<>0 then
  for deriv from 0 to firD+secD do
    if deriv<>0 then
      out:=diff(r(term[1,1][1]-1,term[1,1][2]-firD,fun,deriv));
    else
      out:=fun;
    fi;
    for nxt from 1 to nops(out) do
      for nn from 1 to ntrack[term[1,1][1]+term[sec,1][1]-2
,term[1,1][2]+term[sec,1][2]-firD-secD+deriv] do
        if nbe[term[1,1][1]-1,term[1,1][2]-firD+deriv,nxt,-2]
+nbe[op(term[sec,1]),-2]-(2*Psetup+4)^secD=
nbe[term[1,1][1]+term[sec,1][1]-2,term[1,1][2]+term[sec,1][2]-firD
-secD+deriv,nn,-2] then
          newterm[1,1]:=[term[1,1][1]+term[sec,1][1]-2,term[1,1][2]
+term[sec,1][2]-firD-secD+deriv,nn];
          newterm[1,2]:=term[1,2]*term[sec,2]*out[nxt]*(I*term[1,3])
^(firD+secD-deriv)*nbe[op(term[sec,1]),secD]/4/k;
          newterm[1,3]:=term[1,3]+term[sec,3];
          b:=0;
          for redo from 2 to nterm do
            if redo=sec then
              b:=1;
            else
              newterm[redo-b,1]:=term[redo,1];
              newterm[redo-b,2]:=term[redo,2];
              newterm[redo-b,3]:=term[redo,3];
            fi;
          od;
          if nterm=2 and newterm[1,3]=P1+P2+P3+P4 then
            tot:=tot+fint2(newterm)*newterm[1,2];

```

```

else
  if newterm[1,1]<>[0,0,1] then
    tot:=tot+fint(nterm-1,newterm);
    fi;
  fi;
  fi;
od;
od;
od;
else
  out:=diff(r(term[1,1][1]-1,term[1,1][2]-firD,fun,firD+secD);
  for nxt from 1 to nops(out) do
    for nn from 1 to ntrack[term[1,1][1]+term[sec,1][1]-2
,term[1,1][2]+term[sec,1][2]] do
      if nbe[term[1,1][1]-1,term[1,1][2]+secD,nxt,-2]
+nbe[op(term[sec,1]),-2]-(2*Psetup+4)^secD=nbe[term[1,1][1]
+term[sec,1][1]-2,term[1,1][2]+term[sec,1][2],nn,-2] then
        newterm[1,1]:=[term[1,1][1]+term[sec,1][1]-2,term[1,1][2]
+term[sec,1][2],nn];
        newterm[1,2]:=term[1,2]*term[sec,2]*out[nxt]
*nbe[op(term[sec,1]),secD]/4/k;
        newterm[1,3]:=term[1,3]+term[sec,3];
        b:=0;
        for redo from 2 to nterm do
          if redo=sec then
            b:=1;
          else
            newterm[redo-b,1]:=term[redo,1];
            newterm[redo-b,2]:=term[redo,2];
            newterm[redo-b,3]:=term[redo,3];
          fi;

```

```

od;
if nterm=2 and newterm[1,3]=P1+P2+P3+P4 then
  tot:=tot+fint2(newterm)*newterm[1,2];
else
  if newterm[1,1]<>[0,0,1] then
    tot:=tot+fint(nterm-1,newterm);
  fi;
  fi;
  fi;
od;
od;
fi;
else
  for nn from 1 to ntrack[term[1,1][1]+term[sec,1][1]-2
,term[1,1][2]+term[sec,1][2]] do
    if nbe[op(term[1,1]),-2]+nbe[op(term[sec,1]),-2]-2
=nbe[term[1,1][1]+term[sec,1][1]-2,term[1,1][2]
+term[sec,1][2],nn,-2] then
      newterm[1,1]:=[term[1,1][1]+term[sec,1][1]-2,term[1,1][2]
+term[sec,1][2],nn];
      newterm[1,2]:=term[1,2]*term[sec,2]*nbe[op(term[sec,1]),0]/4/k;
      newterm[1,3]:=term[1,3]+term[sec,3];
      b:=0;
      for redo from 2 to nterm do
        if redo=sec then
          b:=1;
        else
          newterm[redo-b,1]:=term[redo,1];
          newterm[redo-b,2]:=term[redo,2];
          newterm[redo-b,3]:=term[redo,3];
        fi;

```

```

od;
if nterm=2 and newterm[1,3]=P1+P2+P3+P4 then
  tot:=tot+fint2(newterm)*newterm[1,2];
else
  if newterm[1,1]<>[0,0,1] then
    tot:=tot+fint(nterm-1,newterm);
    fi;
    fi;
    fi;
  od;
fi;
od;
od;
if term[1,1][1]>2 then
  for d1 from 0 to nbe[op(term[1,1]),-1]
  while nbe[op(term[1,1]),d1]=0 do od;
  for d2 from d1 to nbe[op(term[1,1]),-1] do
    if ((d1=d2 and nbe[op(term[1,1]),d1]>1) or d1<>d2) and
type(d1+d2,even) and nbe[op(term[1,1]),d2]<>0 then
      for nnew from 1 to ntrack[term[1,1][1]-2,term[1,1][2]-d1-d2]
      while nbe[term[1,1][1]-2,term[1,1][2]-d1-d2,nnew,-2]
<>nbe[op(term[1,1]),-2]-(2*Psetup+4)^d1-(2*Psetup+4)^d2 do od;
      if d1=d2 then
        newterm[1,2]:=term[1,2]*I^(d1+d2)*1^(d1+d2+1)/(d1+d2+1)/8/Pi/k
*(nbe[op(term[1,1]),d2]-1);
      else
        newterm[1,2]:=term[1,2]*I^(d1+d2)*1^(d1+d2+1)/(d1+d2+1)/8/Pi/k
*nbe[op(term[1,1]),d2];
      fi;
      newterm[1,3]:=term[1,3];
      newterm[1,1]:=[term[1,1][1]-2,term[1,1][2]-d1-d2,nnew];

```

```

for n from 2 to nterm do
  newterm[n,1]:=term[n,1];
  newterm[n,2]:=term[n,2];
  newterm[n,3]:=term[n,3];
od;
tot:=tot+fint(nterm,newterm);
fi;
od;
fi;
tot;
end:

```

A.4.2 The S Matrix

There are many different contributions to the S matrix. These arise from the expansions of $\exp(W)$, R and $U(P)U(-P)$. This procedure finds all of the different terms that will required functionally integrating. The procedure `fint` is then used to complete this integration. The momenta in $\exp(iP)$ Ψ_+ and Φ are labelled P_1 , P_2 , P_3 and P_4 . Whilst we will be working in a centre of momentum frame we keep track of these momenta in the exponentials. Only terms that will result in a $\delta(P_1 + P_2 + P_3 + P_4)$ overall factor are kept. The output of `Tmatrix(p)` will be the T matrix but with the delta function assumed. The output will be in terms of the B, C and D coefficients, the momentum cut-off l and other parameters such as k , g and m .

```

with(combinat):
Tmatrix:=proc(p)
global Tout,be;
be[1,0,1,-2]:=nbe[1,0,1,-2];
Tout:=0;
for F1 from 2 by 2 to 2*p-2 do
  for FW from 0 by 2 to 2*p-2-F1 do
    if FW < 0 then

```

The partition function finds the different terms in the expansion of $\exp(W)$.

```

part:=partition(FW/2)*2;
else
part:=[0];
fi;
for NP from 1 to nops(part) do
if part[1]<>0 then
numb1:=F1+5;
cur:=part[NP];

```

We now set up the combinatorics. $\text{dec}[n]$ counts the number of contributions from W_n in each term of e^W . $\text{combs}[n]$ is the coefficient of this term.

```

for NNNP from 2 by 2 to FW do
dec[NNNP]:=0;
od;
for NNP from 1 to nops(cur) do
dec[cur[NNP]]:=dec[cur[NNP]]+1;
od;
comb[NP]:=1;
for NNP from 2 by 2 to FW do
comb[NP]:=comb[NP]/dec[NNP]!;
od;

```

ddcomb is a list of numbers representing the possible number of derivatives for each W contribution

```

for deriv from 0 to (floor((p-F1/2-FW/2-1+1)/2))^(nops(cur))-1 do
if deriv = 0 then
ddcomb:=[0];
else
ddcomb:=2*convert(deriv,base,floor((p-F1/2-FW/2-1+1)/2));
fi;

```

```

if nops(ddcomb)<nops(cur) then
  dcomb:=[op(ddcomb),seq(0,i=nops(ddcomb)+1..nops(cur))];
else
  dcomb:=ddcomb;
fi;
if FW-2*nops(cur)+sum(dcomb[i],i=1..nops(dcomb))<2*p-1-F1 then
  skip:=0;
else
  skip:=1;
fi;
for n from 1 to nops(dcomb) do
  if dcomb[n]=0 and cur[n]=2 then skip:=1 fi;
od;
if skip=0 then

```

tcomb is the number of possible basis elements with fields given by comb and derivatives by dcomb

```

ttcomb:=[seq(track[cur[i],dcomb[i]],i=1..nops(cur))];
for tr from 1 to (max(op(ttcomb))+1)^(nops(cur))-1 do
  tttcomb:=convert(tr,base,max(op(ttcomb))+1);
  if nops(tttcomb)<nops(cur) then
    tcomb:=[op(tttcomb),seq(0,i=nops(tttcomb)+1..nops(cur))];
  else
    tcomb:=tttcomb;
  fi;
  if max(op(tcomb-ttcomb))<=0 and min(op(tcomb))>0 then

```

Now we generate the possible Tmatrix elements for $D \exp(W)$.

```

term[1,1]:=[1,0,1];
term[1,2]:=1;
term[1,3]:=P1;
term[2,1]:=[1,0,1];

```

```

term[2,2]:=1;
term[2,3]:=P2;
term[3,1]:=[4,0,1];
term[3,2]:=g/12;
term[3,3]:=0;
for Wi from 1 to nops(cur) do
  term[3+Wi,1]:=[cur[Wi],dcomb[Wi],tcomb[Wi]];
  if cur[Wi]=2 then
    term[3+Wi,2]:=2*comb[NP]*subs(g=0,subs(Bexp union Bsolo
,B[cur[Wi],dcomb[Wi],tcomb[Wi]]));
  else
    term[3+Wi,2]:=comb[NP]*B[cur[Wi],dcomb[Wi],tcomb[Wi]];
  fi;
  term[3+Wi,3]:=0;
od;
for Fderiv from 0 by 2 to p-F1/2-1-FW/2+nops(cur)-sum(dcomb[i]
,i=1..nops(dcomb)) do
  for FT from 1 to track[F1,Fderiv] do
    term[4+nops(cur),1]:=[F1,Fderiv,FT];
    term[4+nops(cur),2]:=D[F1,Fderiv,FT];
    term[4+nops(cur),3]:=P3+P4;
    Tout:=Tout+fint(nops(cur)+4,term);
  od;
  for F2 from 1 by 2 to F1 do
    for Fderiv2 from 0 by 2 to Fderiv do
      for FT from 1 to track[F2,Fderiv2] do
        for n from 1 to ntrack[F2,Fderiv2] do
          if nbe[F2,Fderiv2,n,-2]=be[F2,Fderiv2,FT,-2] then
            term[4+nops(cur),1]:=[F2,Fderiv2,n];
          fi;
        od;
      od;
    od;
  od;

```

```

    term[4+nops(cur),2]:=C[F2,Fderiv2,FT];
    term[4+nops(cur),3]:=P3;
    for FT2 from 1 to track[F2,Fderiv2] do
      for n from 1 to ntrack[F1-F2,Fderiv-Fderiv2] do
        if nbe[F1-F2,Fderiv-Fderiv2,n,-2]
=be[F1-F2,Fderiv-Fderiv2,FT2,-2] then
          term[5+nops(cur),1]:=[F1-F2,Fderiv-Fderiv2,n];
          fi;
        od;
        term[5+nops(cur),2]:=C[F1-F2,Fderiv-Fderiv2,FT2];
        term[5+nops(cur),3]:=P4;
        Tout:=Tout+fint(nops(cur)+5,term);
      od;
    od;
  od;
  od;
  od;
  od;
  fi;
  od;
  fi;
  od;
else

```

The no W contribution part goes here.

```

    term[1,1]:=[1,0,1];
    term[1,2]:=1;
    term[1,3]:=P1;
    term[2,1]:=[1,0,1];
    term[2,2]:=1;
    term[2,3]:=P2;
    term[3,1]:=[4,0,1];
    term[3,2]:=g/12;

```

```

term[3,3]:=0;
for Fderiv from 0 by 2 to p-1-F1/2 do
  for FT from 1 to track[F1,Fderiv] do
    term[4,1]:=[F1,Fderiv,FT];
    term[4,2]:=D[F1,Fderiv,FT];
    term[4,3]:=P3+P4;
    Tout:=Tout+fint(4,term);
  od;
  for F2 from 1 by 2 to F1 do
    for Fderiv2 from 0 by 2 to Fderiv do
      for FT from 1 to track[F2,Fderiv2] do
        for n from 1 to ntrack[F2,Fderiv2] do
          if nbe[F2,Fderiv2,n,-2]=be[F2,Fderiv2,FT,-2] then
            term[4,1]:=[F2,Fderiv2,n];
            fi;
          od;
          term[4,2]:=C[F2,Fderiv2,FT];
          term[4,3]:=P3;
          for FT2 from 1 to track[F1-F2,Fderiv-Fderiv2] do
            for n from 1 to ntrack[F1-F2,Fderiv-Fderiv2] do
              if nbe[F1-F2,Fderiv-Fderiv2,n,-2]
=be[F1-F2,Fderiv-Fderiv2,FT2,-2] then
                term[5,1]:=[F1-F2,Fderiv-Fderiv2,n];
                fi;
              od;
              term[5,2]:=C[F1-F2,Fderiv-Fderiv2,FT2];
              term[5,3]:=P4;
              Tout:=Tout+fint(5,term);
            od;
          od;
        od;
      od;
    od;
  od;

```

```
    od;  
  od;  
  fi;  
  od;  
  od;  
  od;  
  Tout;  
end:
```

Bibliography

- [1] D. Leonard and P. Mansfield, "Solving the Anharmonic Oscillator: Tuning the Boundary Condition," *J. Phys. A: Math. Theor.* **40** (2007) 10291-10299. [arXiv:quant-ph/0703262].
- [2] D. Leonard and P. Mansfield, "A Modified Borel Resummation Technique," [arXiv:0708.2201]
- [3] K. Symanzik, "Schrödinger Representation And Casimir Effect In Renormalizable Quantum Field Theory," *Nucl. Phys. B* **190** (1981) 1.
- [4] K. Symanzik, "Schrödinger Representation In Renormalizable Quantum Field Theory. (Talk)," *Preprint - SYMANZIK, K. (REC.OCT. 81) 13p*
- [5] F. T. Hioe, D. Macmillen and E. W. Montroll, "Quantum Theory Of Anharmonic Oscillators: Energy Levels Of A Single And A Pair Of Coupled Oscillators With Quartic Coupling," *Phys. Rept.* **43** (1978) 305.
- [6] H. J. Müller-Kirsten "Introduction to Quantum Mechanics" World Scientific Publishing Co. ISBN 981-256-691-0.
- [7] C. M. Bender and T. T. Wu, "Anharmonic oscillator," *Phys. Rev.* **184** (1969) 1231.
- [8] G. H. Hardy, "Divergent Series," Oxford University Press, 1949
- [9] S. Graffi, V. Grecchi and B. Simon, "Borel Summability: Application To The Anharmonic Oscillator," *Phys. Lett. B* **32** (1970) 631.

- [10] J. J. Loeffel, A. Martin, B. Simon and A. S. Wightman, "Padé Approximants And The Anharmonic Oscillator," *Phys. Lett. B* **30** (1969) 656.
- [11] S. R. Coleman, "The uses of instantons," *Subnucl. Ser.* **15** (1979) 805.
- [12] R. Balsa, M. Plo, J. G. Esteve and A. F. Pacheco, "Simple Procedure To Compute Accurate Energy Levels Of A Double Well Anharmonic Oscillator," *Phys. Rev. D* **28** (1983) 1945.
- [13] F. M. Fernandez, A. M. Meson and E. A. Castro, "A simple iterative solution of the Schrödinger equation in matrix representation form," *J. Phys. A* **18** (1985) 1389.
- [14] F. Arias de Saavedra and E. Buenda, "Perturbative-variational calculations in two-well anharmonic oscillators," *Phys. Rev. A* **42** (1990) 5073.
- [15] S. Bravo Yuste and A. Martín Sánchez, "Energy levels of the quartic double well using a phase-integral method," *Phys. Rev. A* **48** (1993) 3478.
- [16] V. Singh, S. N. Biswas and K. Datta, "The Anharmonic Oscillator And The Analytic Theory Of Continued Fractions," *Phys. Rev. D* **18** (1978) 1901.
- [17] M. A. Shifman, "New findings in quantum mechanics (partial algebraization of the spectral problem)," *Int. J. Mod. Phys. A* **4** (1989) 2897.
- [18] W. Balsler, "From Divergent Series to Analytic Functions," LNM 1582. Springer-Verlag, 1994.
- [19] C. M. Bender and T. T. Wu, "Anharmonic Oscillator," *Phys. Rev.* **184** (1969) 1231.
- [20] B. Simon and A. Dicke, "Coupling Constant Analyticity For The Anharmonic Oscillator," *Annals Phys.* **58** (1970) 76.
- [21] P. Mansfield, "The Vacuum functional at large distances," *Phys. Lett. B* **358** (1995) 287 [arXiv:hep-th/9508148].

- [22] P. Mansfield, "Reconstructing the Vacuum Functional of Yang-Mills from its Large Distance Behaviour," *Phys. Lett. B* **365** (1996) 207 [arXiv:hep-th/9510188].
- [23] P. Mansfield, M. Sampaio and J. Pachos, "Short distance properties from large distance behaviour," *Int. J. Mod. Phys. A* **13** (1998) 4101 [arXiv:hep-th/9702072].
- [24] P. Mansfield, "Solving the functional Schroedinger equation: Yang-Mills string tension and surface critical scaling," *JHEP* **0404** (2004) 059 [arXiv:hep-th/0406237].
- [25] W. Magnus, F. Oberhettinger, R. P. Sony "Formulae and Theorems for the Special Functions of Mathematical Physics," 3rd ed., Springer-Verlag, Berlin, 1966.
- [26] C. M. Bender and T. T. Wu, "Large Order Behaviour Of Perturbation Theory," *Phys. Rev. Lett.* **27** (1971) 461.
- [27] C. M. Bender and T. T. Wu, "Anharmonic Oscillator. 2: A Study Of Perturbation Theory In Large Order," *Phys. Rev. D* **7** (1973) 1620.
- [28] V. Kowalenko and A. A. Rawlinson, "Mellin - Barnes regularization, Borel summation and the Bender asymptotics for the anharmonic oscillator," *J. Phys. A* **31** (1998) L663.
- [29] I. G. Halliday and P. Suranyi, "The Anharmonic Oscillator: A New Approach," *Phys. Rev. D* **21** (1980) 1529.
- [30] G. Parisi, "The Perturbative Expansion And The Infinite Coupling Limit," *Phys. Lett. B* **69** (1977) 329.
- [31] C. M. Bender, "Introduction to PT-Symmetric Quantum Theory," *Contemp. Phys.* **46** (2005) 277 [arXiv:quant-ph/0501052].
- [32] B. Hatfield, "Quantum Field Theory of Point Particles and Strings," Perseus Books Publishing (1992) ISBN 0-201-11982-X

- [33] J. H. Yee, "Schrödinger picture representation of quantum field theory," SNUTP-92-40
- [34] R. Floreanini and L. Vinet, "APPLICATIONS OF THE SCHRÖDINGER PICTURE IN QUANTUM FIELD THEORY," MIT-CTP-1517 *Given at Int. Colloquium on Group Theoretical Methods in Physics, Varna Bulgaria, Jun 15-20 1987 and Workshop on High Energy Physics and Field Theory, Protvino, USSR, Jul 6-12 1987 and CAP-NSERC Summer Inst. in Theoretical Physics, Edmonton, Canada, Jul 10-25 1987*
- [35] M. Luscher, "Schrödinger Representation In Quantum Field Theory," Nucl. Phys. B **254** (1985) 52.
- [36] D. M. McAvity and H. Osborn, "Quantum field theories on manifolds with curved boundaries: Scalar fields," Nucl. Phys. B **394** (1993) 728 [arXiv:cond-mat/9206009].
- [37] A. Jaramillo and P. Mansfield, "Finite VEVs from a large distance vacuum wave functional," Int. J. Mod. Phys. A **15** (2000) 581 [arXiv:hep-th/9808067].
- [38] M. D. R. Sampaio, PhD Thesis, University of Durham, UK, (1997).
- [39] J. Pachos, PhD Thesis, University of Durham, UK, (1996).
- [40] R. P. Feynman, "The Qualitative Behavior Of Yang-Mills Theory In (2+1)-Dimensions," Nucl. Phys. B **188** (1981) 479.
- [41] P. Mansfield and M. Sampaio, "Yang-Mills beta-function from a large-distance expansion of the Schroedinger functional," Nucl. Phys. B **545** (1999) 623 [arXiv:hep-th/9807163].
- [42] P. Mansfield and M. Sampaio, "Constructing the leading order terms of the Yang-Mills Schroedinger functional," [arXiv:hep-th/9611109].
- [43] C. M. Bender, S. Boettcher and V. M. Savage, "Conjecture on the Interlacing of Zeros in Complex Sturm-Liouville Problems," J. Math. Phys. **41** (2000) 6381 [arXiv:math-ph/0005012].

- [44] B. A. Lippmann and K. Schwinger, "Variational Principles for Scattering Processes. I," Phys. Rev. **79** (1950) 469
- [45] O. J. P. Eboli, S. Y. P. Pi and M. Samiullah, "RENORMALIZABILITY OF FUNCTIONAL SCHRÖDINGER PICTURE IN ROBERTSON-WALKER SPACE-TIME," Annals Phys. **193** (1989) 102.
- [46] R. Jackiw and A. Kerman, "Time Dependent Variational Principle And The Effective Action," Phys. Lett. A **71** (1979) 158.

